

DP-1457

662696

# **AUTOMATED ABSOLUTE ACTIVATION ANALYSIS WITH CALIFORNIUM-252 SOURCES**

**K. W. MacMURDO and W. W. BOWMAN**



**SAVANNAH RIVER LABORATORY  
AIKEN, SOUTH CAROLINA 29801**

**PREPARED FOR THE U.S. DEPARTMENT OF ENERGY UNDER CONTRACT AT(07-2)-1**

#### NOTICE

This report was prepared as an account of work sponsored by the United States Government. Neither the United States nor the United States Department of Energy, nor any of their contractors, subcontractors, or their employees, makes any warranty, express or implied or assumes any legal liability or responsibility for the accuracy, completeness or usefulness of any information, apparatus, product or process disclosed, or represents that its use would not infringe privately owned rights.

Printed in the United States of America

Available from

National Technical Information Service

U.S. Department of Commerce

5285 Port Royal Road

Springfield, Virginia 22161

Price: Printed Copy \$6.00; Microfiche \$3.00

## **AUTOMATED ABSOLUTE ACTIVATION ANALYSIS WITH CALIFORNIUM-252 SOURCES**

**K. W. MacMURDO and W. W. BOWMAN**

Approved by

E. I. Baucom, Research Manager  
Analytical Chemistry Division

Publication Date: September 1978

---

**E. I. DU PONT DE NEMOURS AND COMPANY  
SAVANNAH RIVER LABORATORY  
AIKEN, SOUTH CAROLINA 29801**

PREPARED FOR THE U. S. DEPARTMENT OF ENERGY UNDER CONTRACT AT(07-2)-1

## ABSTRACT

---

A 100-mg  $^{252}\text{Cf}$  neutron activation analysis facility is used routinely at the Savannah River Laboratory for multielement analysis of many solid and liquid samples. Applications include analysis of metal alloys, coal, fly ash, sediments, rocks, vegetation, inks, and many aqueous process solutions.

An absolute analysis technique converts counting data directly to elemental concentration without the use of classical comparative standards and flux monitors. This absolute technique predicts elemental neutron capture reaction rates from multi-energy 2- and 84-group cross sections and calculated neutron fluxes for different source-moderator-sample arrangements.

With the totally automated pneumatic sample transfer system, cyclic irradiation-decay-count regimes can be pre-selected for up to 40 samples, and samples can be analyzed with the facility unattended. An automatic data control system starts and stops a high-resolution gamma-ray spectrometer and/or a delayed-neutron detector; the system also stores data and controls output modes.

Gamma ray data are reduced by three main programs in the IBM 360/195 computer. In the first program, the 4096-channel spectrum and pertinent experimental timing, counting, and sample data are stored on magnetic tape. In the second program, the spectrum is then reduced to a list of significant photopeak energies, integrated areas, and their associated statistical errors. The third program assigns gamma ray photopeaks to the appropriate neutron activation product(s) by comparing photopeak energies to tabulated gamma ray energies. Photopeak areas are then converted to elemental concentration by using experimental timing and sample data, calculated elemental neutron capture rates, absolute detector efficiencies, and absolute spectroscopic decay data.

Calculational procedures have been developed so that fissile material such as light water reactor plutonium and natural uranium can be analyzed by cyclic neutron activation and delayed-neutron counting procedures. These calculations are based on a 6 half-life group model of delayed neutron emission; calculations include corrections for delayed neutron interference from  $^{17}\text{O}$ . Detection sensitivities of  $\leq 400$  ppb for natural uranium and 8 ppb [ $\leq 0.5$  (nCi/g)] for  $^{239}\text{Pu}$  were demonstrated with 15-g samples at a throughput of up to 140 per day.

Over 40 elements can be detected at the sub-ppm level in the 100-mg  $^{252}\text{Cf}$  facility. Precisions and accuracies of  $\pm 10\%$  for most elements were demonstrated in extensive multielement analyses of standards which include rock standards from the U.S. Geologic Survey, and coal and fly ash standards from the National Bureau of Standards.



## CONTENTS

---

Introduction	13
Description of Facility	17
Irradiation Tank Room	17
Counting Room	26
Rapid Sample Transport System	32
Detection Apparatus	37
Gamma Ray Detectors	37
Ge(Li) Detectors	37
NaI Detectors	39
Delayed Neutron Detector	39
Sample Preparation Facilities and Procedures	39
Basic Principles of $^{252}\text{Cf}$ Neutron Activation Analysis	41
Absolute Activation Analysis	41
Cyclic Activation and Counting	42
Cyclic Sensitivities	44
Master Equation	46
Specific Neutron Capture Reaction Rates	47
Multigroup (84-group) Summation	48
Analytical Function Approximations (2 Groups)	49
Neutron Flux Calculations	51
17-mg $^{252}\text{Cf}$ Facility	51
ANISN Calculations	51
Comparison of Calculated and Experimental Reaction Rates	58
100-mg $^{252}\text{Cf}$ Facility	59
ANISN Calculations	60
Comparison of Calculated and Measured Fluxes	72
Evaluation of the $\text{H}_2\text{O}$ - $\text{D}_2\text{O}$ System	73

Optimized Fissile Material Analysis with Cyclic Neutron Activation and Delayed Neutron Counting	74
Delayed Neutron Analysis	74
Optimization of Cyclic Analysis Procedures for Fissile Materials	75
Effect of Transit Time on Detector Response	78
Optimization Parameters	78
Comparison of Calculated and Measured Detector Responses	84
Oxygen-17 Interference in Analysis of Low-Level Aqueous Samples	85
Computer Data Processing	88
TRANSCRIBE	89
RAGS	89
SIFTER	89
EDIT Data Files	91
SIFTER Flow Diagram	91
Interpretation of SIFTER Output	94
Analysis of Test Mixture	96
Results and Applications	98
Solid Standards	98
Standard Coal (NBS Standard SRM-1632)	98
Standard Fly Ash (NBS Sample SRM-1633)	98
Rock Standards (USGS Samples GSP-1 and BCR-1)	101
Liquid Standards	101
Elemental Detection Limits	101
Summary of Routine Analyses	104
Appendix A: Data Reduction Tables	109
Appendix B: Calculation of Flux Depression Factors	111
Thermal Flux Depression	111
Resonance Flux Depression	112
References	115



## LIST OF TABLES

1	Timers in the Functional Control Unit	35
2	Sensitivity of Cyclic Activation with 17mg $^{252}\text{Cf}$ Source	45
3	Calculated and Measured Neutron Capture Rates for the 17-mg $^{252}\text{Cf}$ Facility	58
4	Flux Calculations for Ideal Systems	66
5	Regions, Distances, and Materials in the 100-mg $^{252}\text{Cf}$ Facility	66
6	Flux Calculations that Include Effects of Stainless Steel	70
7	Calculated Specific Fission Rates in the $^{252}\text{Cf}$ Facility	76
8	Delayed-Neutron Group Half-Lives and Yields for Thermal Fission of $^{233}\text{U}$ , $^{235}\text{U}$ , $^{239}\text{Pu}$ , and $^{241}\text{Pu}$	76
9	Delayed-Neutron Group Half-Lives and Yields for Fast Neutron Fission of $^{238}\text{U}$ and $^{240}\text{Pu}$	76
10	Specific Saturated Delayed-Neutron Emission Rates Calculated for Fissile Isotopes	77
11	Changes in Calculated Detector-Response with Changes in Sample Transit Time for the Optimum Number of Cycles for Natural Uranium	82
12	Optimum Experimental Conditions for Cyclic Analysis of Natural Uranium	83
13	Optimum Experimental Conditions for Cyclic Analysis of Common Fissile Materials	83
14	Delayed-Neutron Signal-to-Noise Ratios for Cyclic Analysis of Natural Uranium in Aqueous Solution	87
15	Coding Format for Header Records	90
16	Analysis of Test Mixture	97

- 17 Analysis of NBS Coal Standard SRM-1632 99
- 18 Analysis of NBS Fly Ash Standard SRM-1633 100
- 19 Analysis of USGS Rock Standard GSP-1 102
- 20 Analysis of USGS Rock Standard BCR-1 103
- 21 Absolute Analysis of Atomic Absorption Liquid Standards 104
- 22 Interference-Free Elemental Detection Limits of the 100-mg  $^{252}\text{Cf}$  Facility 105
- 23 Elemental Concentration Ranges Measured in Typical Samples 107

## LIST OF FIGURES

---

1	$^{252}\text{Cf}$ Neutron Activation Analysis Facility	17
2	Source Tank	18
3	Primary Capsule for $^{252}\text{Cf}$ Source (Series SR-Cf-IX)	19
4	Secondary Capsule for $^{252}\text{Cf}$ Source (Series SR-Cf-100)	20
5	Typical Secondary Capsule for $^{252}\text{Cf}$ Source (Series 100)	21
6	Irradiation Tank Assembly	22
7	Neutron Activation Analysis Facility with $^{252}\text{Cf}$ Sources in Position	23
8	Annular Moderator Tank and Four-Position Source Holder	24
9	Polyethylene Sample Transfer Tubes	25
10	Filter Deionizer System	27
11	Sample Transfer Equipment	28
12	Sample Irradiation Container	28
13	Sample Sealer	29
14	Data Storage Facility	30
15	Shielded Dual Gamma-Ray/Delayed Neutron Detector	31
16	Schematic of Rabbit System	33
17	Sample Transport Control Unit	34
18	Relative Detector Response for Cyclic Activation of Scandium	45
19	Neutron Energy Spectra at 3.81 cm and 10.61 cm as Calculated by ANISN	53
20	Change in Thermal Flux with Distance from Source	53

21	Change in Epithermal Flux with Distance from Source	54
22	Epithermal-to-Thermal Flux Ratio with Distance from Source	54
23	Change in Thermal Flux with Distance from Source to Centers of H <sub>2</sub> O, D <sub>2</sub> O, and Air Moderated Central Regions	55
24	Change in Epithermal-to-Thermal Flux Ratio with Distance from Source to Centers of H <sub>2</sub> O, D <sub>2</sub> O, and Air Moderated Central Regions	56
25	Changes in Calculated and Measured Thermal Fluxes with Distance from Source	57
26	Arrangement of Irradiation Tubes and Sources in 100-mg <sup>252</sup> Cf Facility	60
27	Calculated Thermal Flux for Ideal System with H <sub>2</sub> O Moderator (Case 1)	62
28	Calculated Thermal Flux for Ideal System with H <sub>2</sub> O-D <sub>2</sub> O Moderator (Case 2)	63
29	Calculated Thermal Flux for Ideal Case, H <sub>2</sub> O-D <sub>2</sub> O Moderator with Sample in Outer Ring (Case 3)	64
30	Thermal Flux Ratio for Ideal System (Case 2/Case 1)	65
31	Thermal Flux Ratio for Ideal System (Case 3/Case 1)	65
32	Schematic of Regions Surrounding <sup>252</sup> Cf Sources Used in ANISN Calculations	67
33	Calculated Thermal Flux for Inner Ring in Non-Ideal System with H <sub>2</sub> O Moderator (Case 4)	68
34	Calculated Thermal Flux for Inner Ring in Non-Ideal System with H <sub>2</sub> O-D <sub>2</sub> O Moderator (Case 5)	69
35	Calculated Thermal Flux Ratio for Inner Ring in Non-Ideal System with H <sub>2</sub> O-D <sub>2</sub> O Moderator (Case 5/Case 4)	69
36	Calculated Thermal Flux for Outer Ring in Non-Ideal System with H <sub>2</sub> O Moderator (Case 6)	70
37	Calculated Thermal Flux for Outer Ring in Non-Ideal System with H <sub>2</sub> O-D <sub>2</sub> O Moderator (Case 7)	71

38	Calculated Thermal Flux Ratio in Outer Ring in Non-Ideal System with H <sub>2</sub> O Moderator (Case 7/Case 6)	72
39	Calculated Group Response and Detector Response for Natural Uranium for Transit Time of 0.25 sec	79
40	Calculated Group Response and Detector Response for Natural Uranium for Transit Time of 1.0 sec	80
41	Effect of Sample Transit Time on Detector Response for Natural Uranium	81
42	Relative Detector Response for Fissile Isotopes	84
43	Comparison of Calculated and Measured Detector Responses for Cyclic Analysis of <sup>235</sup> U	85
44	Calculated Detector Response for Aqueous Samples Containing 10 ppm Natural Uranium	86
45	Data Reduction Flowsheet	90
46	SIFTER Program Flowsheet	92



## INTRODUCTION

---

The usefulness of neutron activation analysis (NAA) as a multielement analytical tool has been demonstrated over the past thirty years. During 1950-1970, many publications described successful use of NAA in the trace analysis of samples for geology, biology, archeology, chemistry, and criminology application. For multielement activation analysis, either complete exhaustive chemical separation and counting of products or some type of gamma ray spectroscopy is used. With the earliest spectroscopic technique of gamma ray absorption, resolution was extremely poor. In 1948, Hofstadter<sup>1</sup> pioneered the development of NaI (Tl) scintillation crystals; this development opened a new dimension in gamma ray spectrometry. Further improvements in the early 1960's included Ge(Li) detectors which made high-resolution gamma ray spectrometry possible.<sup>2</sup> With NaI detectors and early Ge(Li) detectors, energy resolution was very poor compared to today's standards, and elements were separated by chemical group before counting. By the early 1970's, the technique of NAA, once regarded as the ultimate method of trace analysis, was in a recognized decline.<sup>3</sup> This decline was caused by development of better instrumental techniques and by a limited understanding of basic NAA principles. The users of activation analysis assumed that NAA was basically a chemical technique, and therefore its development was hindered because advances in the basic physics of the technique were ignored. Neutron activation analysis is a nuclear technique, not a chemical technique. In fact, the most serious limitation has been the low sample throughput of NAA because chemical separations were required.

The basic physical principles of NAA, though understood for 30 years, have been used mainly for teaching purposes and have not been incorporated into routine analytical procedures. Most activation analysts use the standard comparative technique basic to all analysis techniques. In these techniques, a standard of almost identical matrix and similar trace constituents is analyzed simultaneously with the sample. The comparative technique requires estimates of sample composition, preparation, packaging, irradiation, and counting of both samples and standards; sample throughput is necessarily reduced. With the standard comparative technique, the analysis procedure is reduced to a determination of counting ratios because the following basic factors are eliminated:

- Uncertainties in radioactive decay parameters such as half-life and absolute decay abundance.
- Variations in effective element response to the particular irradiation conditions and sample matrix.
- Changes in neutron flux and energy distribution which accompany changes in reactor power level and fuel burnup.

In recent years, major advances have been made by nuclear chemists and physicists in the measurement of multigroup cross sections and in the development of neutron shielding and neutron transport codes used to calculate isotope production in reactors. Significant advances have been made in the measurement of spectroscopic decay data and in the determination of decay schemes for most isotopes. Because of improvements in the efficiency and resolution of Ge(Li) detectors and associated electronics, separations can be done electronically rather than chemically.

The sensitivity and multielement capabilities of neutron activation analysis made it a highly desirable technique for use at Savannah River Laboratory. Because production reactors were not a convenient source of neutrons for activation, large  $^{252}\text{Cf}$  sources available in the laboratory were used to develop neutron activation analysis. However, the relatively low thermal neutron flux (a factor of  $\sim 1000$  below that available from a small reactor) limited elemental sensitivities and hampered diversified applications because of low sample throughput.

A facility at the Savannah River Laboratory was first designed for a 17-mg  $^{252}\text{Cf}$  source. Analysis capabilities of this facility were later expanded when this source was replaced by four 25-mg  $^{252}\text{Cf}$  sources. An absolute technique (eliminating comparative standards) was also developed which uses accurately known neutron capture cross sections<sup>4</sup> and the constant spectral and spatial distributions of  $^{252}\text{Cf}$  neutrons calculated from neutron transport codes.<sup>5</sup> Sample throughput was further increased by using automated sample handling and data reduction procedures and tabulated spectrometric data.<sup>6</sup> The rapid sample transport system also improved detection sensitivities of certain elements by using cyclic activation and counting regimes. These regimes were designed for analysis of elements with neutron capture products with half-lives  $\leq 60$  sec. Other design features were included in the facility to increase sample throughput and to compensate for the relatively low flux of isotopic neutron sources. These features include 18 irradiation tubes in two concentric rings around the source, a  $\text{D}_2\text{O}$  moderator annulus to increase the thermal flux in 9 of the irradiation tubes, provision for irradiating sample volumes up to  $11\text{ cm}^3$ , a shielded counting room, and high-efficiency detectors.



This report is written in four main parts: 1) a complete description of the facility; 2) a discussion of the principles and techniques developed for the facility; 3) a section describing practical application of these principles and techniques, and 4) appendices describing the computer programs developed and currently used in the  $^{252}\text{Cf}$  facility.



## DESCRIPTION OF FACILITY

### IRRADIATION TANK ROOM

The current neutron activation analysis facility (Figure 1) contains four nominal 25-mg  $^{252}\text{Cf}$  sources near the bottom of a 1/4-inch stainless steel tank which is 12-1/2 ft deep and 4-ft in diameter. The tank (Figure 2) was constructed from two cylindrical sections and a hemispherical bottom section seal-welded together. A 1-ft-thick concrete shell surrounding the tank supports the tank and prevents loss of tank water to the ground in the unlikely event of tank rupture. The interior of the tank is painted with white epoxy for improved visibility. The doubly encapsulated  $^{252}\text{Cf}$  sources are attached to a four-position zircaloy source holder assembly extending approximately two feet up from the tank bottom. Figures 3-5 show the primary (inner) and secondary (outer) zircaloy source capsules. Figure 6 shows the irradiation tank assembly.

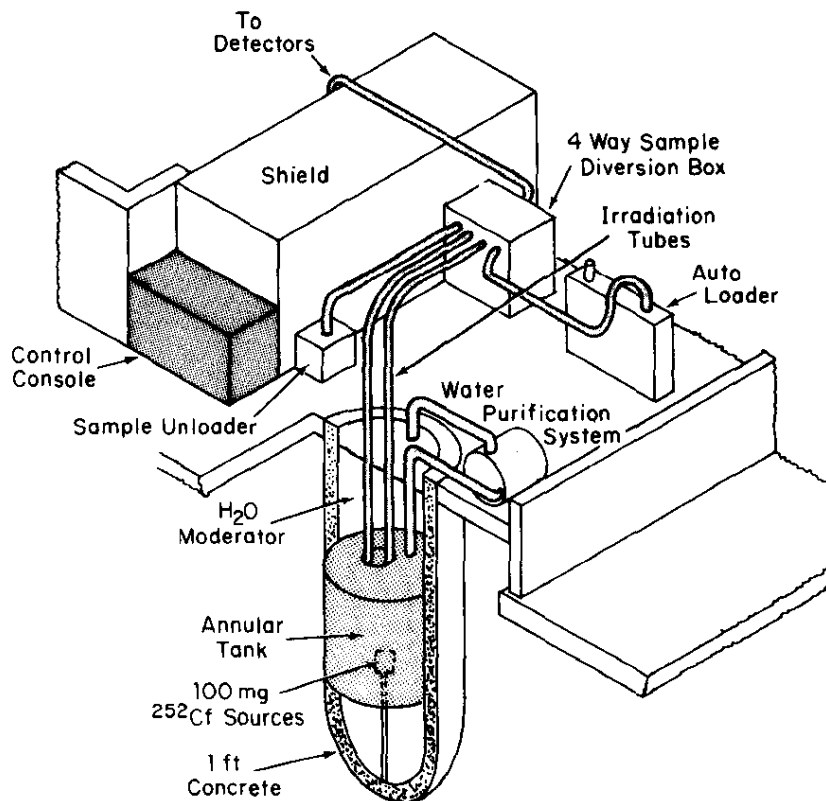


FIGURE 1.  $^{252}\text{Cf}$  Neutron Activation Analysis Facility

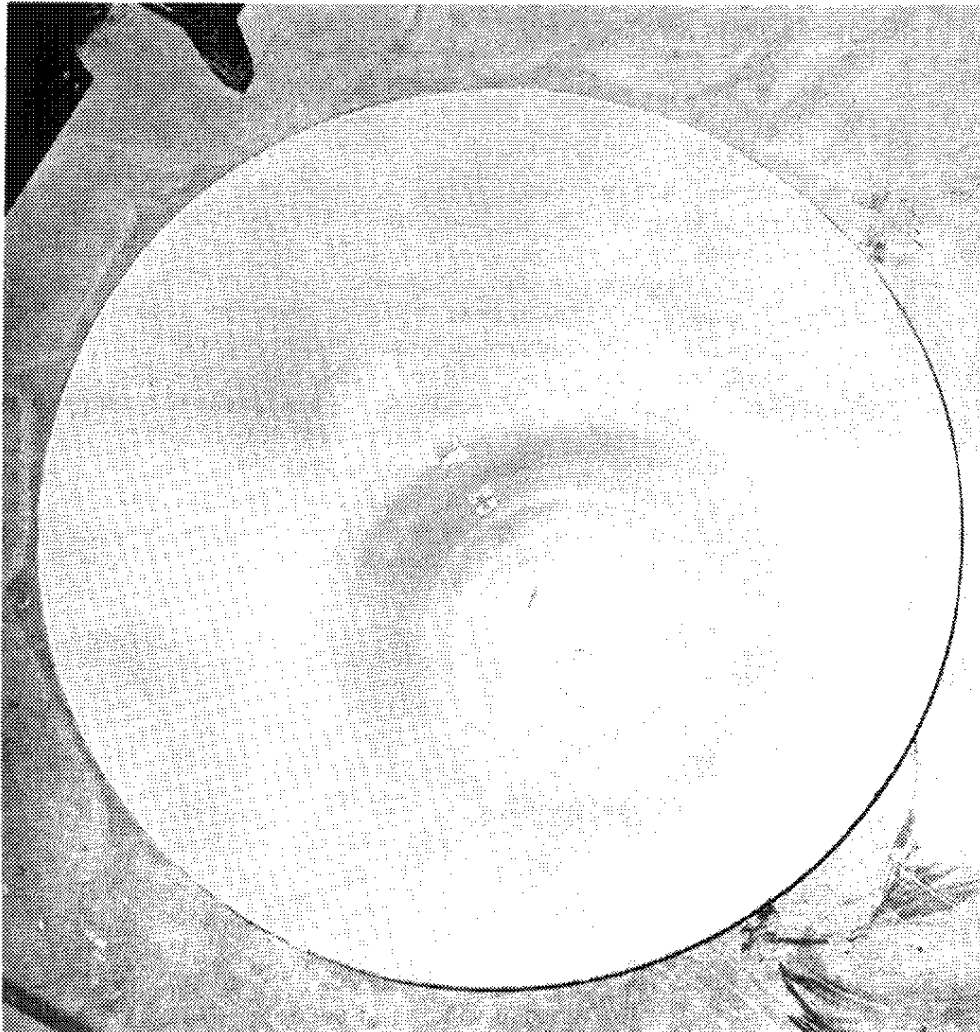


FIGURE 2. Source Tank

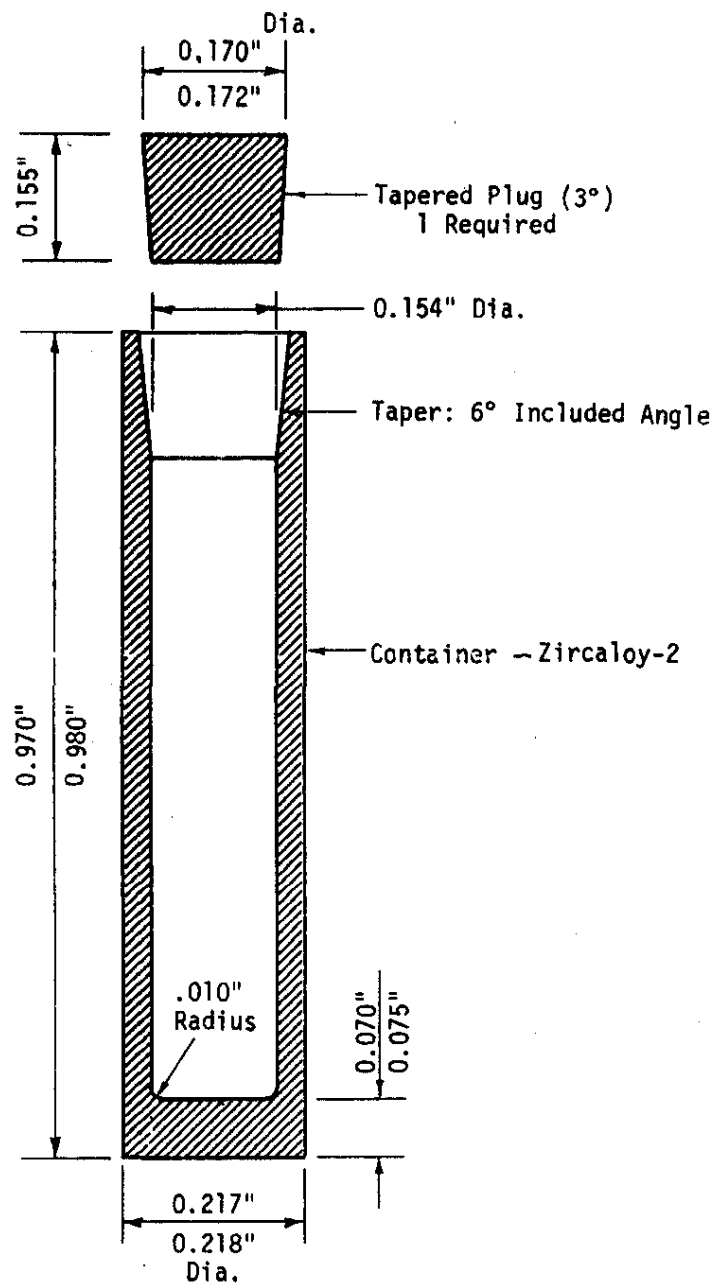


FIGURE 3. Primary Capsule for  $^{252}\text{Cf}$  Source  
(Series SR-CF-IX)

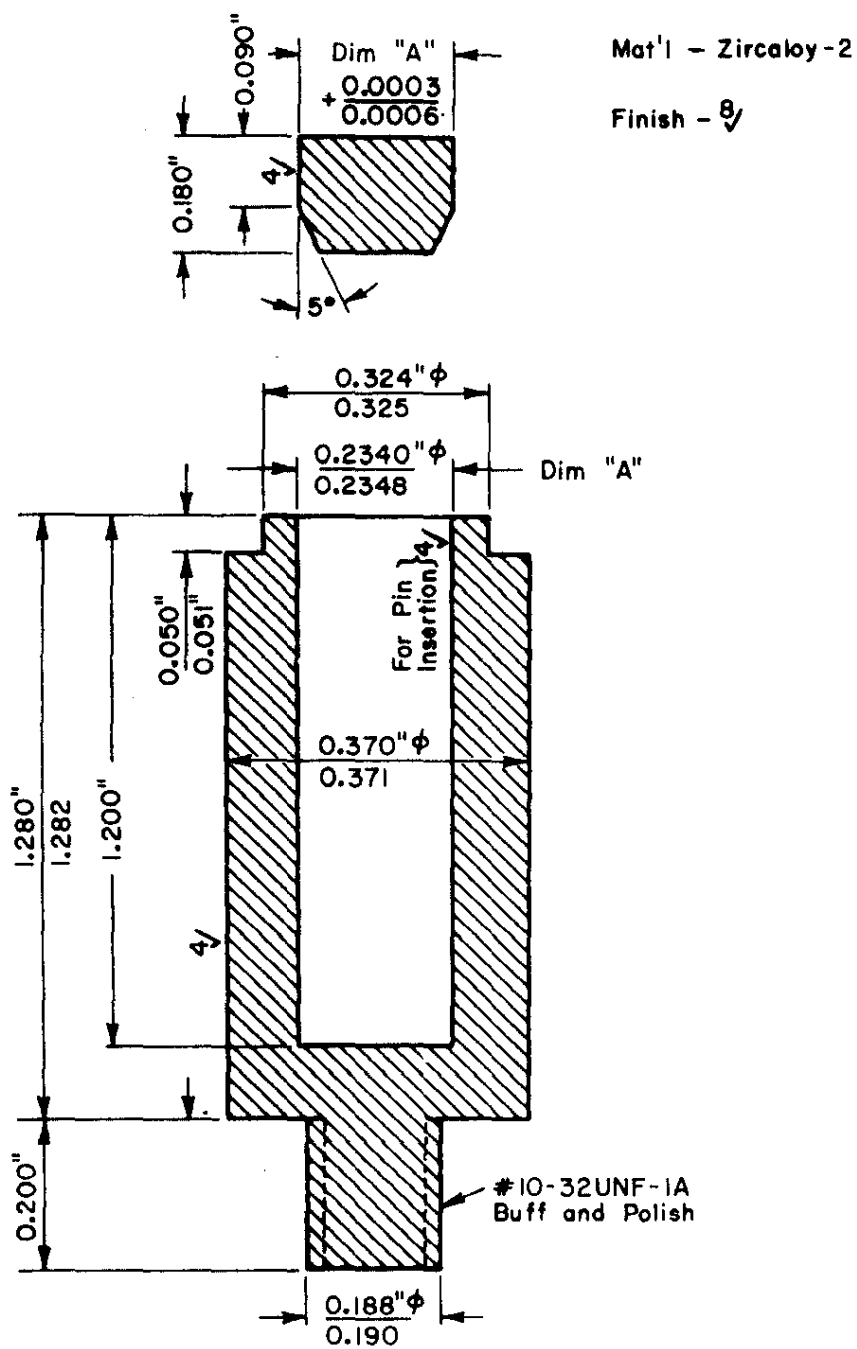


FIGURE 4. Secondary Capsule for  $^{252}\text{Cf}$  Source  
(Series SR-CF-100)

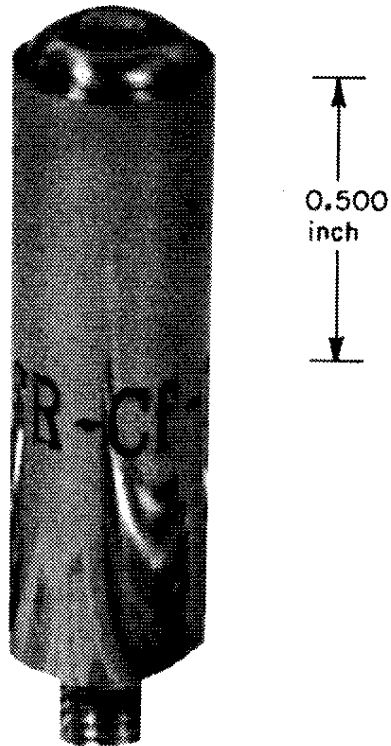


FIGURE 5. Typical Secondary Capsule for  $^{252}\text{Cf}$  Source  
(Series 100)

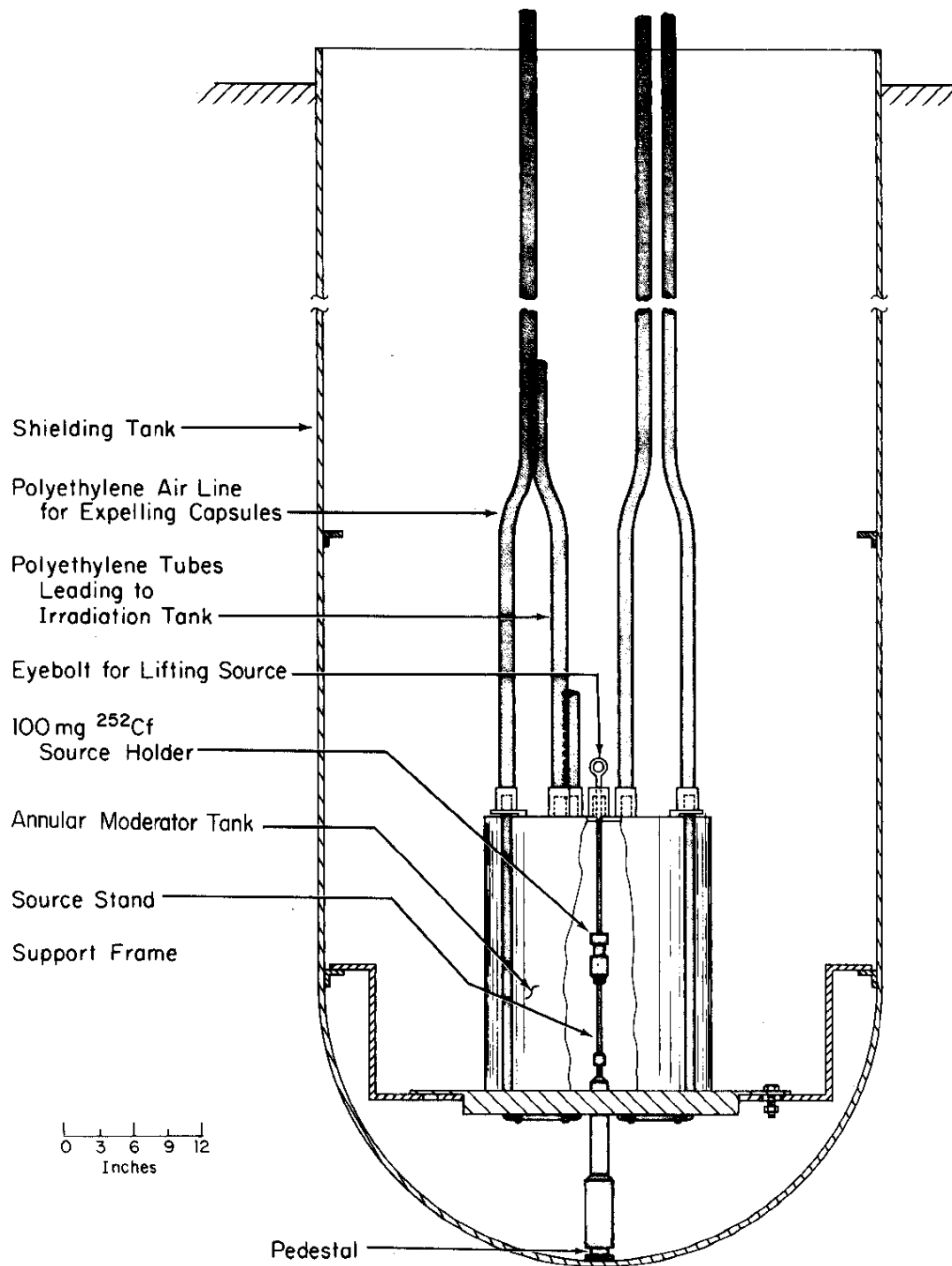


FIGURE 6. Irradiation Tank Assembly



A cylindrical region of deionized light water of 4.68-cm radius surrounds the source (Figure 7). A seal-welded stainless steel annular tank containing  $D_2O$  surrounds the  $H_2O$  region. The outer diameter of the  $D_2O$  annulus is 22.77 cm, and the wall thickness of the tank is 0.1588 cm. Fittings on the tank permit addition and removal of  $D_2O$ ,  $H_2O$ , or air for adjustment of the neutron energy spectrum. Figure 8 shows the annular tank and the four-position source holder. Nine stainless steel sample irradiation tubes are located within the  $H_2O$ -moderated region. Three of these sites are connected to a pneumatic, rapid sample transfer system designed for short half-life studies and cyclic irradiation and counting procedures. Nine additional drop tube irradiation sites are within the annular  $D_2O$  tank. All irradiation sites are stainless steel tubes of 2.54-cm outer diameter and 0.0089-cm wall thickness.

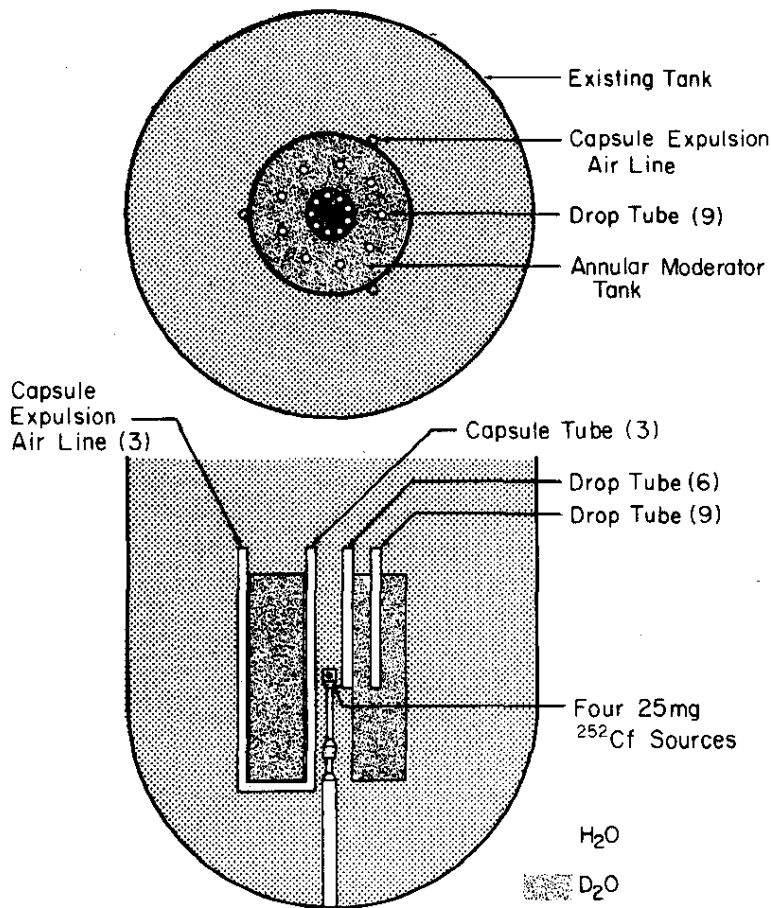


FIGURE 7. Neutron Activation Analysis Facility with  $^{252}Cf$  Sources in Position

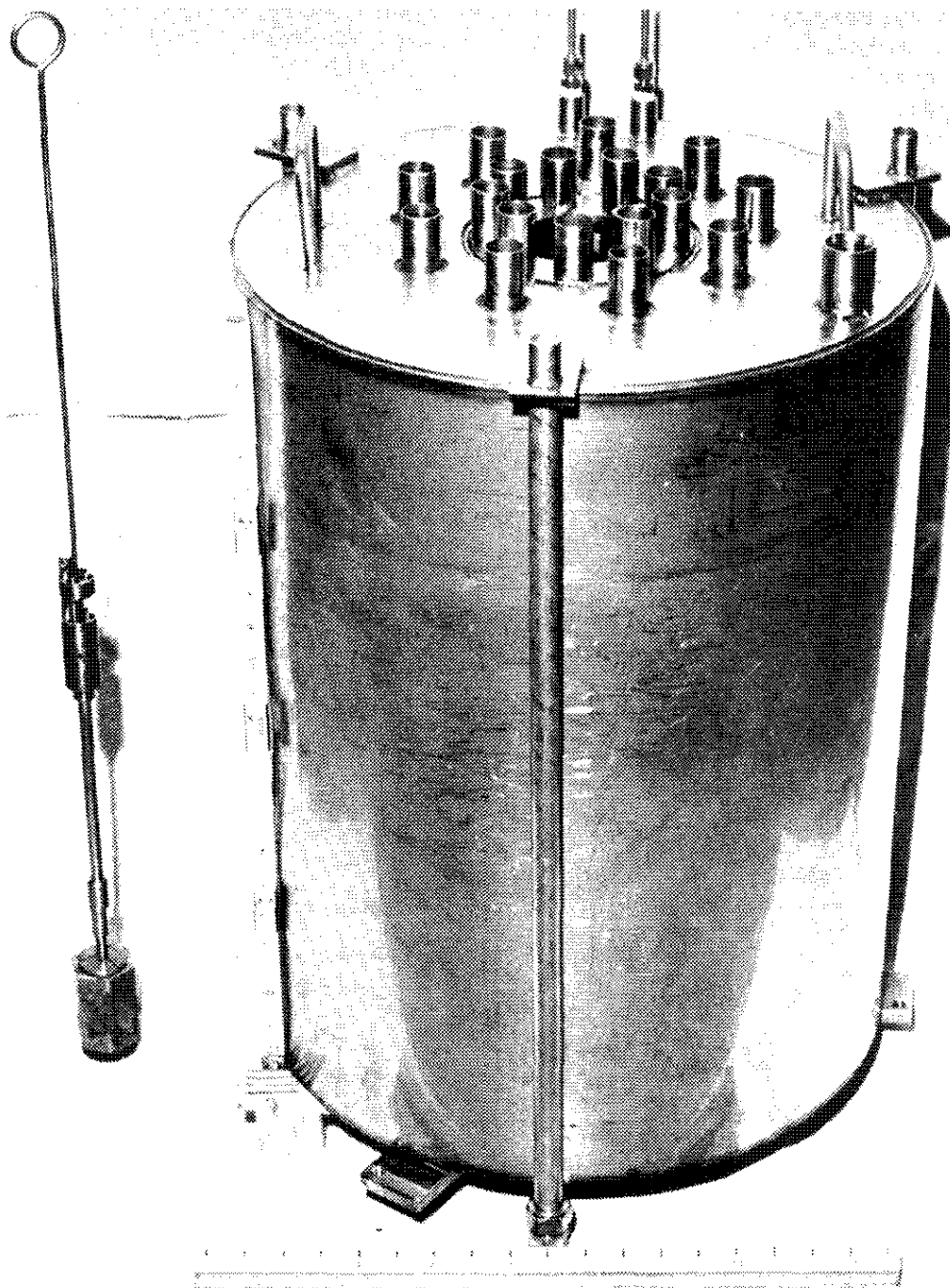


FIGURE 8. Annular Moderator Tank and Four-Position Source Holder

Samples to be irradiated are heat-sealed within high-density polyethylene containers called rabbits of  $\sim 11 \text{ cm}^3$  internal volume. Samples are introduced to the irradiation site either manually or automatically from the pneumatic sample transfer system through 2.85-cm-outer diameter polyethylene transfer tubes. These tubes spiral downward from the working level to the stainless steel irradiation tubes (Figure 9). The polyethylene transfer tubes are clamped to the stainless steel irradiation tubes at about 40 cm from the sources to prevent radiation damage to the polyethylene.

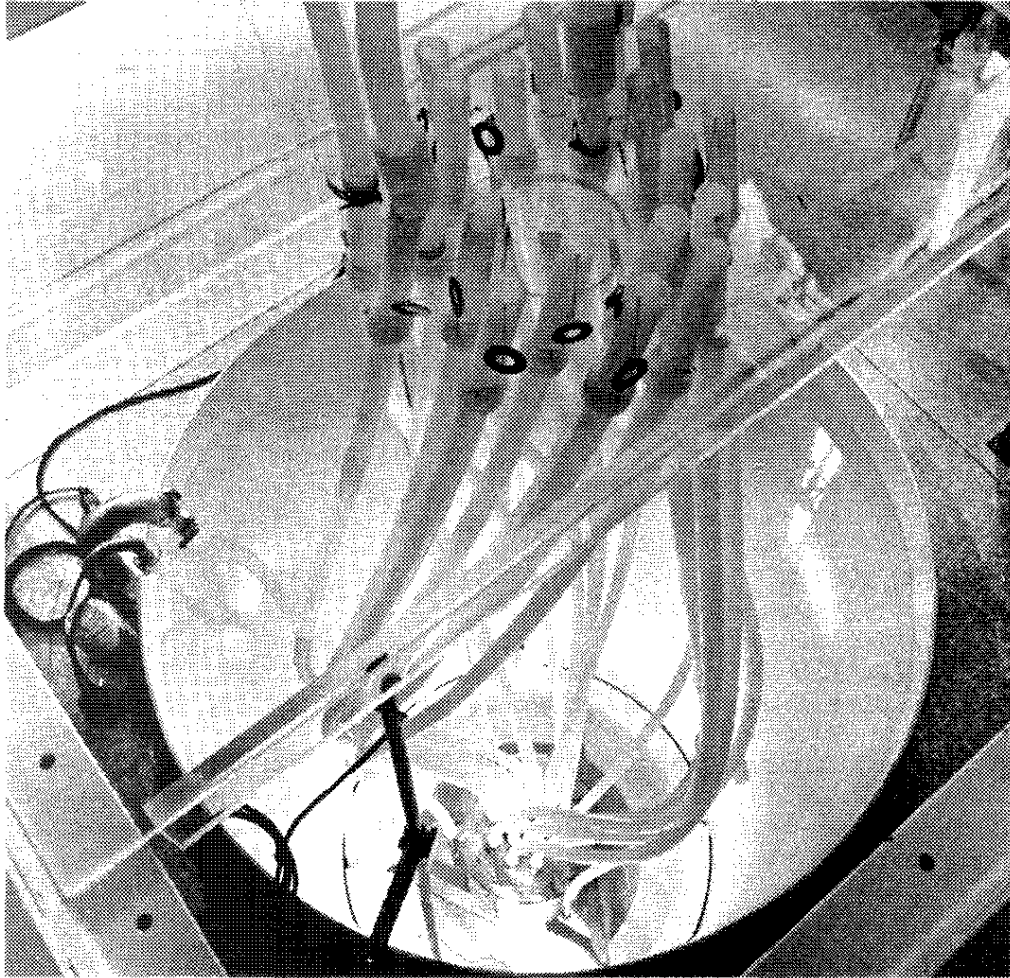


FIGURE 9. Polyethylene Sample Transfer Tubes

The source tank is filled with 1100 gallons of distilled water for moderation and radiation shielding. This water is circulated continuously through a mixed-bed cation-anion demineralizer and filtration system (Figure 10) to prevent buildup of radioactive activation products within the moderator. The ion exchange bed is monitored continuously for gamma and neutron radioactivity which would result from a breached source or sample. The neutron monitor alarm automatically shuts off the moderator circulation pump. The neutron monitor and a beta-gamma air activity monitor are connected to the building alarm panel.

A four-foot square table with a stainless steel framework and acrylic sides and top covers the tank. The tank cover is vented to the laboratory exhaust system. Shielded floodlamps with a 12-V DC power supply provide underwater lighting in the source tank.

The source tank room contains a sample transfer control unit, an automatic sample loader, an unloader, a four-way sample diversion unit, and sample preparation equipment (Figure 11). Sample preparation equipment includes a Class 100 clean bench and a Class 100 fume hood. Polyethylene irradiation containers (Figure 12) are heat-sealed with a pneumatically operated sealer (Figure 13) which moves a resistance-heated wire coil over the threaded end of the rabbit. Then the containers are automatically pressed into an aluminum cooling block.

## COUNTING ROOM

Irradiated samples are counted in a concrete-shielded vault of 4-ft wall thickness. Within this vault, secondary lead shields of minimum 2-inch thickness surround the two Ge(Li) gamma ray spectrometers, a NaI detector, and a BF<sub>3</sub> delayed neutron detector. The dual BF<sub>3</sub>-Ge(Li) spectrometer system within the vault is shown in Figure 15. The dual counting system is part of the automated sample transfer system and is activated automatically through the data storage control module.

Instruments for data acquisition are adjacent to the shielded counting vault (Figure 14). A Canberra Model 8100 multichannel analyzer receives gamma ray spectra from irradiated samples. Accumulated spectra are transferred to nine-track magnetic tape with a Canberra Model 8531 magnetic tape controller and a Wang Model 7 tape transport.

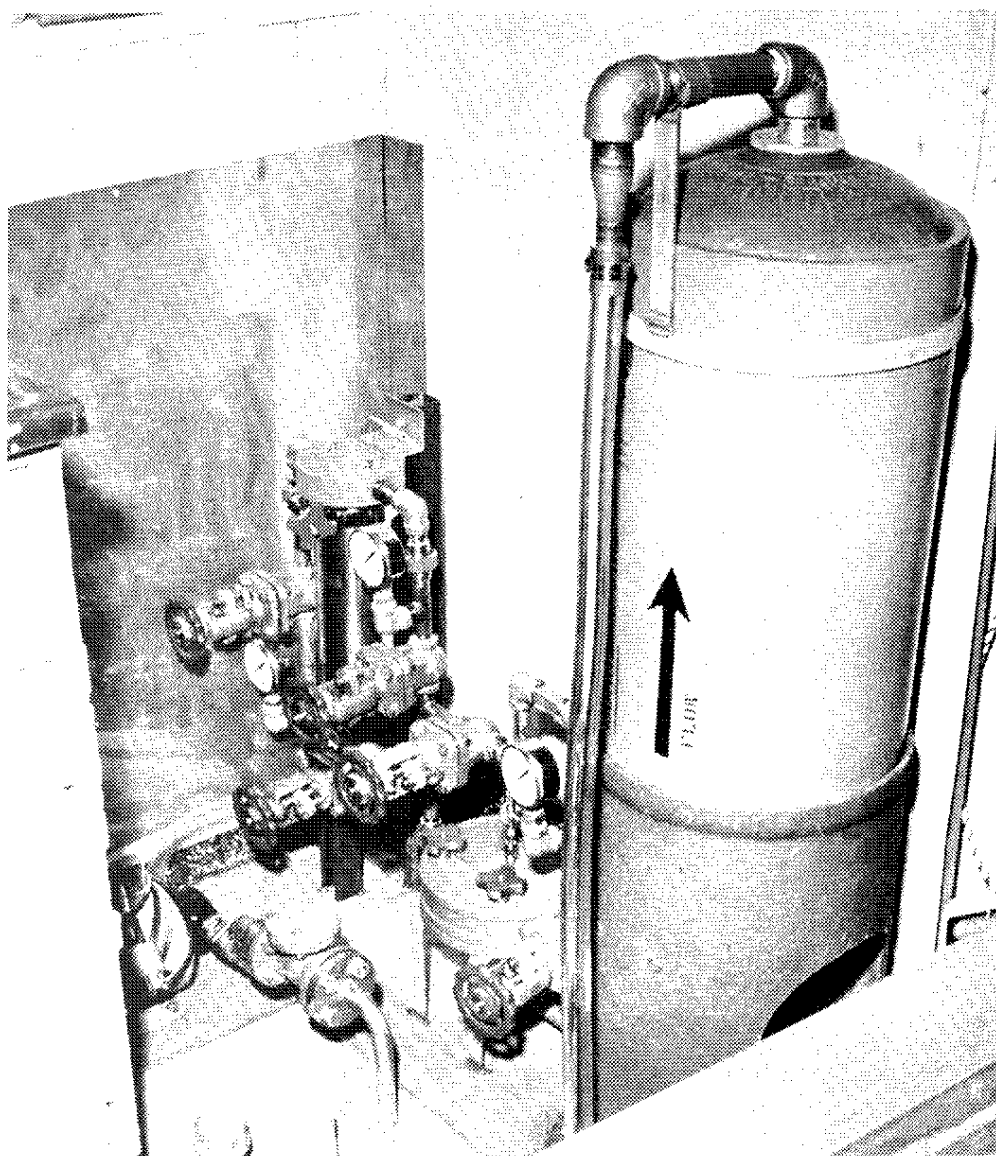


FIGURE 10. Filter-Deionizer System

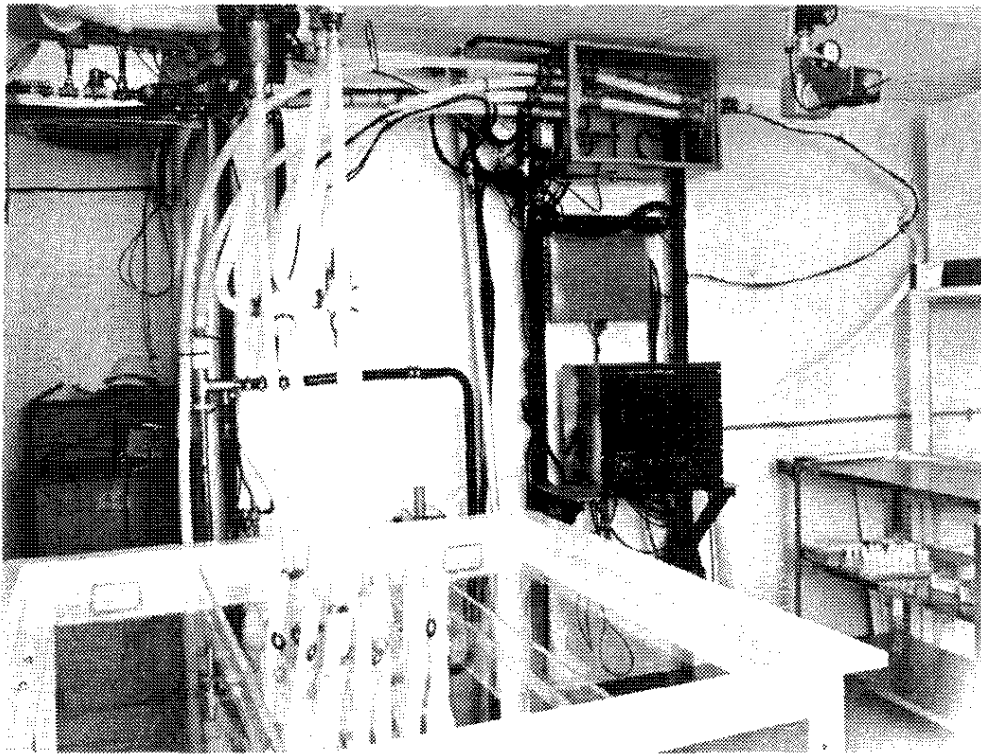
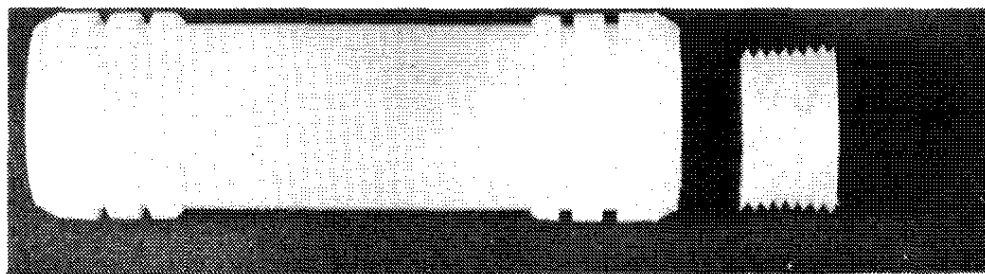


FIGURE 11. Sample Transfer Equipment



0 1 2 3 4 5 6 7 8 9 10  
cm SAVANNAH RIVER LABORATORY

FIGURE 12. Sample Irradiation Container

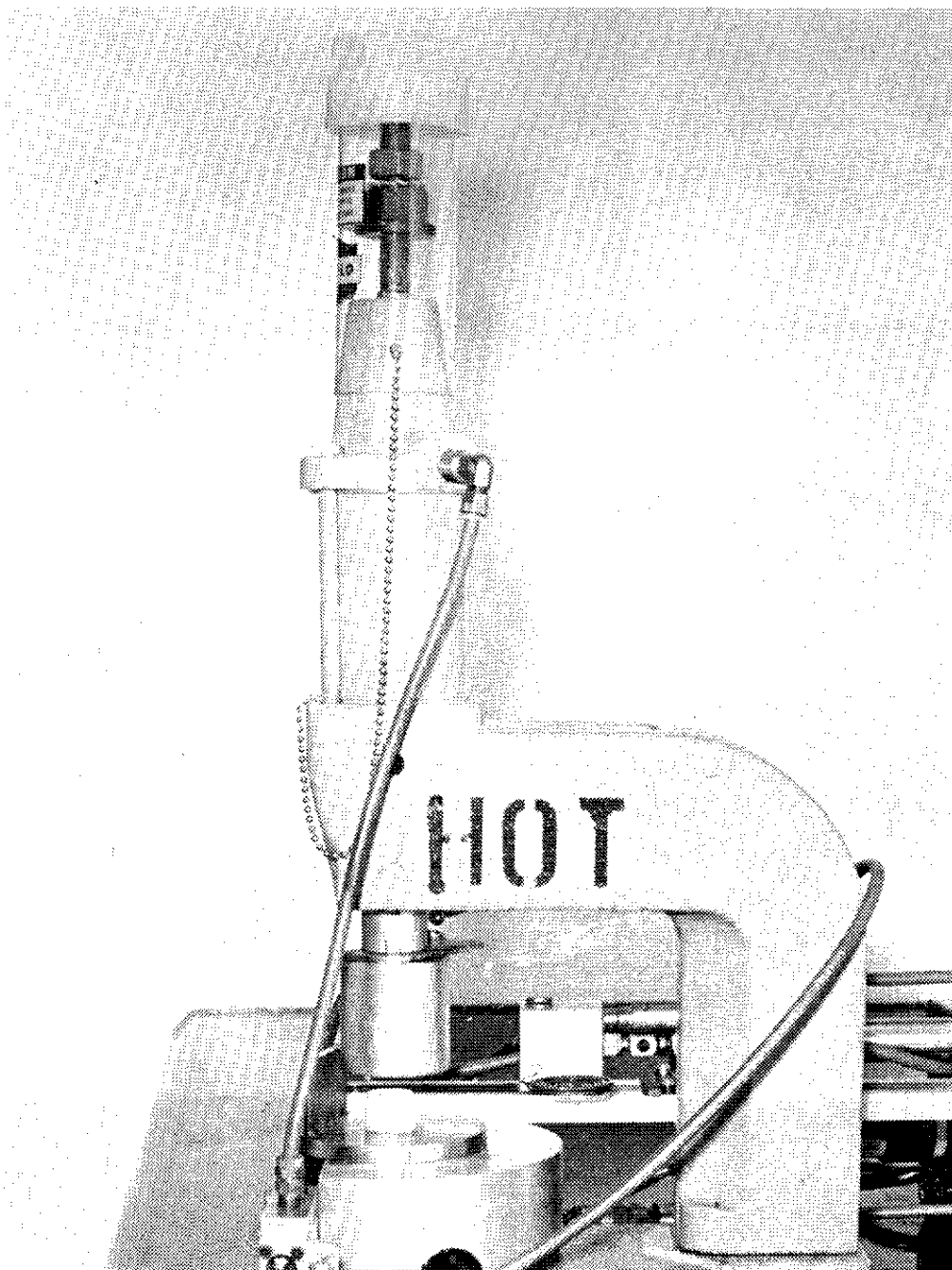


FIGURE 13. Sample Sealer

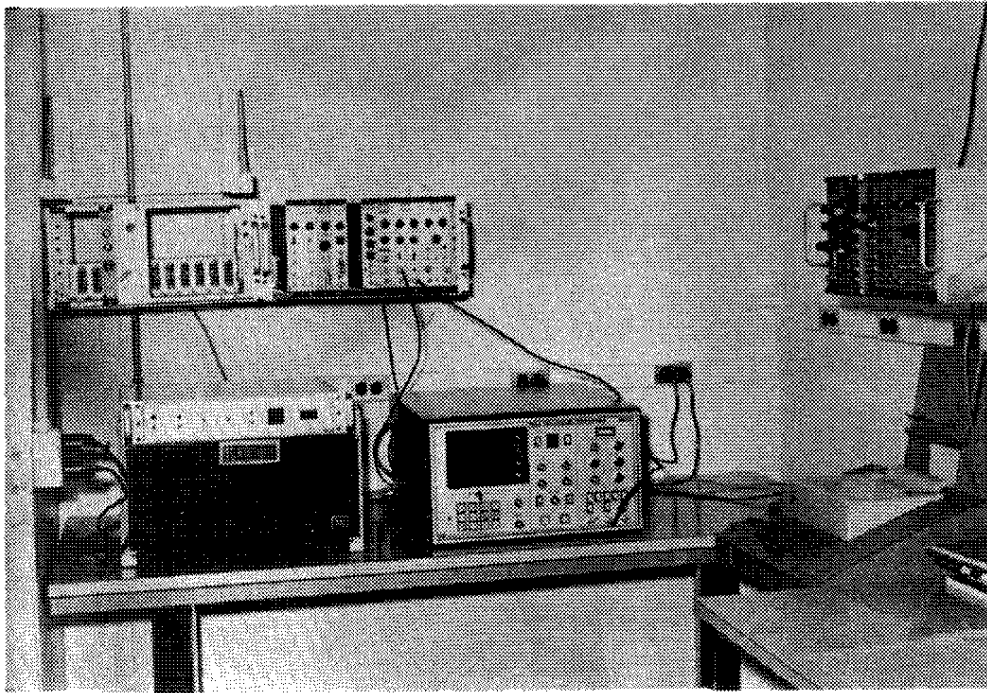


FIGURE 14. Data Storage Facility



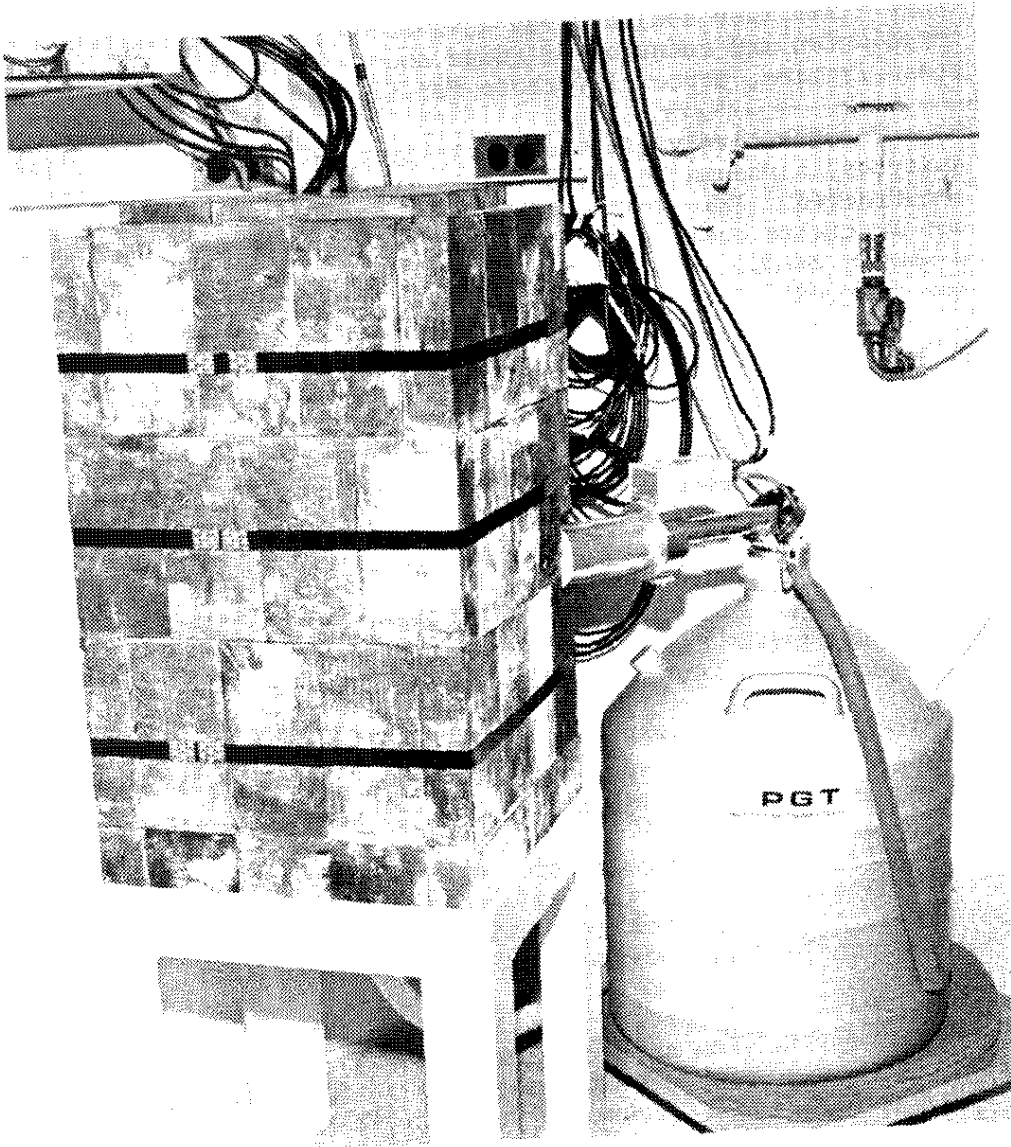


FIGURE 15. Shielded Dual Gamma Ray, Delayed Neutron Detector

## RAPID SAMPLE TRANSPORT SYSTEM

Analysis times can be decreased for many elements by detecting short-lived ( $\leq 60$  sec) neutron activation products. Cyclic neutron irradiation and counting of these short-lived products also improves sensitivities, especially those for fissile materials.

To effectively use the short-lived products for activation analyses, a pneumatic rapid sample transfer system (rabbit) was constructed. This system includes several features which were not available commercially. Main system specifications assumed a sample volume of 10 ml and a transit time of  $\leq 1.5$  sec. The key features of this system are:

- Completely automatic sequencing of each rabbit throughout the system.
- Automatic self-loading and unloading of samples without operator attention.
- Accurate preselection of irradiation, decay, and counting intervals.
- Recycle capabilities (up to 100 times) for identical irradiation, decay, and counting regimes.
- Simultaneous sequencing of two samples (dual mode) through identical regimes by using two sample irradiation positions and one counting position.
- Completely automatic control of the multichannel analyzer for accumulating gamma ray spectra, storing data on magnetic tape, and automatically routing spectra into the appropriate analyzer memory location for dual mode operation.
- A data control interface which allows the counting mode (delayed neutron and/or gamma counting) to be preselected and allows delayed neutron data to be automatically routed to a scaler and gamma data to a multichannel analyzer.
- An automatic system abort mode (with audio and visual alarms and system depressurization if a rabbit should fail to complete a selected path).
- Visual display of the next function to be undertaken by the control unit and current location of all rabbits in the system.

- A display indicating the number of cycles completed for each rabbit being irradiated and digital readout of the irradiation, decay, and counting times.
- Air-cushioning of samples upon arrival at all locations within the system.
- Exhaust of all air used within the system to laboratory exhaust system.

The transport system is shown schematically in Figure 16.

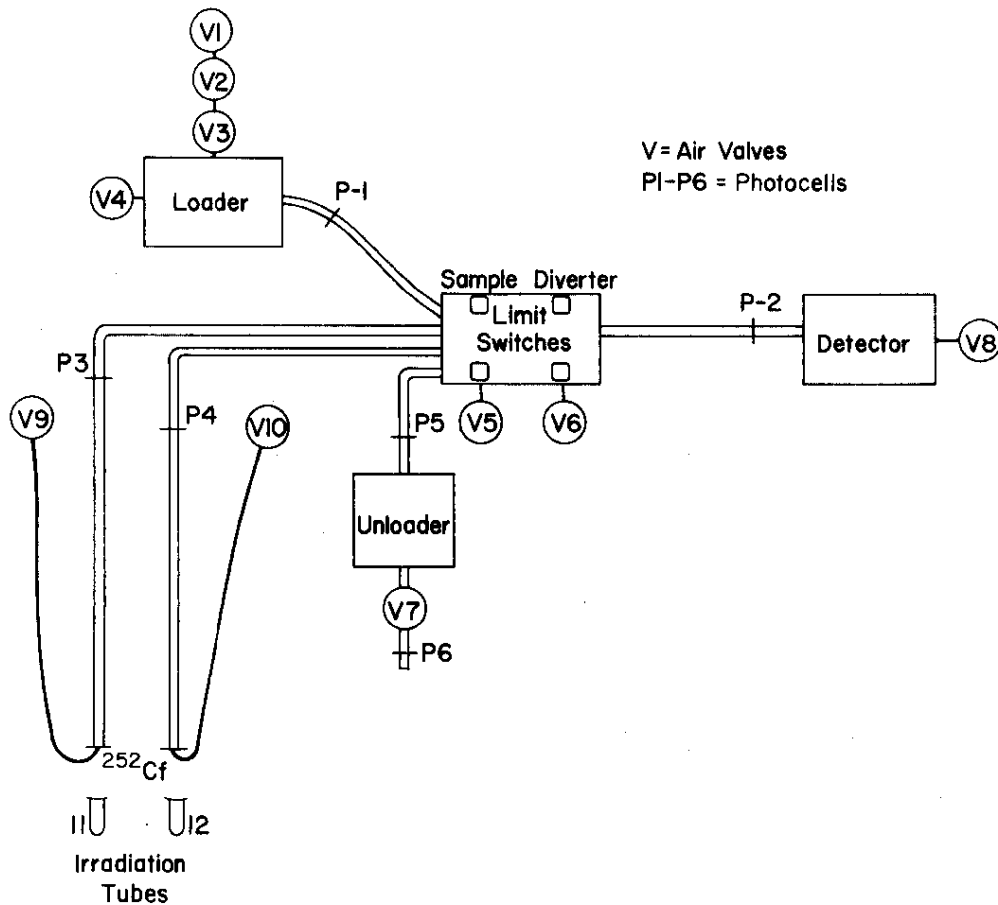


FIGURE 16. Schematic of Rabbit System

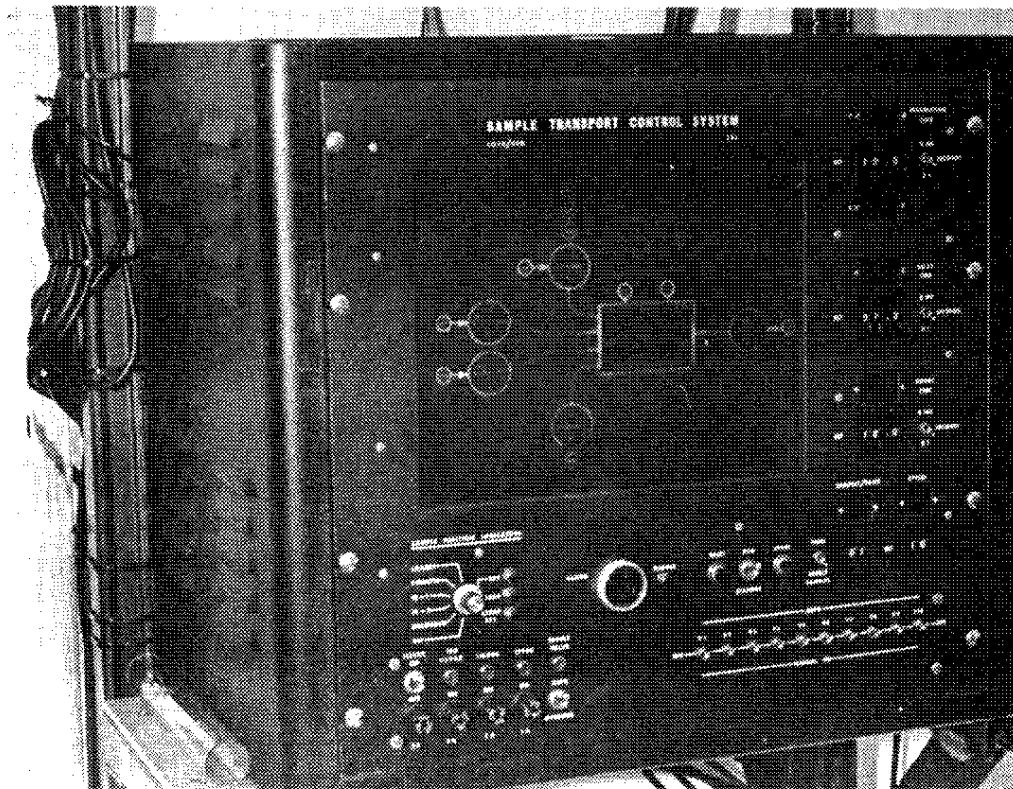


FIGURE 17. Sample Transport Control Unit

Figure 17 is a photograph of the sample transport control unit. The transport system consists of the following hardware in addition to the control unit:

- Two irradiation tubes which are used to transport and position the samples near the four sources.
- An automatic rabbit loader.
- An automatic rabbit unloader.
- A detection end observed by a  $\text{Ge}(\text{Li})$  detector and/or a delayed neutron detector.
- A four-way sample diverter which connects the detector site to the other portions of the system.
- Two air valves, V5 and V6, which actuate the switching in the four-way diverter.
- Four limit switches which verify the state of the four-way diverter.

- Four air valves, V4, V8, V9, and V10, which propel the rabbits from location to location.
- Three loading valves, V1, V2, and V3, which load samples into the system one at a time; and a ball valve, V7, which unloads samples after sequencing at the unloader.
- Six photocells P1-P6, which signal rabbit passage at key locations.

Sequencing is accomplished with stepping relays. Table 1 lists timers in the functional control unit. All timers are crystal-controlled oscillators, which provide both high accuracy and stability in the timing of analysis regimes. A single-cycle regime (load, irradiate, count, and unload), proceeds as follows:

TABLE 1

Timers in the Functional Control Unit

<i>Timer</i>	<i>Function</i>
T1	Irradiation timer for Tube I1
T2	Delay timer for Tubes I1 and I2
T3	Counter timer
T4	Irradiation time for Tube I2

- Valves 1 and 2 (V1 and V2) sequence, one rabbit is dropped beyond opening of V4 verified by a signal from photocell 1 (P1), and analyzer memory is cleared.
- V3 seals the loader end of the transport line and permits V4 to be activated. The rabbit is then propelled through the previously positioned four-way diverter box (V5 and V6 off verified by L1-L4) to the detector site.
- A signal from P2 confirms passage of the rabbit, actuates V5 (which selects irradiation tube I1 for next path), and permits actuation of V8 (which fires the rabbit toward the  $^{252}\text{Cf}$  source through irradiation tube I1).
- A P3 signal closes V8 and starts the irradiation timer (T1).
- At end of T1, V9 is actuated, P3 starts decay timer T2, and P2 closes V9 and opens V5 and V6 (which selects unloader for next path).

- At end of T2, the analyzer or the scaler-timer and count-timer T3 are activated by the Data Control Module.
- At end of T3, the analyzer or scaler-timer records or prints out counting data. V8 is actuated (P5 signals closure of V8 and opens V7; P6 signals closing of V7).
- At the end of the analyzer or printer readout, the control unit is automatically reset to the beginning of the next cycle.
- After the next rabbit is loaded, V4 clears the analyzer memory.

If a rabbit should get stuck in the system, no signal will be received by the photocell at the destination. If this signal is not received within 15 sec after valve firing, the control unit alarms (audibly and visually) and shuts off the main air supply. No additional action can be taken by the system without operator intervention.

As described above, a single rabbit irradiation uses only one function at a time, i.e., one irradiation tube (and timer), decay timer, or detector (count timer). In the dual mode of operation, two rabbits may be analyzed concurrently, if the sum of the times on T2 and T3 is less than the time on T1. In concurrent analyses:

- Rabbit 1 is loaded into the system and moved to irradiation in irradiation tube I1 (and starts T1), and Rabbit 2 is immediately loaded into the detector site.
- Just before T1 counts down, Rabbit 2 is moved to irradiation tube I2, and the irradiation timer (T4) for tube T2 is started.
- When T1 counts down, Rabbit 1 is transferred to the detector, and T2 and T3 are started.
- When T3 counts down, Rabbit 1 stays at the detector until just before T4 counts down. Then Rabbit 1 is transferred back to irradiation tube I1 for its second irradiation (or to unload at the end of the regime).
- When T4 counts down, Rabbit 2 is transferred to the detector, and T2 and T3 are started.
- The system is now in the same configuration as in Step 1, and both rabbits can now be recycled.

The data are routed into the appropriate location in the analyzer memory depending on the status of T1. If T1 is counting, Rabbit 2 is at the detector, and the spectrum is stored in one part of memory. If T1 is not counting, Rabbit 1 is at the detector and the spectrum is stored in another part of memory. Both spectra are retained in memory until Rabbit 2 is unloaded. When Rabbit 2 is unloaded, the analyzer output mode begins.

## DETECTION APPARATUS

### Gamma-ray Detectors

Most activation products are gamma-ray emitters; therefore, emphasis is placed on detecting these gamma-rays with efficiency and with highest resolution. Two practical detector types currently available commercially are NaI and Ge(Li). NaI detectors have higher efficiency and lower resolution than Ge(Li) detectors. Ge(Li) detectors are normally used except when the gamma-ray energy is very high ( $>4$  MeV) or when only one element with a simple (1 or 2 steps) gamma-ray decay scheme is only weakly activated.

#### *Ge(Li) Detectors*

Many laboratories use Ge(Li) detectors for activation analysis; however, the comparative technique uses only the ratio of detector responses. With the absolute technique used at SRL's neutron activation analysis facility, the detector must be accurately calibrated for detector efficiency vs energy for each sample-detector arrangement used (such as sample-detector distance and sample size).

Two Ge(Li) detectors are currently used in the  $^{252}\text{Cf}$  neutron activation analysis facility. One detector is a Canberra Industries\* detector of 15% efficiency relative to a 3x3-inch NaI detector and of 2.04 keV FWHM (full width at half-maximum) resolution at 1332.495 keV. This detector is used exclusively for drop tube sample counting, and it has three detector-sample arrangements for which absolute efficiency vs. energy calibrations have been performed (identified as positions 01, 04, and 05). The other detector is a Princeton Gamma Tech\*\* detector of 16% efficiency and a resolution of 1.88 keV FWHM at 1332.495 keV. This detector is used exclusively in the rabbit system, and it has two detector-sample arrangements for which absolute efficiency vs. energy calibrations have been made (positions 03 and 06).

\* Canberra Industries, Meriden, CN

\*\* Princeton Gamma Tech, Inc., Princeton, NJ

These absolute efficiency curves are stored as EFFCAL data files on disk with the IBM 360/195 computer. The EFFCAL data files are listed in Appendix, Table A-6.

The absolute efficiency vs. energy curve for each detector-sample arrangement is determined in a two-step process. First, the general shape of the curve (log efficiency vs. log energy) is determined by counting nuclides such as  $^{182}\text{Ta}$ ,  $^{169}\text{Yb}$ ,  $^{125}\text{Sb}$ ,  $^{133}\text{Ba}$ , and  $^{166\text{m}}\text{Ho}$ . These isotopes have complex decay schemes which yield a distribution of abundant gamma rays with well-known energies and relative intensities. Second, National Bureau of Standards Reference Materials (absolute gamma ray standards) are counted to determine several absolute log energy vs. log efficiency points. The relative and absolute data are combined to produce an efficiency curve for each counting arrangement.

When one of these nuclides is used as a calibration source, the efficiency calibration curve is determined as follows: 1) spectra are accumulated with at least 10,000 net counts in the photopeaks, 2) the photopeak areas are determined in the same manner that any sample spectrum is analyzed, 3) the relative detector efficiency is calculated by dividing the relative gamma-ray intensity by the photopeak area, 4) for each source, the logarithm of the relative efficiency is plotted against the logarithm of the gamma-ray energy, 5) these plots are superimposed and the best single relative curve is constructed, 6) because no single theoretical function adequately describes the data, the curve is drawn by hand and not determined by computer least squares analysis.

A certified calibration source converts the relative efficiency curve to an absolute curve. One of the best sources is available from the National Bureau of Standards (NBS 4243E). It consists of a solution containing accurately known quantities of  $^{109}\text{Cd}$ ,  $^{57}\text{Co}$ ,  $^{139}\text{Ce}$ ,  $^{203}\text{Hg}$ ,  $^{113}\text{Sn}$ ,  $^{85}\text{Sr}$ ,  $^{137}\text{Cs}$ ,  $^{60}\text{Co}$ , and  $^{88}\text{Y}$ . This solution is packaged in a container identical to those used for samples, and spectra are collected. Absolute detector efficiencies are determined for these gamma rays. The relative curve is then scaled so that it best intersects with these absolute points.

For computerized data reduction, these efficiencies are listed for selected energies. The computer interpolates the efficiency for a desired energy by using a second-order least-squares fit to the four nearest log efficiency-log energy points.

Table A-6 lists the absolute efficiencies used in the  $^{252}\text{Cf}$  facility. The first block contains the selected energies, and the second block contains the corresponding reciprocal of the absolute counting efficiency.



### NaI Detector

A NaI detector is also used for gamma-ray detection for specific analyses. For oxygen analysis, the 6.2-MeV gamma-ray from the  $^{16}\text{O}(\text{n},\text{p})\ ^{16}\text{N}(\text{T}_{1/2} = 7.11 \text{ sec})$  activation reaction product is the most sensitive indicator. For such analyses, a 3x3-inch NaI detector\* with 6.5% resolution at 662 keV is used with the rabbit system. For analyses where only one element is activated and a product emits only one gamma-ray, the NaI detector in the secondary shielded vault provides maximum gamma-ray detection sensitivity and lowest possible detection limit. No absolute activation analyses are performed routinely with the NaI detector.

### Delayed Neutron Detector

Many samples from plant processes require analysis for fissile isotopes such as  $^{235}\text{U}$ ,  $^{239}\text{Pu}$ , and natural uranium. The most specific and sensitive method for such analyses is to detect beta-delayed neutron decay. A high-efficiency (12% absolute) assembly was designed and constructed to detect neutrons with energy distributions characteristic of beta-delayed neutron emitters. Twelve tubes (92%  $^{10}\text{BF}_3$  at 70 cm pressure) are symmetrically arranged around the sample. High-density polyethylene is used to thermalize the neutrons for most efficient detection. The average delayed neutron has an energy of ~500 keV; thus, only 4.12 cm of moderator is required between source and detectors. In the shielded facility, the neutron detector background averages only 4 counts/min. Cyclic irradiation and delayed neutron counting are optimized for analysis of different fissile materials.

### SAMPLE PREPARATION FACILITIES AND PROCEDURES

Because of the sensitivity of activation analysis, samples are prepared for irradiation in a clean environment. A clean bench and a clean fume hood (Agnew Higgins) provide a Class 100 environment for sample preparation.

Samples are weighed on an auto-taring, rapid-readout Mettler Model H-64 balance with a sensitivity of 10  $\mu\text{g}$  over a 160-g range. Solid samples are weighed into pre-cleaned polyethylene rabbits; liquid samples are pipetted.

Frequently, the physical forms of samples are changed before irradiation. These changes include:

---

\* Bicorn, Incorporated, Cleveland, OH.

- Grinding of samples to reduce particle sizes.
- Blending of small samples.
- Freeze drying of biological samples.
- Compaction of samples into pellets (especially freeze-dried samples).
- Moistening of all powdered samples with enough water to complete the 10-cc volume followed by vortexing to ensure complete mixing.

All of the above are done in a clean environment.

Ion exchange concentration procedures were developed especially for analysis of very dilute solutions. These procedures involve batch-contacting of 1 liter of the dilute aqueous solution with equal equivalent amounts of mixed cation-anion exchange resins. Detection sensitivities are improved 100-fold for almost every element dissolved in the water by direct activation analysis of the resin. With this technique, 5 ppb of natural uranium in water can be detected. The resin was specially purified by BioRad Laboratories, Richmond, CA.

## BASIC PRINCIPLES OF $^{252}\text{Cf}$ NEUTRON ACTIVATION ANALYSES

### ABSOLUTE ACTIVATION ANALYSIS

One of the unique features of the  $^{252}\text{Cf}$  neutron activation analysis facility is that it can perform rapid multielement analyses without the routine use of comparative standards. In the absolute technique, the master equation of activation analysis is used to relate a measured detector response to the multielement concentration of the sample. Many factors enter into the absolute calculation of detector response. These factors include absolute decay data, sample weight, experimental irradiation, decay, and counting times; absolute detection efficiency; and, most important, elemental neutron capture reaction rates, which are calculated from measured flux and cross section data.

During irradiation of a sample, the instantaneous change in the number of atoms of some activated product species ( $N$ ) present in the sample is:

$$\frac{dN}{dt} = (\text{rate of production}) - (\text{rate of decay}) = r - \lambda N \quad (1)$$

where

$\lambda$  = decay constant of the product,  $\text{sec}^{-1}$

$r$  = production rate, atoms/sec

Integrating this equation over the irradiation time (from 0 to  $T_1$ ) yields

$$N_1 = \frac{r}{\lambda} [1 - \exp(-\lambda T_1)] = \frac{rS}{\lambda} \quad (2)$$

where

$T_1$  = irradiation time, sec

$N_1$  = number of product atoms present at  $T_1$

$S = [1 - \exp(-\lambda T_1)]$ ; the irradiation saturation factor

If the sample is removed from the neutron flux at  $T_1$  and then allowed to decay during time,  $T_2$ , the number of atoms remaining at the end of  $T_2$  is

$$N_2 = N_1 \exp(-\lambda T_2) = \frac{rSD}{\lambda} \quad (3)$$

where

$D = \exp(-\lambda T_2)$ ; the decay factor.

At the end of  $T_2$ , the sample is counted for a time,  $T_3$ .  
At the end of  $T_3$ , the number of product atoms remaining is

$$N_3 = N_2 \exp(-\lambda T_3) \quad (4)$$

The number of atoms which decayed during the counting period is given by

$$\Delta N = N_2 - N_3 = N_2 [1 - \exp(-\lambda T_3)] = \frac{rSDC}{\lambda} \quad (5)$$

where

$C = [1 - \exp(-\lambda T_3)]$ , the counting factor.

The number of counts  $G$  observed by the detector is

$$G = EI\Delta N \quad (6)$$

where

$E$  = the absolute detector efficiency for the gamma ray counted

$I$  = the absolute decay abundance of the radiation, number of gamma rays emitted per decay.

Thus, the number of counts observed for an activated species found in a single irradiation-decay-count cycle is given by

$$G = \frac{EIrSDC}{\lambda} \quad (7)$$

## CYCLIC ACTIVATION AND COUNTING

Cyclic activation and counting is used to enhance the sensitivity of analyses of short-lived species. Because the production and decay rates are the same at saturation, and because saturation is achieved quickly for short-lived product species, detection sensitivity does not increase when the irradiation and counting intervals are increased beyond a few half-lives. In fact, for analysis times which are much larger than the product half-life, a significant gain in detection sensitivity is achieved by cyclically activating and counting a sample several times during the analysis.

As in Equations 2-4,  $T_1$ ,  $T_2$ , and  $T_3$  are the irradiation, decay, and counting intervals, respectively. If  $T_4$  is defined at the time required to transport the sample from the counter back into the neutron flux, then the total time required for each cycle is

$$T_c = T_1 + T_2 + T_3 + T_4 \quad (8)$$

For the first cycle,  $G$  counts are recorded. For the second cycle,  $G$  counts are accumulated from the second irradiation, and  $G \exp(-\lambda T_c)$  counts are accumulated from the activity remaining from the first irradiation. For the third cycle,  $G$  counts are accumulated from Irradiation 3,  $G \exp(-\lambda T_c)$  counts are accumulated from Irradiation 2, and  $G \exp(-\lambda T_c) \exp(-\lambda T_c)$  counts are accumulated from the activity remaining from the first irradiation. The number of counts accumulated during the counting time for each cycle is

<i>Cycle</i>	<i>Counts</i>
1	$G$
2	$G + GQ$
3	$G + GQ + GQ^2$
4	$G + GQ + GQ^2 + GQ^3$
:	:
.	.
M	$G + GQ + \dots GQ^{M-1}$

where

$$Q = \exp(-\lambda T_c)$$

The total time required for the cyclic analysis is

$$T_A = MT_c \quad (9)$$

Thus, after  $M$  cycles, the total number of counts  $K$  collected is the sum of the counts for each cycle, or

$$\begin{aligned} K &= MG + (M-1)GQ + (M-2)GQ^2 + \dots GQ^{M-1} \\ &= G [M + (M-1)Q + (M-2)Q^2 + \dots Q^{M-1}] \end{aligned}$$

The finite series in brackets may be expressed as the difference between two infinite series (which are each expansions of analytical expressions) as follows:

$$M + (M-1)Q + (M-2)Q^2 + \dots + Q^{M-1} = \frac{M}{1-Q} - \frac{Q(1-Q^M)}{(1-Q)^2} = F \quad (10)$$

Replacing this series by F yields

$$K = GF$$

By substitution, the number of counts recorded during a cyclic irradiation and counting regime is

$$K = \frac{E I r S D C F}{\lambda} \quad (11)$$

For a fixed total analysis time  $T_A$ , K would be maximized when the irradiation and counting times are equal ( $T_1 = T_3$ ) and when the transit times  $T_2$  and  $T_4$  are zero. For a given total analysis time  $T_A$  and finite values for  $T_2$  and  $T_4$ , there is a particular number of cycles for which K is a maximum. The analysis procedure is optimized with this equation for a given isotope.

A maximum total analysis time is usually determined by the number of samples to be analyzed within a certain time period.  $^{46}\text{mSc}$ , with an 18.7-second neutron capture product, is a good example to demonstrate the effect of optimized cyclic activation and counting regimes. The maximum analysis time is assumed to be 200 seconds, the irradiation and counting intervals are assumed to be equal, and the sample transfer times are assumed to be 1.0 second. The curve in Figure 18 shows the relative number of  $^{46}\text{mSc}$  counts as a function of the number of cycles calculated from Equation 11. The experimental response was determined with a scandium standard; the response is normalized to the calculated curve. The optimum number of cycles is about 4; thus, the irradiation and counting intervals for maximum sensitivity is 24 seconds for the assumed analysis conditions.

### Cyclic Sensitivities

Table 2 compares interference-free detection limits calculated for elements which yield short half-life neutron activation products suitable for analysis when irradiated. For single-cycle manual irradiation, the calculation was based on the most sensitive isotope that can be produced by activating that element regardless of half-life. The maximum analysis time allowed was 190 hours. For 100-cycle automatic irradiation, the calculation was based on the cyclic activation product indicated. The maximum analysis time allowed was 16 hours. For the elements fluorine through cobalt, the advantages of cyclic activation are that both analysis time and detection limits are greatly improved. For other elements,

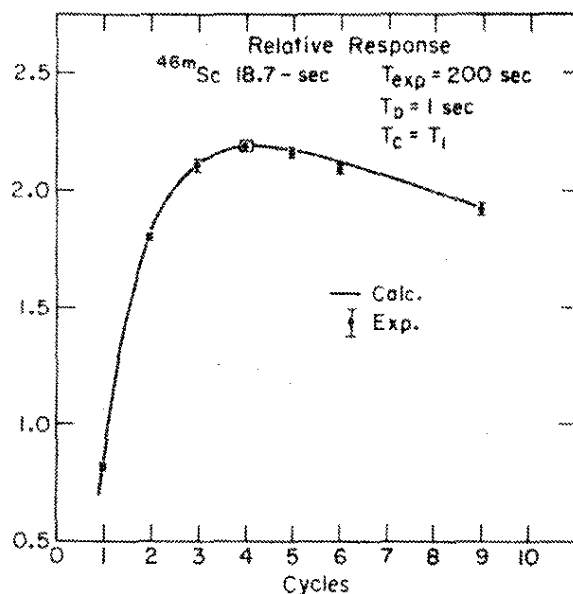


FIGURE 18. Relative Detector Response for Cyclic Activation of Scandium

TABLE 2

Sensitivity of Cyclic Activation with 17 mg  $^{252}\text{Cf}$  Source

Element	Cyclic Activation Product	Single Cycle Manual		100-Cycle Automatic	
		Limit, $\mu\text{g}$	Time, hr	Limit, $\mu\text{g}$	Time, hr
F	11.1-s $^{20}\text{F}$			800	0.7
In	14.2-s $^{116}\text{In}$			20	0.8
Se	17.5-s $^{77\text{m}}\text{Se}$	0.9	190	0.6	1.1
Dy	1.24-m $^{165\text{m}}\text{Dy}$	3	26	0.2	4.2
Gd	3.67-m $^{161}\text{Gd}$	10	26	3	12
Cu	5.1-m $^{65}\text{Cu}$	80	26	5	16
Co	10.5-m $^{60\text{m}}\text{Co}$	0.6	190	0.1	16
Sc	18.7-s $^{46\text{m}}\text{Sc}$	0.02	190	0.3	1.1
Br	17.4-m $^{80}\text{Br}$	0.2	53	0.4	1.6
$^{235}\text{U}$	Delayed Neutron	1.3	0.1	0.03	1.2
Ag	24.6-s $^{110}\text{Ag}$	60	0.6	1.0	1.4
Rh	42-s $^{104}\text{Rh}$	600	0.2	20	2.4
Al	2.24-m $^{28}\text{Al}$	60	0.5	2	7.5
V	3.76-m $^{52}\text{V}$	3	0.9	0.09	13
Ti	5.77-m $^{51}\text{Ti}$	250	1.3	10	16
Nb	6.27-m $^{94\text{m}}\text{Nb}$	3400	1.5	130	16
Ca	8.7-m $^{49}\text{Ca}$	5000	2.0	290	16
Mg	9.4-m $^{27}\text{Mg}$	1700	2.2	100	16

the particular experimental requirement on analysis time or detection limit will determine whether cyclic activation is used. For both scandium and bromine, the analysis time is greatly reduced, but the detection limit is somewhat higher. For silver through magnesium, the analysis times are increased, but the detection limits are improved. All calculations in Table 2 assume a 17-mg  $^{252}\text{Cf}$  source and a flux of  $3.5 \times 10^8$  n/(cm<sup>2</sup> sec).

## MASTER EQUATION

A master activation analysis equation can be derived from the rate of production shown in Equation 11, r, which may also be expressed as

$$r = nR \quad (12)$$

where

n = number of parent (target) atoms present in the sample,  
and

R = specific neutron capture reaction rate leading to the  
product [captures/(sec-atom)]\*

The number of target atoms in the sample of weight, W in grams, containing P parts per million of that element is

$$n = \frac{P W B N_0}{10^6 A} \quad (13)$$

where

B = isotopic abundance of parent nuclide

A = atomic weight of parent nuclide

$N_0$  = Avagadro's number

Substituting Equations 12 and 13 into Equation 11 gives

$$K = \frac{N_0 P W B E I S C D F R}{10^6 A \lambda} \quad (14)$$

---

\* The ability to predict the specific neutron capture reaction rate by calculation is the basis of the absolute technique and is discussed in later sections.



solving for P

$$P = \frac{K A \lambda 10^6}{W B E I N_0} \cdot \frac{1}{S D C F} \cdot \frac{1}{R} \quad (15)$$

Equation 15 is the master activation analysis equation. As with most equations which are derived for nuclear processes, simplifying assumptions have been made to reduce the complexity of the expression. The assumptions implied in the preceding derivation and the range of applicability of this master equation are as follows:

- The fraction of target nuclei activated during the total irradiation is very small, i.e., target burnup is neglected. This assumption is realistic if  $nRT_1 \ll 1$  (which is true except for very high neutron fluxes, very large cross sections, and/or very long irradiations).
- Multiple neutron captures are neglected, i.e., product burnup is neglected.
- R is constant over the total irradiation time. This assumption may not be valid for reactor activation because both the neutron flux magnitude and energy distribution change as a function of power level and fuel burnup. For isotopic neutron sources, this condition is met if the total irradiation time is a small fraction of the source half-life. In the 100-mg  $^{252}\text{Cf}$  facility, a maximum irradiation time of 14 days is normal; therefore, the decrease in flux is  $<1\%$  during irradiation.
- The detector and associated electronics have negligible dead time. This condition can be met by using small samples or by counting the sample at low detection efficiency. If these steps are undesirable, there are electronic procedures which allow for dead time compensation.
- The time of transit of samples into and out of the flux is very short compared to the irradiation time. This condition is generally met with manual irradiation because only long-lived species are being considered. Using the rabbit system, transit times are reduced by increasing the transport velocity.

In practice, Equation 15 is solved by computer. As discussed earlier, specific neutron capture reaction rates, R, are calculated from the moderated  $^{252}\text{Cf}$  fission neutron spectrum, an important feature in the absolute technique.

#### SPECIFIC NEUTRON CAPTURE REACTION RATES

Each nucleus has a neutron capture cross section,  $\sigma$ , which is an effective area of interaction with a point neutron moving

at some speed  $s$ . The number of neutrons passing through (into and out of) an area per unit time is the flux  $\phi$ . The specific neutron capture reaction rate can be expressed as the product

$$R = \sigma \phi$$

Both  $\sigma$  and  $\phi$  are functions of the neutron speed, such that

$$R = \int [\sigma(s) \phi(s)] ds \quad (17)$$

The flux may be expressed as a speed distribution

$$\phi(s) = n(s) s \quad (18)$$

Where  $n(s)$  is the number of neutrons per unit volume having speed  $s$ .

Thus

$$R = \int [\sigma(s) n(s) s] ds \quad (19)$$

To date no analytical functions accurately describe either  $\sigma(s)$  or  $n(s)$  for any real experiment. Two approaches to approximating  $R$  have developed: 1) multigroup summations, and 2) analytical function approximations.

#### Multigroup (84-group) Summation

Equation 19 may be expressed by a sum of many integrals over small regions of  $s$  by

$$R = \sum_{i=1}^M \int_{s_i}^{s_{i+1}} [\sigma(s) n(s) s] ds \quad (s_1 = 0; s_{m+1} = \infty) \quad (20)$$

If  $M$  is large and the neutron distribution is smooth between  $s_i$  and  $s_{i+1}$ , each rate may be expressed by

$$R_i = \phi_i \bar{\sigma}_i \quad (21)$$

where

$\phi_i$  = the flux in group  $i$  (number of neutrons/(cm<sup>2</sup>-sec) with speeds between  $s_i$  and  $s_{i+1}$ , and

$\bar{\sigma}_i$  = the average cross section over the neutron speed range.

Each  $\bar{\sigma}_i$  is obtained by weighting  $\sigma(s)$  by some function of  $s$  for each speed group. In practice,  $\sigma(s)$  is calculated from a measured smooth cross section component and the measured resonance parameters superimposed on this smooth component;  $\sigma(s)$  is then weighted by the

microscopically smooth flux distribution (in 84 speed groups) supplied for the rate calculation. The 84-group approximation assumes that the flux distribution within a speed group is microscopically smooth and that the cross section retains its resonance fluctuations. The description of the microscopic cross section requires a large number of parameters for each nuclide. Unfortunately, only a limited number of nuclides has been studied in detail sufficient to provide all these data; even more unfortunate is the fact that, of the well-studied nuclides, only a few of interest to activation analysis have their parameters coded into the computer data libraries. The multigroup description of the neutron flux distribution will be discussed later.

### Analytical Function Approximations (2-Group)

The second approach to calculating the specific neutron capture rates is to divide  $R$  into two components, i.e.,

$$R = R_T + R_E = \int_0^{s_0} [\sigma(s) n_T(s) s] ds + \int_{s_0}^{s_1} [\sigma(s) n_E(s) s ds] \quad (22)$$

Where  $R_T$  and  $R_E$  are the thermal and epithermal components to the rate, and  $s_0$  is the speed of the neutrons at the thermal/epithermal boundary (called the cadmium cutoff energy).

By approximating the thermal and epithermal fluxes and the cross section by analytical expression,  $R$  can be expressed as,

$$R = a\sigma_T \cdot \phi_T + b\sigma_E \cdot \phi_E \quad (23)$$

which contains only two parameters for the cross section,  $\sigma_T$  and  $\sigma_E$ , two parameters for the flux distribution,  $\phi_T$  and  $\phi_E$ , and two constants  $a$  and  $b$ . The analytical functions which are normally assumed are listed below:

- The thermal flux  $n_T(s)$  is Maxwellian, i.e.

$$n_T(s) = \frac{4m}{\sqrt{\pi}} \frac{s^2}{s_T^3} \exp(-s^2/s_T^2) \quad (24)$$

where

$$s^2 = 2kT/m$$

$T$  = moderator temperature, °K

$m$  = neutron mass, g

$k$  = Boltzmann constant

$s_T$  = the most probable thermal speed  
(where  $dn_T(s)/ds = 0$ )

- The cross section is proportional to  $\frac{1}{s}$ , (usually expressed as  $1/v$ )

$$\sigma(s) = \sigma_0 s_0 / s \quad (25)$$

where

$s_0$  is some standard speed, usually 2200 m/s ( $s_T$  at 293°K)

$\sigma_0$  is the  $\frac{1}{s}$  cross section at  $s_0$  (usually  $\sigma_{2200}$ )

- The epithermal flux is proportional to  $\frac{1}{s^2}$  (usually expressed as  $\frac{1}{E}$  such that

$$\int_{s_0}^{s_1} [\sigma(s) n(s) s] ds = k \int_{s_0}^{s_1} \frac{\sigma(s) ds}{s} = K I \quad (26)$$

where

$I$  is the so-called resonance integral, which is the average epithermal cross section weighted by the  $\frac{1}{s^2}$  flux spectrum, and

$$K = \beta \phi_E$$

$\phi_E$  = the epithermal flux ( $s > s_0$ ), and

$$\beta = \ln \frac{E_1}{E_0} \text{ (if } \phi \propto \frac{1}{s^2} \text{ and } \sigma(s) \propto \frac{1}{s} \text{)} \quad (27)$$

With these assumed functions, the two-group specific neutron capture reaction rate  $R$  is

$$R = \alpha \sigma_{2200} \phi_T + \beta I \phi_E \quad (28)$$

where

$$\alpha = \left( \frac{\pi}{4} \frac{T_0}{T} \right)^{1/2} = 0.886 \text{ if } T = T_0 = 293^\circ\text{K}$$

$$\beta = 0.0603 \text{ if } E_0 = 0.625 \text{ eV; } E_1 = 10 \text{ MeV, or}$$

$$\beta = 0.0597 \text{ if } E_0 = 0.4 \text{ eV; } E_1 = 10 \text{ MeV}$$

(choice of  $E_0$  depends on the values used to determine  $\phi_E$  and  $I$ )

The applicability of the two-group technique to calculations of R for nuclei in real fluxes is reasonable within rather strict limitations:

- Epithermal resonances should be small and evenly spaced (in  $\frac{1}{E}$ ) for maximum  $R_E$  accuracy.
- Nuclides with resonances below  $E_0$  (subcadmium resonances) will not be properly calculated, i.e.,  $^{239}\text{Pu}$ .
- The epithermal flux must be proportional to  $\frac{1}{E}$  to properly account for the epithermal contribution to R. (An additional approximation which treats  $\beta$  as a variable may be used for non- $\frac{1}{E}$  fluxes.)
- Reactions which have thresholds [most neutron-induced reactions except (n, $\gamma$ ) reactions] cannot be treated by the two-group approximation.

## NEUTRON FLUX CALCULATIONS

To accurately predict absolute neutron capture reaction rates, the moderated neutron energy spectrum and flux at the sample irradiation site must be calculated. As described earlier, these flux and spectrum calculations and the multigroup (2 or 84) cross section data form the basis of the absolute technique used in the  $^{252}\text{Cf}$  activation analysis facility. The results of the neutron energy spectral calculations will first be discussed for the original 17-mg  $^{252}\text{Cf}$  facility with all  $\text{H}_2\text{O}$  moderator and then for the more-complex 100-mg  $^{252}\text{Cf}$  facility with  $\text{H}_2\text{O}/\text{D}_2\text{O}$  moderator.

### The 17-mg $^{252}\text{Cf}$ Facility

#### *ANISN Calculations*

The neutron transport code ANISN<sup>4</sup> was used to calculate the neutron spectrum in 84 energy groups for the 17-mg  $^{252}\text{Cf}$  facility. Modification of this calculation provided the thermal and epithermal flux in the 2-group reaction rate method. ANISN assumes one-dimensional spherical geometry in calculating neutron transport into and out of moderator and tank material zones (distances) surrounding the source. ANISN also accounts for scattering and absorption in each energy group in these zones. The details of ANISN are outside the scope of this report; however, the results consist of tables of unit neutron fluxes at each zone for each of the 84 energy subgroups. In the design of the source tank hardware, care was taken to approximate the spatial geometry assumption in ANISN: a point source surrounded as nearly as possible with a sphere of moderator. Samples contained in the hexagonal

array of polyethylene irradiation tubes were fixed between solid polyethylene rods to displace air. The source-to-sample distances (center-to-center) for the two concentric rings were 3.81 cm and 10.16 cm. The results of the 84-group neutron spectrum calculation for a single source surrounded by a sphere of water at 298°K is shown in Figure 19. Key features are:

- The large thermal Maxwellian centered at 0.0525 eV (0.0263 eV if plotted  $\phi$  vs E).
- The unmoderated fission spectrum centered at about 2.3 MeV.
- The slightly non-1/E epithermal distribution (especially for the 3.81 cm distance).

For the two-group approximation, which assumes a cadmium cutoff energy of 0.632 eV and a maximum fission neutron energy of 10 MeV, the thermal flux is obtained by summing fluxes  $\phi_i$  in the energy groups below the cadmium cutoff energy. The epithermal flux is obtained by summing fluxes  $\phi_i$  in the energy groups above the cadmium cutoff energy. Plots of  $\phi_T$  and  $\phi_E$  and the ratios of  $\phi_E/\phi_T$  for an all-H<sub>2</sub>O-moderated system are illustrated in Figures 20-22 for the 17-mg <sup>252</sup>Cf facility. For these calculations, a total source emission rate of  $3.51 \times 10^{10}$  neutrons/sec (15 mg of <sup>252</sup>Cf) was used. Note the steep decline in the epithermal-to-thermal flux ratio with a minimum of 0.24 at about 15 cm. The steep decline in flux with distance results in a thermal flux dropoff of ~25% and an epithermal flux dropoff of 33% across an aqueous sample (2.5 cm diameter).

ANISN calculations were also performed for hypothetical cases in which the H<sub>2</sub>O moderator was replaced with spherical regions (30 cm radius) of D<sub>2</sub>O and H<sub>2</sub>O. The calculated changes in  $\phi_T$  and  $\phi_E/\phi_T$  with distance for D<sub>2</sub>O and air are shown in Figures 23 and 24. H<sub>2</sub>O is the most efficient moderator; however, it has a larger absorption cross section than does D<sub>2</sub>O; therefore, a higher thermal flux is observed at distances close to the <sup>252</sup>Cf source (0 to 10 cm) for an all-H<sub>2</sub>O-moderated system. Because the absorption cross section is lower for D<sub>2</sub>O, the decrease in thermal flux with distance is less, and useful sample irradiation region around the source is greater. Figure 24 shows the softer (lower  $\phi_E/\phi_T$  ratio) spectrum achievable with the D<sub>2</sub>O-moderated system at greater distances from the sources. For example, for H<sub>2</sub>O, the minimum ratio is 0.24 at ~15 cm where  $\phi_T \sim 2.5 \times 10^7$  n/(cm<sup>2</sup>-sec<sup>-1</sup>). For D<sub>2</sub>O, at 30 cm from the source, the flux ratio is ~0.08; however, the thermal flux is still  $\sim 3 \times 10^7$  n/(cm<sup>2</sup>-sec).

In the 17-mg <sup>252</sup>Cf facility, absolute thermal neutron flux was determined by irradiating gold wires. Measurements were made across the first irradiation position at distances of 2.72, 3.18,

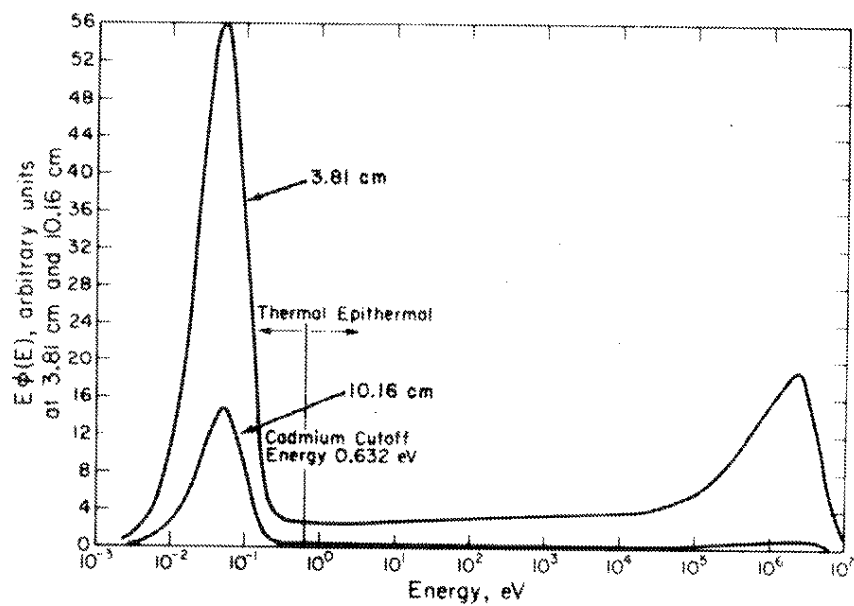


FIGURE 19. Neutron Energy Spectra at 3.81 cm and 10.16 cm as Calculated by ANISN

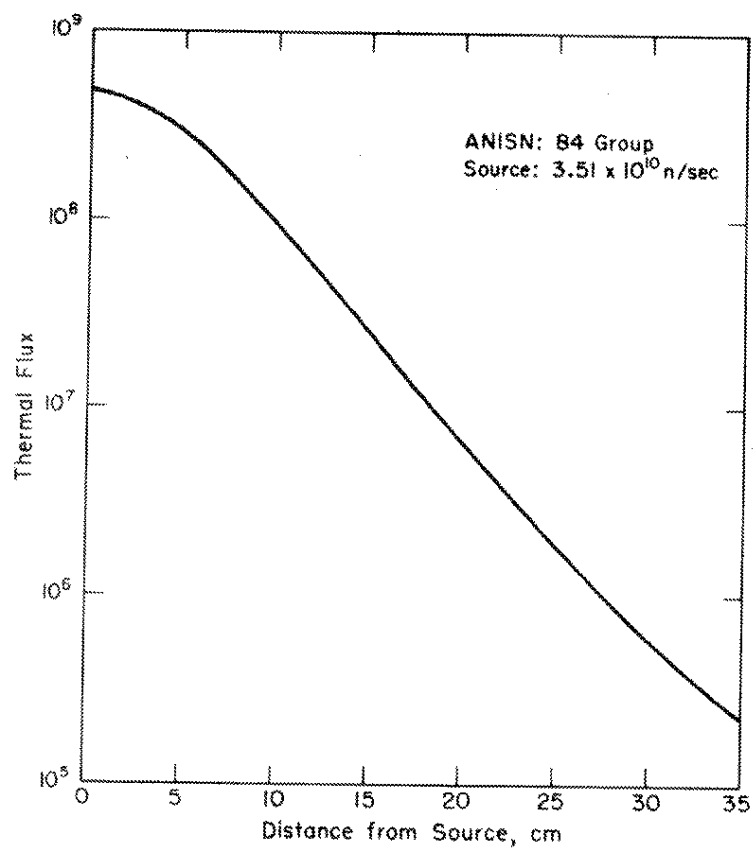


FIGURE 20. Change in Thermal Flux with Distance from Source

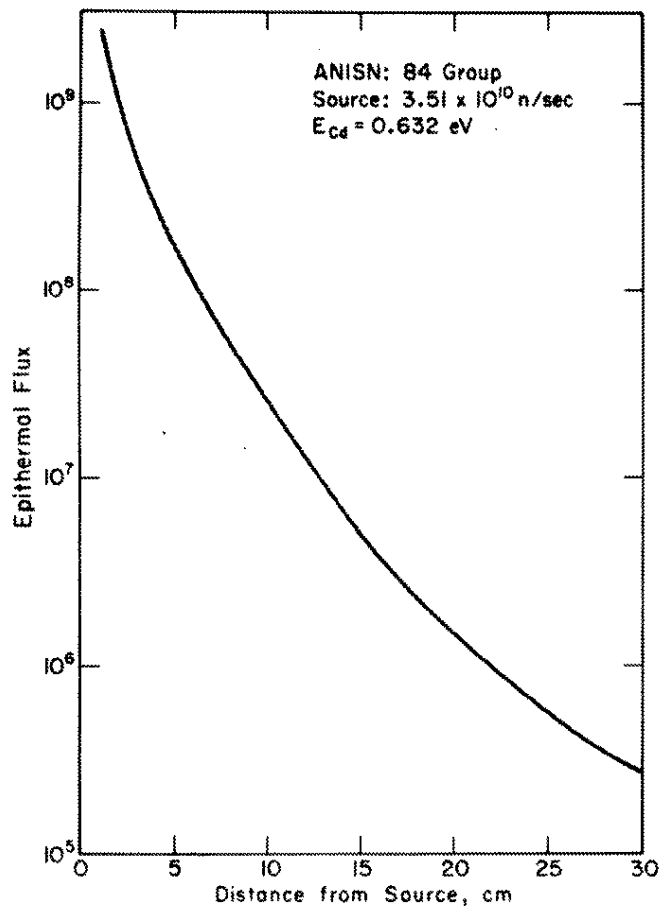


FIGURE 21. Change in Epithermal Flux with Distance from Source

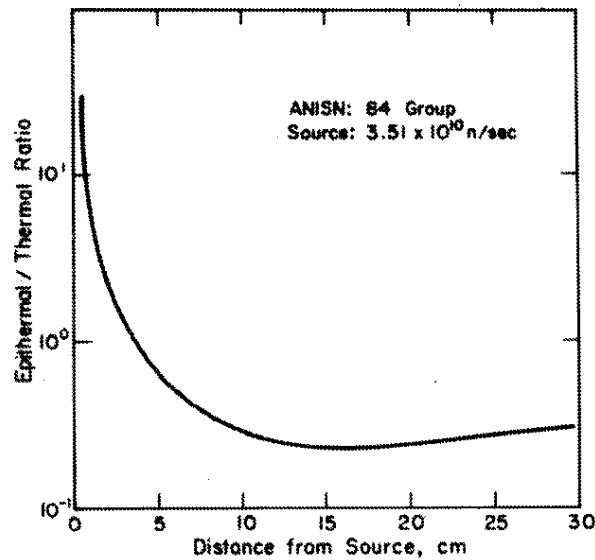


FIGURE 22. Change in Epithermal-to-Thermal Flux Ratio with Distance from Source



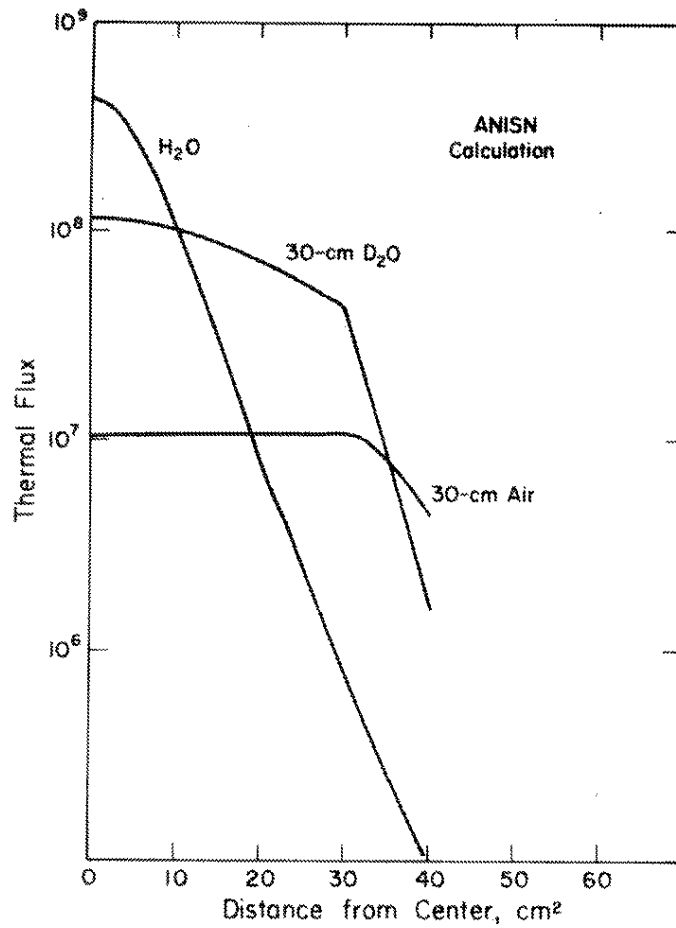


FIGURE 23. Change in Thermal Flux with Distance from Source to Centers of H<sub>2</sub>O, D<sub>2</sub>O, and Air-Moderated Central Regions

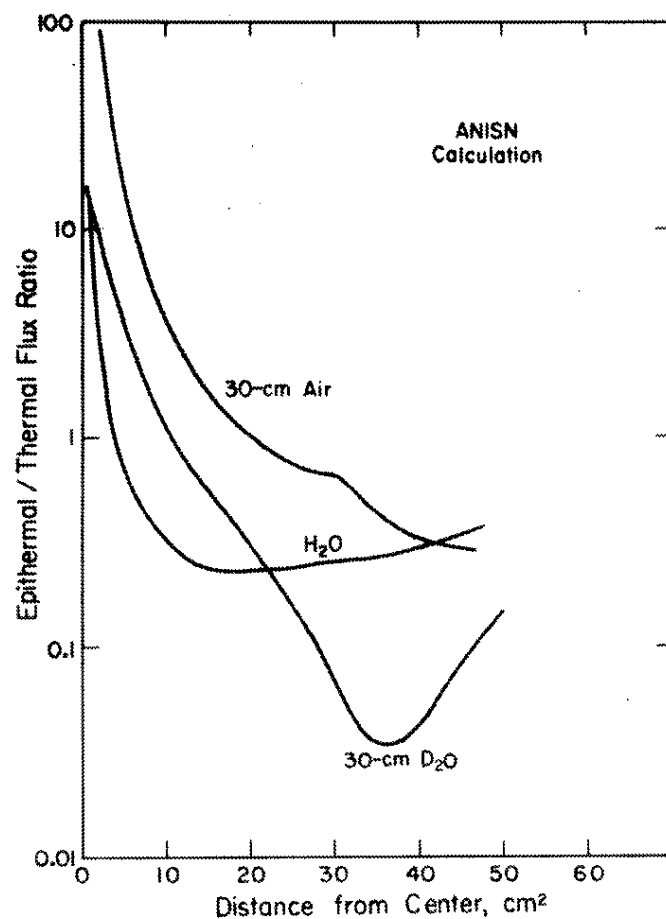


FIGURE 24. Change in Epithermal/Thermal Flux Ratio with Distance from Source for H<sub>2</sub>O, D<sub>2</sub>O, and Air-Moderated Central Regions

3.81, 4.45, and 4.90 cm and at the center of the second and third irradiation tubes at 10.16 and 20.32 cm. Results of these measurements and of integral measurements for standard gold solutions agreed within  $\pm 3\%$  of those calculated by ANISN at the 3.81-cm irradiation position. Agreement was  $\pm 10\%$  at the seldom-used irradiation distances of 10.16 and 20.32 cm. Appendix B summarizes the calculation of flux depression factors for the gold wires used in these experiments. Figure 25 summarizes results of the thermal flux measurements.

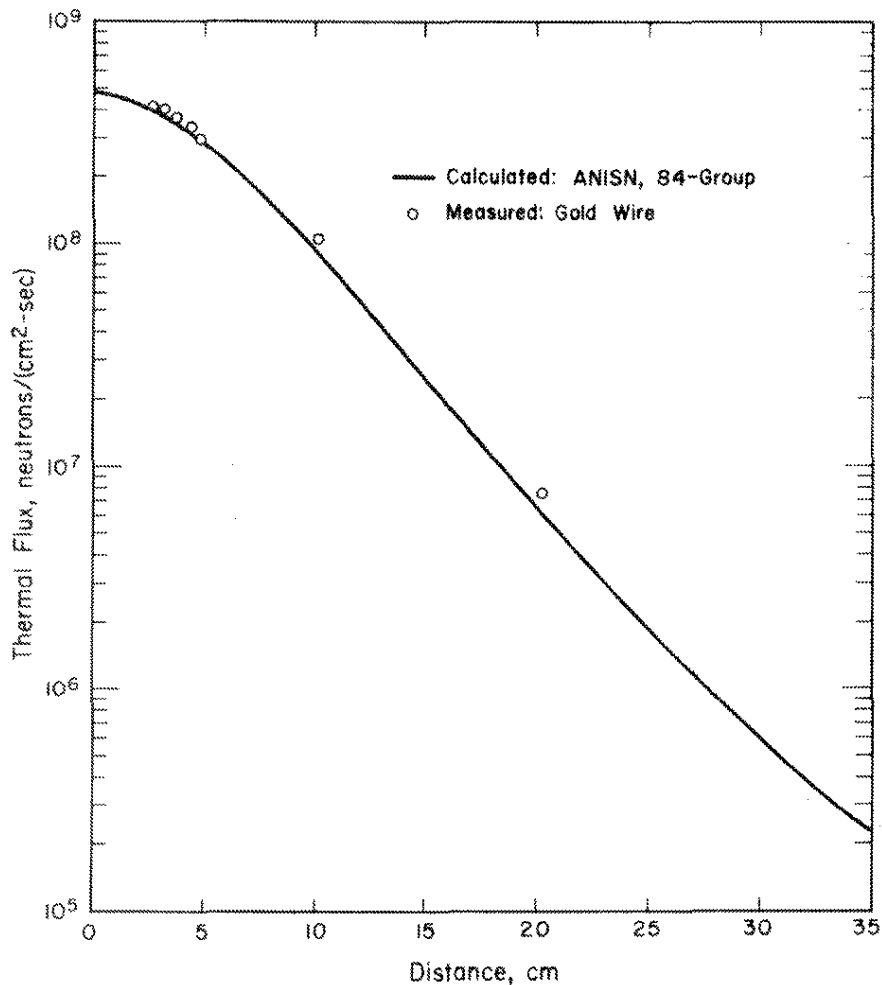


FIGURE 25. Changes in Calculated and Measured Thermal Fluxes with Distance from Source

# Comparison of Calculated and Experimental Reaction Rates

Two-group reaction rates were calculated from Equation 28 for 17 elements (Table 3).

with  $\alpha = 0.886$  (using  $T = 293^\circ\text{K}$ ) and

$\beta = 0.023$  (as experimentally determined using Au and Co standard solutions to account for the non- $\frac{1}{E}$  epithermal spectrum and the unmoderated neutron peak  $E$  at  $\sim 2.1$  MeV)

As described earlier, the 84-group reaction rates were calculated for nine elements from

$$R = \sum_{i=1}^{84} \sigma_i(E) \phi_i(E) \quad (84\text{-group}) \quad (29)$$

TABLE 3

Calculated and Measured Neutron Capture Rates for the 17 mg  $^{252}\text{Cf}$  Facility

Element	Capture Product	Calculated Captures/(sec-mg)		Experimental <sup>a</sup> Captures/(sec-mg)
		84-Group	2-Group	
Au	$^{198}\text{Au}$	$1.27 \times 10^5$	$1.20 \times 10^5$	$1.22 \times 10^5$ ( $\pm 1\%$ )
Al	$^{27}\text{Al}$	$1.45 \times 10^3$	$1.48 \times 10^3$	$1.45 \times 10^3$ ( $\pm 5\%$ )
Dy	$^{165}\text{Dy}$	$2.46 \times 10^6$	$2.82 \times 10^6$	$2.21 \times 10^6$ ( $\pm 5\%$ )
Co	$^{60}\text{Co}$	$1.10 \times 10^5$	$1.13 \times 10^5$	$1.13 \times 10^5$ ( $\pm 2\%$ )
Mn	$^{55}\text{Mn}$	$4.07 \times 10^4$	$4.24 \times 10^4$	$3.84 \times 10^4$ ( $\pm 1\%$ )
As	$^{76}\text{As}$	$1.44 \times 10^4$	$1.35 \times 10^4$	$1.37 \times 10^4$ ( $\pm 1\%$ )
V	$^{52}\text{V}$	$1.56 \times 10^4$	$1.66 \times 10^4$	$1.66 \times 10^4$ ( $\pm 2\%$ )
I	$^{127}\text{I}$	-	$8.26 \times 10^3$	$9.76 \times 10^3$ ( $\pm 5\%$ )
Na	$^{23}\text{Na}$	-	$3.99 \times 10^3$	$3.63 \times 10^3$ ( $\pm 1\%$ )
K	$^{41}\text{K}$	$5.02 \times 10^3$	$5.27 \times 10^3$	$5.45 \times 10^3$ ( $\pm 6\%$ )
Zn	$^{69\text{m}}\text{Zn}$	-	$1.50 \times 10^2$	$1.50 \times 10^2$ ( $\pm 9\%$ )
Mo	$^{99}\text{Mo}$	-	$4.13 \times 10^2$	$4.45 \times 10^2$ ( $\pm 7\%$ )
Cd	$^{115}\text{Cd}$	-	$1.05 \times 10^3$	$0.95 \times 10^3$ ( $\pm 2\%$ )
Eu	$^{152\text{m}}\text{Eu}$	-	$2.89 \times 10^6$	$2.79 \times 10^6$ ( $\pm 3\%$ )
Hg	$^{197}\text{Hg}$	-	$2.10 \times 10^6$	$2.17 \times 10^6$ ( $\pm 1\%$ )
Se	$^{77\text{m}}\text{Se}$	-	$4.15 \times 10^4$	$3.94 \times 10^4$ ( $\pm 3\%$ )
Se	$^{75}\text{Se}$	$1.30 \times 10^5$	$1.46 \times 10^5$	$1.42 \times 10^5$ ( $\pm 5\%$ )

a. Uncertainties represent only counting statistics.

The  $\sigma_{2200}$  values and resonance integrals  $I$  were taken from the recommended values of the *Chart of the Nuclides*, 1972 edition.<sup>7</sup> The multigroup cross section data,  $\sigma_i(E)$ , were taken from the ENDF-B cross section library.

For experimental measurements, 17 elemental standard solutions were prepared. During sequential irradiations, all other irradiation tubes were removed to approximate more closely the assumption of spherical moderator arrangement. Sample irradiation, decay, and counting intervals were carefully timed, and a calibrated detector was used for absolute counting. Results are shown in Table 3. Eighty-four group reaction rates were calculated for those nine isotopes for which multigroup cross sections are available. In general, the results of the 2-group method are as reliable as those of the more-sophisticated 84-group technique. However, the limitations of the two-group approach listed earlier must be considered. Except in the cases of gold and arsenic, >90% of the total reaction rate is the result of thermal neutron capture. The simple two-group approach to the calculation of neutron capture reaction rates appeared adequate for the particular experimental conditions within the 17-mg  $^{252}\text{Cf}$  facility in which  $\phi_E/\phi_T$  is about 1.0. Thus, only two-group reaction rates are used in the 100-mg  $^{252}\text{Cf}$  facility.

In the 17-mg  $^{252}\text{Cf}$  facility, six irradiation tubes in a hexagonal array were located around the  $^{252}\text{Cf}$  source. The presence of these tubes and of samples located within them reduce the thermal flux somewhat by displacing moderator. Quantitative measurements were performed to determine and to correct for this effect. The net effect of the presence of the other five irradiation tubes containing aqueous samples was to reduce the calculated thermal flux by 11% and the epithermal flux by 3%. These flux reduction factors were used in the data reduction programs used for routine analysis in the 17-mg  $^{252}\text{Cf}$  facility.

#### The 100-mg $^{252}\text{Cf}$ facility

To take advantage of the rapid moderation of  $\text{H}_2\text{O}$  and the low absorption cross section of  $\text{D}_2\text{O}$ , an  $\text{H}_2\text{O}$ - $\text{D}_2\text{O}$  moderated system was installed in the 100-mg  $^{252}\text{Cf}$  facility. As shown in Figures 6 through 8, the first concentric ring of 9 irradiation tubes is located in the  $\text{H}_2\text{O}$ -moderated region, and the second ring of tubes is in the  $\text{D}_2\text{O}$  region. This arrangement was based on ANISN calculations in an attempt to increase the thermal flux at the second ring of irradiation sites over an all- $\text{H}_2\text{O}$ -moderated system. However, because stainless steel is used in the moderator tank, the expected increase was only partly realized.

### ANISN Calculations

The one-dimensional ANISN code again was used to calculate the thermal and epithermal neutron fluxes and the neutron energy distribution in 13 energy groups at the sample irradiation sites. Figure 26 is a scaled drawing of the H<sub>2</sub>O-D<sub>2</sub>O-moderated system showing the locations of the rotating four-source holder (Zircaloy-2), the H<sub>2</sub>O-moderated region containing the first ring of irradiation sites, and the annular D<sub>2</sub>O tank containing the second ring of irradiation tubes. For one-dimensional ANISN calculations, the distance zones of the different construction, moderator, and sample materials are assumed to be concentric spheres. Thus these calculations only approximate the complex three-dimensional array.

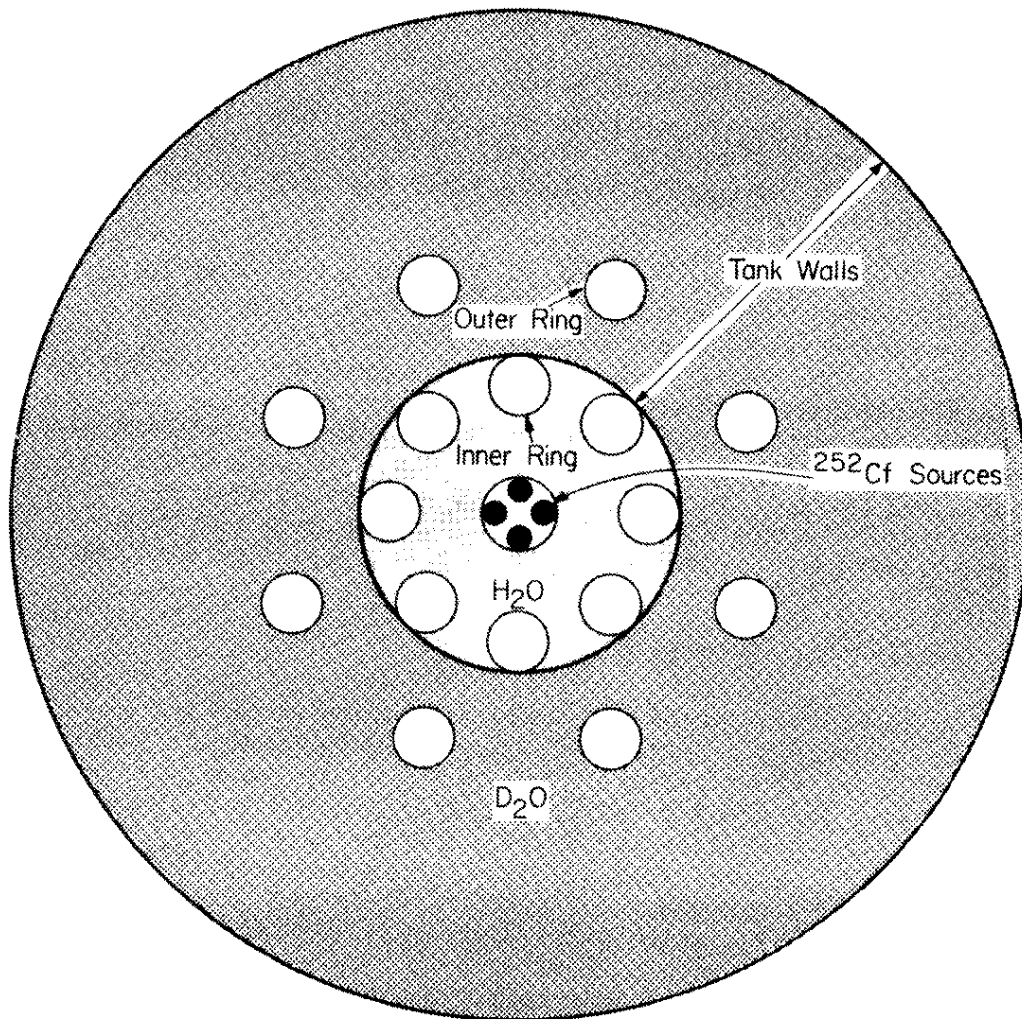


FIGURE 26. Arrangement of Irradiation Tubes and Sources in 100-mg <sup>252</sup>Cf Facility

Two basic sets of calculations were performed. The first set of calculations assumed ideal systems; a spherical source and spherical regions of moderator were assumed. The stainless steel in both the moderator tank and the sample irradiation tubes were not included in the calculations. The second more realistic set of calculations included the effects of stainless steel. In all calculations, the actual source neutron emission rate ( $2.53 \times 10^{11}$ ) neutrons/sec) was used.

Figure 27 shows the calculated change in thermal flux with distance for an ideal all-H<sub>2</sub>O-moderated system surrounding the zircaloy <sup>252</sup>Cf source holder (Case 1). This curve is superimposed on several other curves for reference purposes.

Figure 28 shows the results of ANISN for an ideal H<sub>2</sub>O-D<sub>2</sub>O moderator system (Case 2). Actual D<sub>2</sub>O tank dimensions and the 0.692 cm radius of the zircaloy source holder are shown. The effects of stainless steel and of an aqueous sample in the outer ring are not included. As expected, the flux is increased by ~70% in the D<sub>2</sub>O-moderated region (outer ring sample irradiation site) over that expected from an all-H<sub>2</sub>O-moderated system.

Figure 29 shows ANISN results for an ideal H<sub>2</sub>O-D<sub>2</sub>O moderator system using actual tank and source dimensions. The effect of an aqueous sample located in the second ring irradiation site is included (Case 3). The thermal neutron absorption within the aqueous sample itself (outer ring sample region of 10.01 to 12.32 cm) reduces the net increase in thermal flux at the center of the sample (11.19 cm) to ~60% over the all-H<sub>2</sub>O-moderated system.

Figures 30 and 31 show the calculated ratios of thermal fluxes for Case 2/Case 1 and for Case 3/Case 1; shaded areas indicate the locations of the two irradiation rings. Flux ratio values greater than one indicate a thermal flux enhancement relative to the all-H<sub>2</sub>O-moderated system. Averaged over the entire inner sample irradiation region (4.69 to 7.05 cm), the effect of adding D<sub>2</sub>O to the inner ring is negligible because neutrons from the D<sub>2</sub>O region do not reflect back into the H<sub>2</sub>O region. However, the net flux gain in the outer ring is significant even when the absorbing effect of the aqueous sample is included (Case 3/Case 1). Table 4 summarizes these calculated results at the center of two rings of irradiation sites for the ideal systems.

The second, more realistic, set of calculations include the effect of the stainless steel irradiation tubes and annular tank walls. Again, because of the one-dimensional limitation of the ANISN flux calculations, simplifying assumptions were made. Because of the staggered arrangement (Figure 26) of inner and outer rings of irradiation tubes, flux ratios for inner and outer

irradiation tubes were calculated separately. In all calculations, however, the steel walls of the D<sub>2</sub>O tank were included. Table 5 lists the regions, distance intervals, materials, and explanations of these regions shown schematically in Figure 32. Regions 4 and 9 are the inner and outer ring sample irradiation positions.

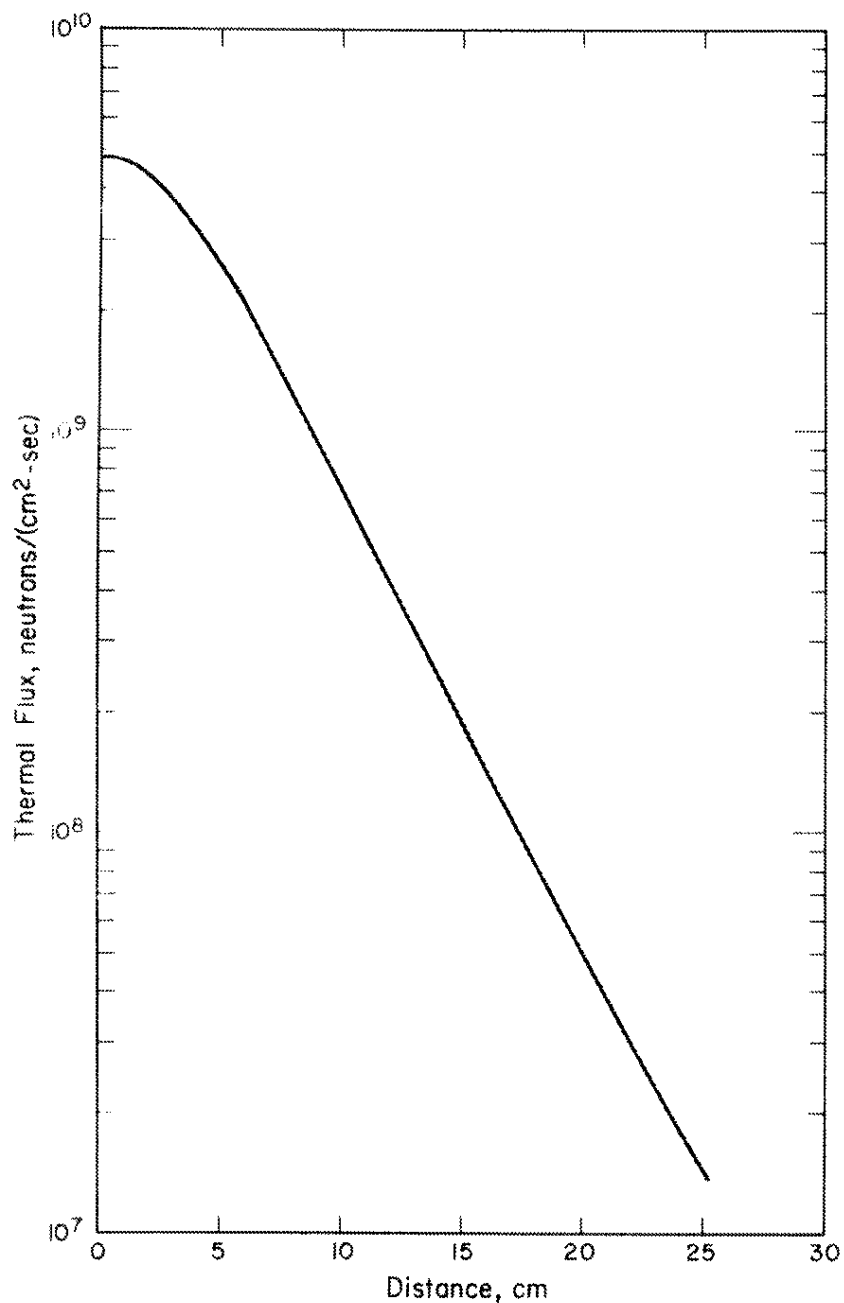


FIGURE 27. Calculated Thermal Flux for Ideal System with H<sub>2</sub>O Moderator (Case 1)



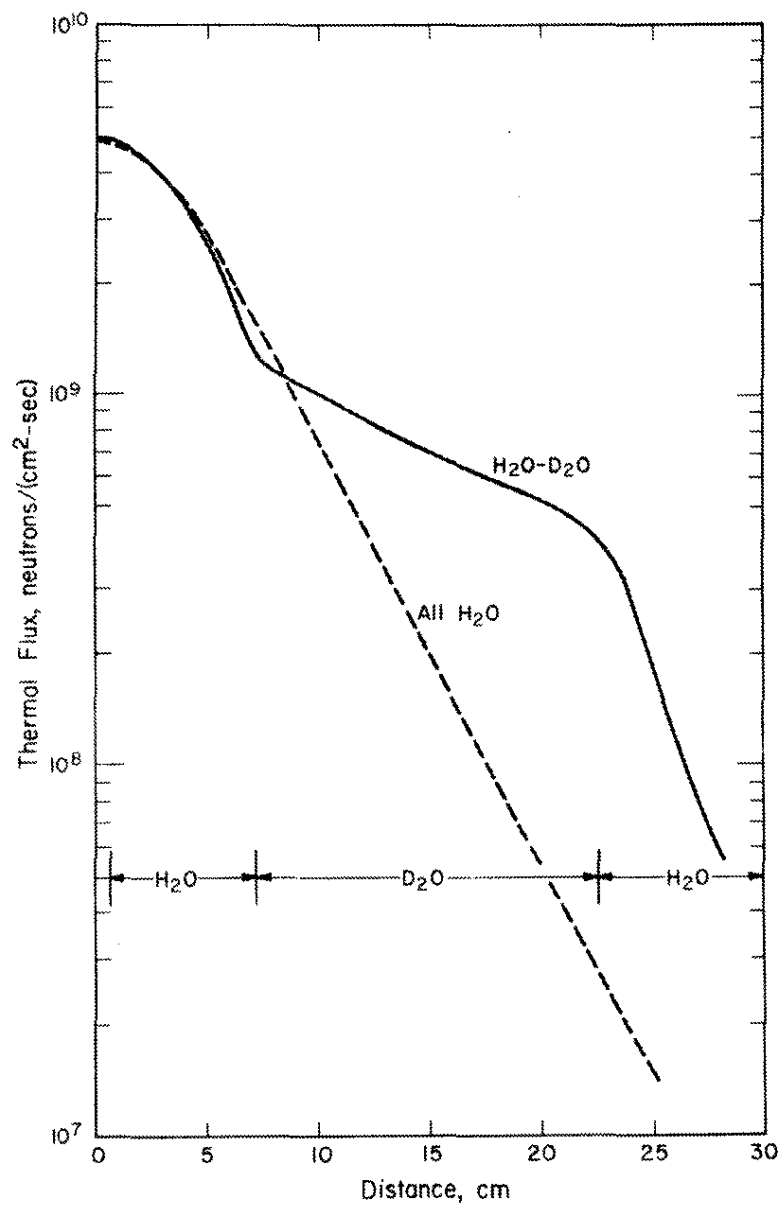


FIGURE 28. Calculated Thermal Flux for Ideal System with H<sub>2</sub>O-D<sub>2</sub>O Moderator (Case 2)

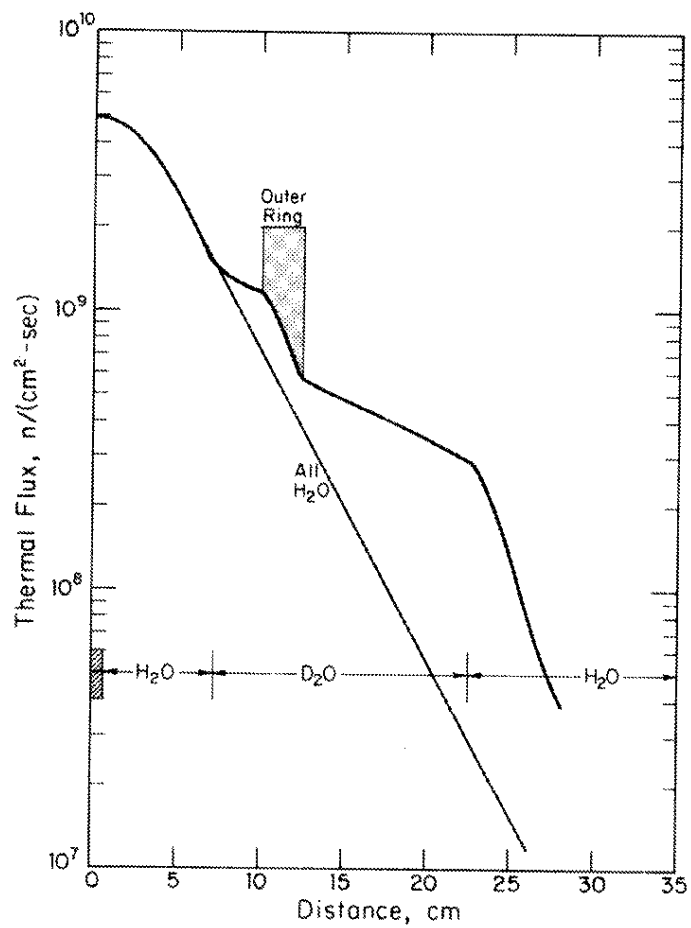


FIGURE 29. Thermal Flux for Ideal Case,  $H_2O$ - $D_2O$  Moderator with Samples in Outer Ring (Case 3)

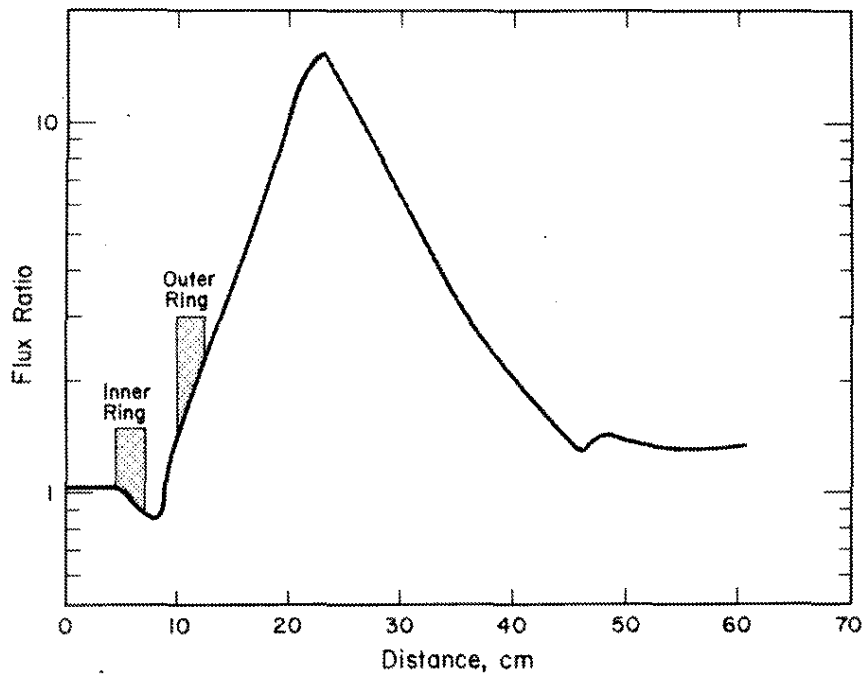


FIGURE 30. Thermal Flux Ratio for Ideal System (Case 2/Case 1)

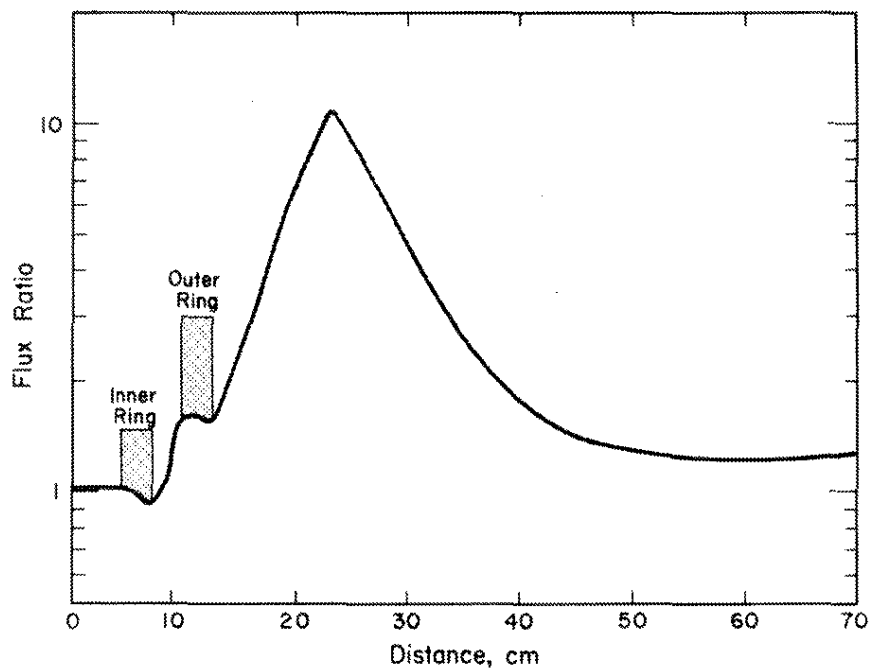


FIGURE 31. Thermal Flux Ratio for Ideal System (Case 3/Case 1)

TABLE 4

Flux Calculations for Ideal Systems<sup>a</sup>

	<i>Case 1</i>		<i>Case 2</i>		<i>Case 3</i>	
	<i>Inner Ring</i>	<i>Outer Ring</i>	<i>Inner Ring</i>	<i>Outer Ring</i>	<i>Inner Ring</i>	<i>Outer Ring</i>
$\phi_T$	$2.09 \times 10^9$	$5.33 \times 10^8$	$2.05 \times 10^9$	$9.19 \times 10^8$	$2.08 \times 10^9$	$8.51 \times 10^8$
$\phi_E$	$9.51 \times 10^8$	$1.44 \times 10^8$	$1.07 \times 10^9$	$3.27 \times 10^8$	$1.03 \times 10^9$	$2.25 \times 10^8$
$\phi_E/\phi_T$	0.45	0.27	0.52	0.35	0.50	0.26

- a. Case 1, all H<sub>2</sub>O moderator;  
 Case 2, H<sub>2</sub>O-D<sub>2</sub>O moderators; and  
 Case 3, H<sub>2</sub>O-D<sub>2</sub>O moderator and outer ring aqueous sample.

The effects of stainless steel were not included in these calculations.

TABLE 5

Regions, Distances and Materials  
in the 100-mg <sup>252</sup>Cf Facility (see Figure 32)

<i>Region</i>	<i>Interval, cm</i>	<i>Material</i>	<i>Explanation</i>
1	0 - 0.6922	Zircaloy	<sup>252</sup> Cf source holder
2	0.6922 - 4.602	H <sub>2</sub> O	H <sub>2</sub> O Moderator Around <sup>252</sup> Cf Source
3	4.602 - 4.691	Stainless Steel	Near-Wall Inner Irradiation Ring
4	4.691 - 7.054	H <sub>2</sub> O	Aqueous Sample Inner Ring
5	7.054 - 7.143	Stainless Steel	Far-Wall Inner Irradiation Ring
6	7.143 - 7.301	Stainless Steel	Near-Wall of Annular Moderator Tank
7	7.301 - 9.921	D <sub>2</sub> O	D <sub>2</sub> O Moderator
8	9.921 - 10.010	Stainless Steel	Near-Wall Outer Irradiation Ring
9	10.010 - 12.372	H <sub>2</sub> O	Aqueous Sample Outer Ring
10	12.372 - 12.461	Stainless Steel	Far-Wall Outer Irradiation Ring
11	12.461 - 22.460	D <sub>2</sub> O	D <sub>2</sub> O Moderator
12	22.460 - 22.619	Stainless Steel	Far-Wall Annular Moderator Tank
13	22.619 -	H <sub>2</sub> O	H <sub>2</sub> O Shielding and Moderator

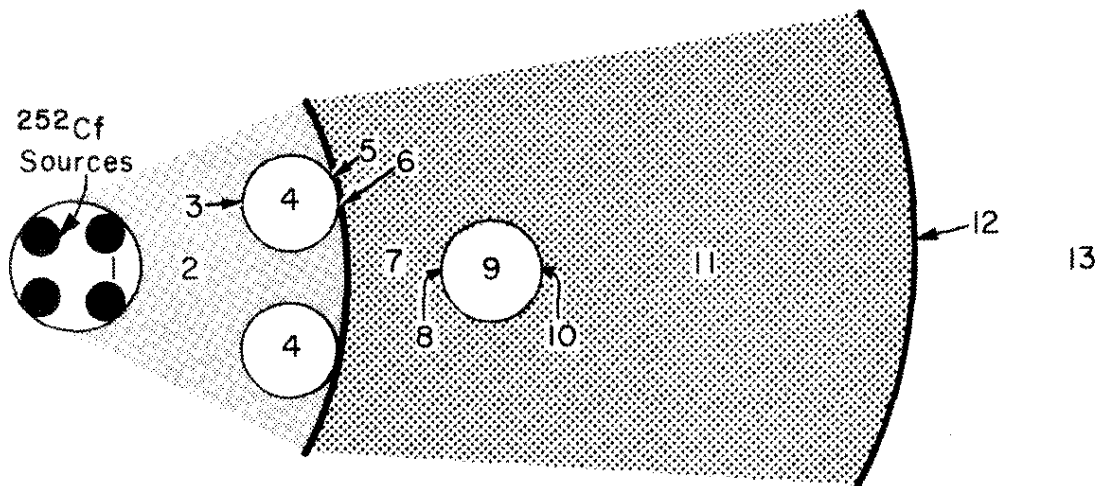


FIGURE 32. Schematic of Regions Surrounding  $^{252}\text{Cf}$  Sources Used in ANISN Calculations (see Table 5)

Figure 33 (Case 4) shows the change in calculated thermal flux with distance for the inner irradiation ring for an all- $\text{H}_2\text{O}$ -moderated system. (Regions 1 through 6 are as indicated in Table 5; however, the outer ring is not considered and regions 7 through 11 are assumed to be  $\text{H}_2\text{O}$ ). Flux depressions are seen in Figure 33 for the near and far walls of the inner ring and for the moderator tank wall. A net loss of  $\sim 30\%$  in thermal flux at the inner ring compared to the ideal Case 1 (superimposed) occurs because of neutron absorption in the steel walls.

Figure 34 (Case 5) is the calculated change in thermal flux with distance for the inner irradiation ring of an  $\text{H}_2\text{O}$ - $\text{D}_2\text{O}$ -moderated system (i.e., Regions 7 through 11 are  $\text{D}_2\text{O}$ ). As shown in Table 6, replacing the  $\text{H}_2\text{O}$  with  $\text{D}_2\text{O}$  does not raise the thermal flux significantly at the inner ring. The stainless steel reduces the thermal flux 27.3% at the inner ring compared to Case 2. Figure 35 shows the calculated ratios of thermal fluxes (Case 5/Case 4). Averaged over an entire inner ring volume, this ratio does not deviate significantly from one; thus the flux-enhancement is no greater with  $\text{D}_2\text{O}$  moderator than that with  $\text{H}_2\text{O}$  moderator.

Figure 36 (Case 6) shows the calculated change in thermal flux with distance for the outer stainless steel irradiation ring for an all  $\text{H}_2\text{O}$ -moderated system. Compared to the ideal case, the thermal flux is reduced by  $\sim 30\%$  [from  $5.33 \times 10^8$  to  $3.75 \times 10^8$  neutron/( $\text{cm}^2$ -sec)] by inclusion of the stainless steel.

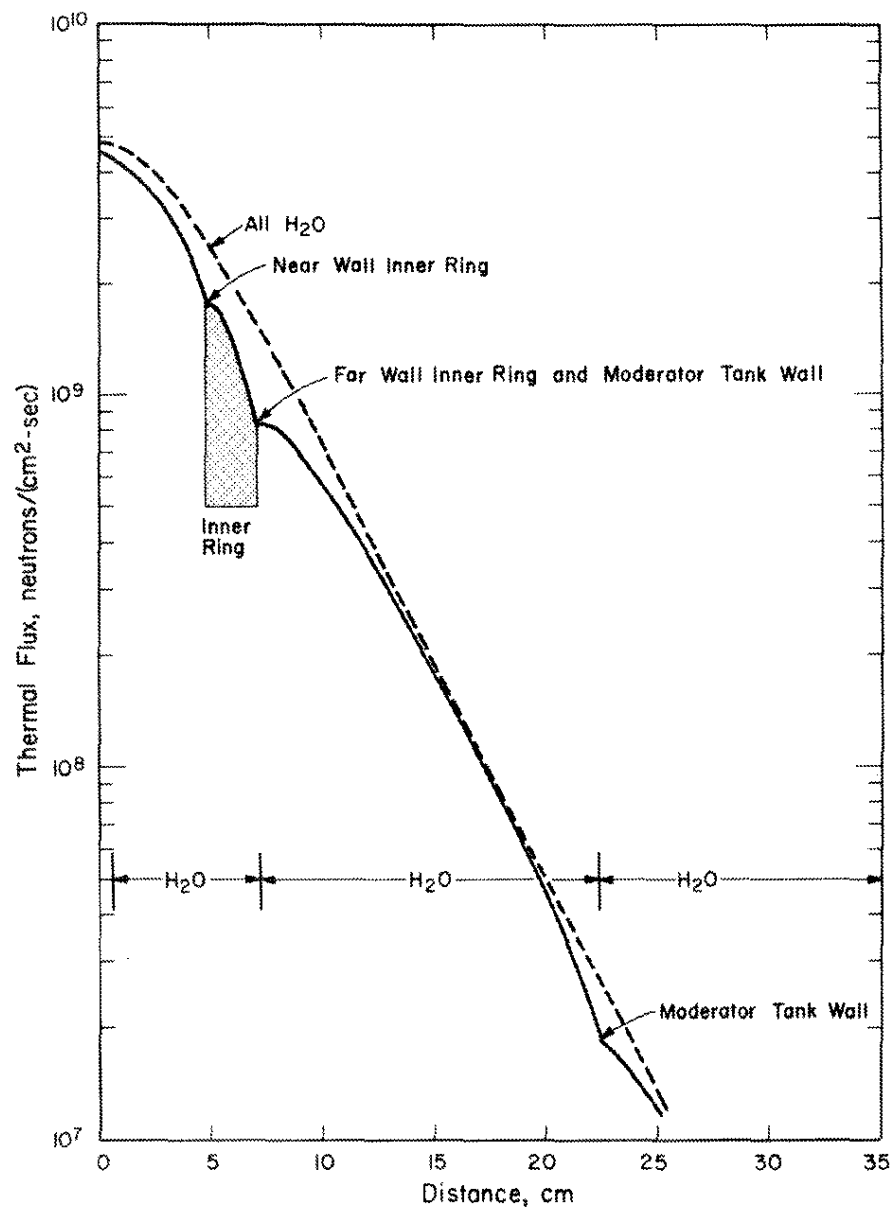


FIGURE 33. Calculated Thermal Flux for Inner Ring in Non-Ideal System with H<sub>2</sub>O Moderator (Case 4)

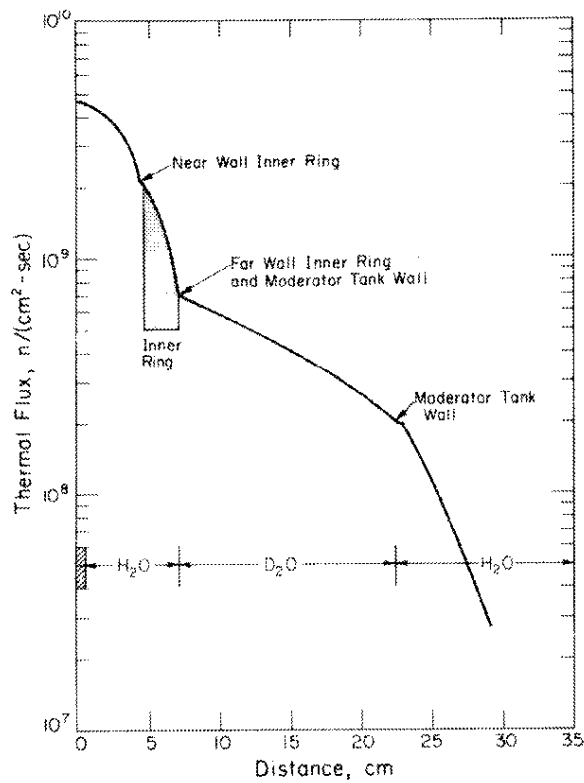


FIGURE 34. Calculated Thermal Flux for Inner Ring in Non-Ideal System with H<sub>2</sub>O-D<sub>2</sub>O Moderator (Case 5)

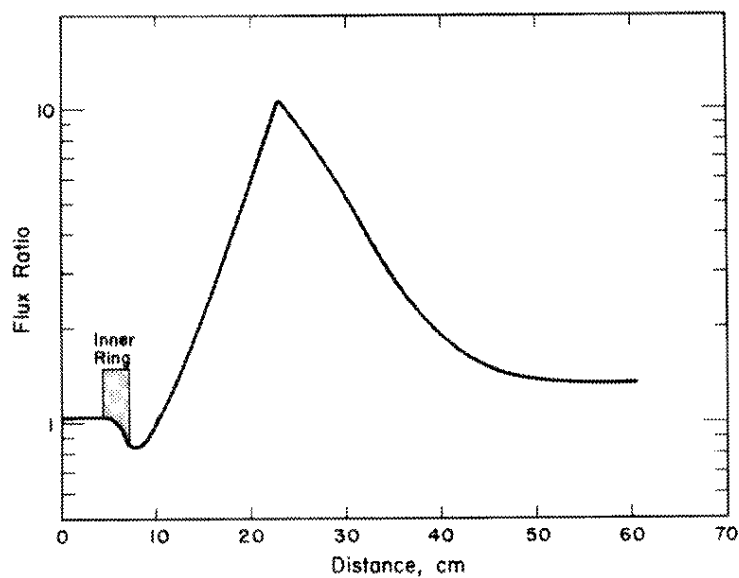


FIGURE 35. Calculated Thermal Flux Ratio for Inner Ring in Non-Ideal System with H<sub>2</sub>O-D<sub>2</sub>O Moderator (Case 5/Case 4)

TABLE 6

Flux Calculations that Include  
Effects of Stainless Steel<sup>a</sup>

	Case 4 (Inner Ring)	Case 5 (Inner Ring)	Case 6 (Outer Ring)	Case 7 (Outer Ring)
$\phi_T$	$1.46 \times 10^9$	$1.49 \times 10^9$	$3.75 \times 10^8$	$5.15 \times 10^8$
$\phi_E$	$9.80 \times 10^8$	$1.10 \times 10^9$	$1.48 \times 10^8$	$2.25 \times 10^8$
$\phi_E/\phi_T$	0.67	0.74	0.40	0.44

a. Case 4, all H<sub>2</sub>O moderator and aqueous sample inner ring;  
Case 5, H<sub>2</sub>O-D<sub>2</sub>O moderator and aqueous sample inner ring;  
Case 6, all H<sub>2</sub>O moderator and aqueous sample outer ring; and  
Case 7, H<sub>2</sub>O-D<sub>2</sub>O moderator and aqueous sample outer ring.  
Cadmium cutoff energy is 0.414 eV.

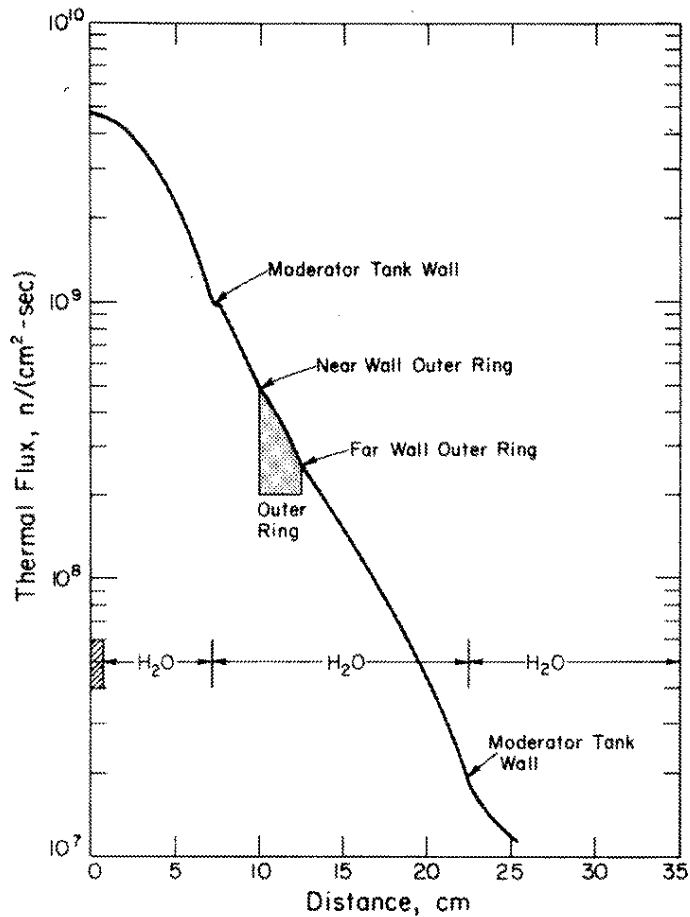


FIGURE 36. Calculated Thermal Flux for Outer Ring  
in Non-Ideal System with H<sub>2</sub>O Moderator  
(Case 6)



Figure 37 (Case 7) shows the calculated change in thermal flux with distance for the outer stainless steel irradiation ring for the H<sub>2</sub>O-D<sub>2</sub>O moderated system. Compared to Case 6, the D<sub>2</sub>O increases the thermal flux at the center of the outer ring over an all-H<sub>2</sub>O-moderated system by ~37%. Compared to Case 2, the combined effects of the stainless steel and thermal neutron absorption within the aqueous sample itself reduce the thermal flux by 44% [from  $9.19 \times 10^8$  to  $5.15 \times 10^8$  neutrons/(cm<sup>2</sup>-sec)]. Compared to Case 3, which is identical to Case 7, except that no stainless steel was assumed to be present, neutron absorption by the steel reduces the thermal flux by 39%.

Figure 38 shows the thermal flux ratio of Case 7/Case 6. A gain in thermal flux of ~30% over the outer ring sample region is seen for the H<sub>2</sub>O-D<sub>2</sub>O moderator system.

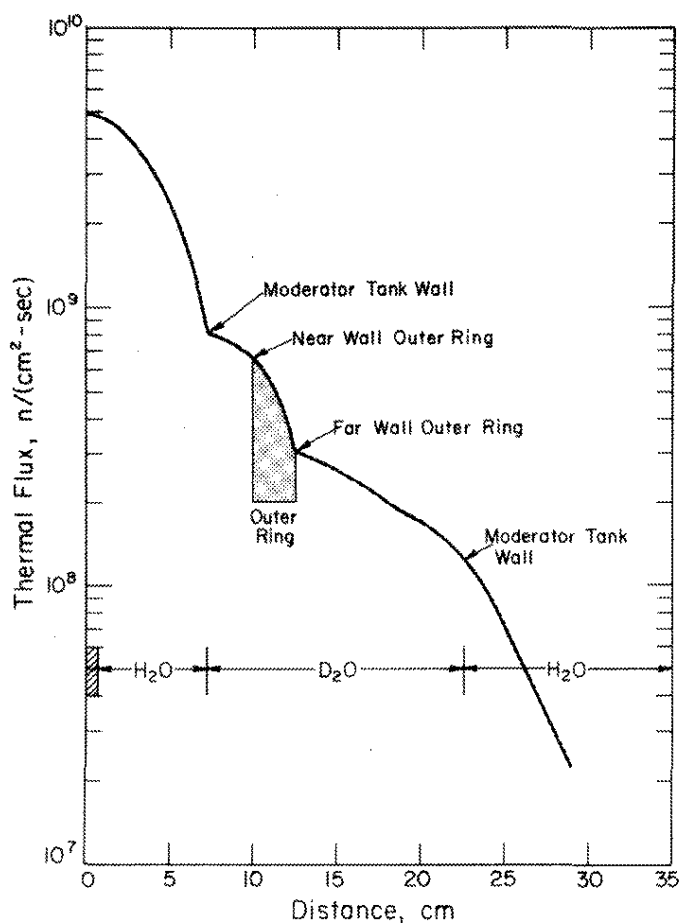


FIGURE 37. Calculated Thermal Flux for Outer Ring in Non-Ideal System with H<sub>2</sub>O-D<sub>2</sub>O Moderator (Case 7)

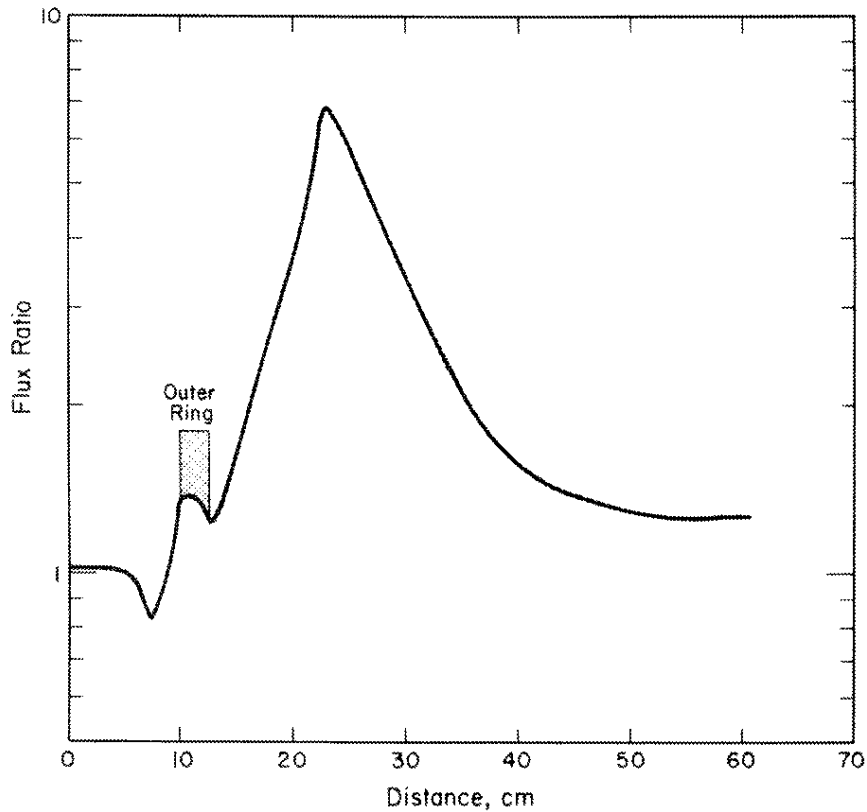


FIGURE 38. Calculated Thermal Flux Ratio in Outer Ring in Non-Ideal System with H<sub>2</sub>O Moderator (Case 7/Case 6)

#### *Comparison of Calculated and Measured Fluxes*

Pure gold wires and gold wires within cadmium tubes of 0.002-inch-diameter were irradiated at the center of both the inner and outer rings of irradiation sites. During these measurements, the other tubes were filled with polyethylene. The irradiated wires were dissolved and counted with a calibrated detector. The net thermal-induced <sup>198</sup>Au specific activities were obtained by subtracting the measured epithermal specific activities of wires irradiated inside the cadmium tubes. The saturated gold activity (thermal)  $A_{sat}^{th}$ , at the end of irradiation is then related to the thermal flux by

$$\phi_T = \frac{A_{sat}^{th}}{N_{197} \left( \frac{\pi T}{4 T_0} \right)^{1/2} \sigma_{2200}} \times \frac{1}{F_{th}} \quad (30)$$

where

$N_{197}$  = Number of gold atoms in each wire

$$\left( \frac{\pi T}{4 T_0} \right)^{1/2} = 0.886 \text{ at } 298^\circ\text{K}$$

$\sigma_{2200} = 98.8$  barns

$F_{th}$  = thermal flux depression factor = 0.976

The measured thermal neutron fluxes with the  $\text{H}_2\text{O}-\text{D}_2\text{O}$  moderator system for the center of the inner and outer irradiation rings (5.87 cm and 11.19 cm) were  $(1.21 \pm 0.10) 10^9$  and  $(4.25 \pm 0.20) 10^8$  neutron/( $\text{cm}^2\text{-sec}$ ) using the gold wire technique.

Because of the limitations of the one-dimensional ANISN flux calculation, the calculated thermal fluxes for Case 5 and Case 7 only approximate experimental conditions. The experimental-to-calculated thermal flux ratio is 0.812 for the inner irradiation rings and 0.825 for the outer irradiation ring. This discrepancy is caused by limitations of the calculational technique. When calculating the thermal flux in the inner ring, the effect of stainless steel outer irradiation was not considered. When calculating the thermal flux in the outer ring, the effect of stainless steel inner tubes was not considered. The effect of one ring on the other as well as the effect of adjacent steel irradiation tubes could account for most of the observed flux depression.

## EVALUATION OF THE $\text{H}_2\text{O}-\text{D}_2\text{O}$ SYSTEM

Three separate methods are used to evaluate the  $\text{H}_2\text{O}-\text{D}_2\text{O}$  moderator system. First, the ANISN calculations (Table 4) for ideal systems (Case 1 and Case 3) indicate no net thermal flux increase in the inner sample irradiation zone compared to an all- $\text{H}_2\text{O}$ -moderated system [ $2.09 \times 10^9$  compared to  $2.08 \times 10^9$  neutron/( $\text{cm}^2\text{-sec}$ )]. In theory, however, the  $\text{H}_2\text{O}-\text{D}_2\text{O}$  moderator system is advantageous because the thermal flux in the outer sample irradiation zone is increased significantly. In practice, the stainless steel construction material offsets this advantage. Stainless steel was selected as the construction material for the irradiation tubes and annular tank because it is readily available and structurally strong and because more ideal materials, such as zircaloy and aluminum, are more difficult to fabricate. Calculationally, inclusion of the steel is shown to reduce the thermal fluxes compared to the ideal systems by  $\sim 29\%$  for inner rings and  $39\%$  for outer rings (compare Case 5/Case 1 and Case 7/Case 1). Calculationally, however, inclusion of

stainless steel does not affect the gain in thermal flux in the outer sample ring for the H<sub>2</sub>O-D<sub>2</sub>O moderator system [gain is  $3.75 \times 10^8$  to  $5.15 \times 10^8$  neutron/(cm<sup>2</sup>-sec)] for a net gain of 37% (Case 6/Case 7).

The benefit of the H<sub>2</sub>O-D<sub>2</sub>O moderator also has been demonstrated experimentally. The experimental ratio of thermal fluxes (outer-to-inner) was 0.351 compared to that calculated from the ideal all-H<sub>2</sub>O system of 0.255. The calculated ratio including the effect of steel of 0.346 agrees well with the experimental value. Results of the definitive experimental flux measurement using gold solutions with H<sub>2</sub>O and D<sub>2</sub>O in the outer ring indicate a gain of 28.3% in thermal flux, the absolute thermal fluxes are  $3.40 \times 10^8$  neutron/(cm<sup>2</sup>-sec) for H<sub>2</sub>O and  $4.33 \times 10^8$ , neutrons/(cm<sup>2</sup>-sec) for D<sub>2</sub>O. The experimental flux measurements indicate that D<sub>2</sub>O reduces the thermal flux in the inner ring by about 3%. The measured thermal flux in the inner ring for the all-H<sub>2</sub>O system was  $9.6 \times 10^8$  neutrons/(cm<sup>2</sup>-sec) compared to  $9.3 \times 10^8$  neutrons/(cm<sup>2</sup>-sec) for the dual systems.

An alternate construction material such as aluminum would have been better than stainless steel in the H<sub>2</sub>O-D<sub>2</sub>O moderator system.

#### OPTIMIZED FISSILE MATERIAL ANALYSIS WITH CYCLIC NEUTRON ACTIVATION AND DELAYED NEUTRON COUNTING

Several laboratory programs, including the National Uranium Resource Evaluation program, require rapid, specific, and sensitive assays of natural uranium and other fissile isotopes, e.g., <sup>233</sup>U, <sup>239,241</sup>Pu, and <sup>245</sup>Cm. Automated neutron activation analysis based on cyclic neutron activation and delayed neutron counting was developed using the 17-mg <sup>252</sup>Cf facility. Procedures have been optimized for as many as 200 samples/day. Sensitivities are  $\leq 0.5$  ppm for natural uranium and  $\leq 10$  ppb for <sup>239</sup>Pu in the 100-mg <sup>252</sup>Cf facility. Cyclic irradiation and counting procedures are used to improve analytical sensitivity for measuring short half-life ( $\leq$ minute) activated species.

#### Delayed Neutron Analysis

A rigorous mathematical optimization for assaying fissile material by cyclic neutron activation analysis is not yet possible because the factors that determine neutron detector response for a particular fissile isotope are complex. The fission process itself is complex. For <sup>235</sup>U, fission is known to yield over 50 beta-delayed, neutron-emitting precursors, each with a characteristic half-life and delayed neutron emission probability.<sup>8,9</sup>

The fission yield of each of these precursors is dependent on the mass of the fissioning nucleus (especially those products with lighter mass), charge distribution characteristics, and on the energy of the incident neutron on the fissioning nucleus. An additional mathematical complexity is the growth and decay of isobaric short-lived fission products that decay by delayed neutron emission; examples<sup>10</sup> are  $^{92,93}\text{Kr}$ ,  $^{92,93}\text{Rb}$ ,  $^{141,141}\text{Xe}$ , and  $^{141,142}\text{Cs}$ . A final complexity in estimating the delayed-neutron detector response is the effect of the different neutron energy groups emitted from the different activation products.<sup>8,11</sup>

Delayed neutron emission has long been a matter of great importance in reactor control and design. Although a large number of delayed-neutron precursors have been identified, reactor kineticists are in almost universal agreement that a simplified six-group treatment is adequate for treatment of the phenomena. Efforts to identify other delayed groups and to refine the group yields reported by Keepin<sup>12</sup> have not resulted in significant revision of the six-group theory.<sup>13-15</sup>

### Optimization of Cyclic Analysis Procedures for Fissile Material

The six-group model of delayed neutron emission is used to optimize procedures for cyclic analysis of different fissile materials. The multigroup flux calculations were combined with multigroup fission cross sections from the ENDF-B library<sup>5</sup> to calculate specific saturated fission rates for each fissile material,  $R_f$ . The thermal neutron flux and the specific fission rates (Table 7) were shown experimentally to be accurate to within  $\pm 5\%$ .

The number of counts recorded in a cyclic irradiation and counting procedure for a single, short-lived activation species is

$$K = \frac{EIrSDCF}{\lambda} \quad (11)$$

where  $r$  is the saturated production rate for the particular product being measured and  $F$  is the cyclic gain factor.

In the six-group model of delayed neutron emission, the specific saturated rate of production of each of the six half-life, delayed-neutron groups  $r_i$  is given by the product of the specific fission rate  $R_f$  and the delayed neutron group yields  $Y_i$  listed in Tables 8 and 9.

$$r_i = R_f Y_i \quad (31)$$

TABLE 7

Calculated Specific Fission Rates in the  $^{252}\text{Cf}$  Facility

Isotopes	Fission Rate, <sup>a</sup> (fissions/(sec-mg))
$^{233}\text{U}$	$3.99 \times 10^5$
$^{235}\text{U}$	$4.44 \times 10^5$
$^{238}\text{U}$	$1.14 \times 10^2$
Natural U	$3.31 \times 10^3$
$^{239}\text{Pu}$	$6.21 \times 10^5$
$^{240}\text{Pu}$	$4.97 \times 10^2$
$^{241}\text{Pu}$	$7.90 \times 10^5$

a. Calculated from 84-group neutron flux and cross section data. The thermal and epithermal flux values (0.632-eV cutoff) are  $3.53 \times 10^8$  n/(cm<sup>2</sup>-sec) and  $3.22 \times 10^8$  n/(cm<sup>2</sup>-sec), respectively.

TABLE 8

Delayed-Neutron Half-Lives and Yields for Thermal Fission of  $^{233}\text{U}$ ,  $^{235}\text{U}$ ,  $^{239}\text{Pu}$ , and  $^{241}\text{Pu}$ 

Group	$^{233}\text{U}$		$^{235}\text{U}$		$^{239}\text{Pu}$		$^{241}\text{Pu}$	
	Half-Life, sec	Yield, %	Half-Life, sec	Yield, %	Half-Life, sec	Yield, %	Half-Life, sec	Yield, %
1	55.0	0.057	55.72	0.052	54.28	0.021	54.0	0.015
2	20.57	0.197	22.72	0.346	23.04	0.182	23.2	0.365
3	5.00	0.166	6.22	0.310	5.60	0.129	5.6	0.275
4	2.13	0.184	2.30	0.624	2.13	0.199	1.97	0.620
5	0.615	0.034	0.61	0.182	0.618	0.052	0.43	0.290
6	0.277	0.022	0.23	0.066	0.257	0.027	-	-
Total		0.66		1.58		0.61		1.57

TABLE 9

Delayed-Neutron Half-Lives and Yields for Fast Neutron Fission of  $^{238}\text{U}$  and  $^{240}\text{Pu}$ 

Group	$^{238}\text{U}$		$^{240}\text{Pu}$	
	Half-Life, sec	Yield, %	Half-Life, sec	Yield, %
1	52.38	0.054	53.56	0.022
2	21.58	0.564	22.14	0.238
3	5.00	0.667	5.14	0.162
4	1.93	1.599	2.08	0.315
5	0.49	0.927	0.51	0.119
6	0.17	0.309	0.17	0.024
Total		4.12		0.88

Table 10 lists these specific saturated emission rates for delayed neutrons calculated for natural uranium, plutonium, and specific isotopes irradiated in the  $^{252}\text{Cf}$  activation facility.

From Equation 11, the neutron response for the  $i_{\text{th}}$  delayed neutron group is

$$K_i = G_i F_i \quad (32)$$

where

$$G_i = \frac{r_i S_i C_i D_i E}{\lambda_i} \quad \text{and} \quad (33)$$

$$F_i = \frac{M}{1-Q_i} - \frac{Q_i(1-Q_i)^M}{(1-Q_i)^2} \quad (34)$$

Neutron detection efficiencies for all groups are assumed equal. The detector response  $R_d$  actually recorded is the sum of the six groups:

$$R_d = \sum_{i=1}^6 G_i F_i \quad (35)$$

TABLE 10

Specific Saturated Delayed-Neutron Emission Rates Calculated for Fissile Isotopes

Isotope	Delayed Neutron Emission Rate by Group, Neutron/(sec-mg)					
	1	2	3	4	5	6
$^{233}\text{U}$	227	786	662	734	136	88
$^{235}\text{U}$	231	1536	1376	2769	808	293
$^{238}\text{U}$	0.061	0.64	0.76	1.82	1.05	0.35
Natural U	1.72	11.82	10.66	21.75	6.85	2.45
$^{239}\text{Pu}$	130	1131	801	1236	323	168
$^{240}\text{Pu}$	0.1	1.4	1.0	1.9	0.7	0.1
$^{241}\text{Pu}$	119	2883	2173	4898	2291	-
LWR Pu <sup>a</sup>	122	1077	763	1189	317	157

a. Assumed Pu isotopic concentrations:

Mass No.	Atom %
238	1.2
239	59.2
240	23.7
241	11.9
242	4.0

The delayed neutron emission rates for specific groups listed in Table 10 are combined with Equations 33 and 34 to calculate the group responses  $K_i$  and detector response  $R_d$  as functions of different experimental parameters.

Figures 39-44 show delayed neutron detector responses calculated for samples containing 1 mg of fissile material analyzed in the 17-mg  $^{252}\text{Cf}$  facility by the cyclic technique. Calculations are based on the six-group model.

### Effect of Transit Time on Detector Response

Figure 39 shows the group response  $K_i$  for each of the six groups and the expected measurable response  $R_d$  (the sum of the six groups) for a cyclic irradiation and counting regime for natural uranium. The total analysis time is 600 sec, and the sample transit time is 0.25 sec. Figure 40 shows the effect of increasing the transit time to 1.0 sec. The major difference is that the response from the 2.30 sec delayed-neutron group is less because of an increased decay during transit in the latter case. The calculated detector response  $R_d$  (Figure 41) for a range of transit times for natural uranium is based on an assumed total analysis time of 600 sec.

### Optimization Parameters

Table 11 shows the percentage of the detector response, by group, at the optimum number of cycles for different transit times. Table 12 summarizes the optimum experimental parameters for natural uranium analysis. As the transit time is increased from 0.25 sec to 2.50 sec, the optimum number of cycles decreases from 83 to 20 and the detector response decreases from 6048 to 2868. The overall detector response (Table 11) is controlled largely by the 22.72, 6.22, and 2.30-sec half-life groups. The 55.72 sec group does not make a major contribution even for the 2.50-sec transit time. The relative contribution of the 2.30 sec group decreases rapidly with increasing transit time. Table 13 lists the optimum experimental parameters for cyclic analysis of different fissile isotopes.

Figure 42 compares the calculated detector response  $R_d$  for 1 mg of the common fissile isotopes. For these calculations, a transit time of 1.0 sec and an experiment time of 600 sec were assumed. Although the thermal fission cross section for  $^{239}\text{Pu}$  is 742 barns compared to 580 barns for  $^{235}\text{U}$ , the detector response is much higher for  $^{235}\text{U}$  because of the high delayed neutron group yields for this isotope.



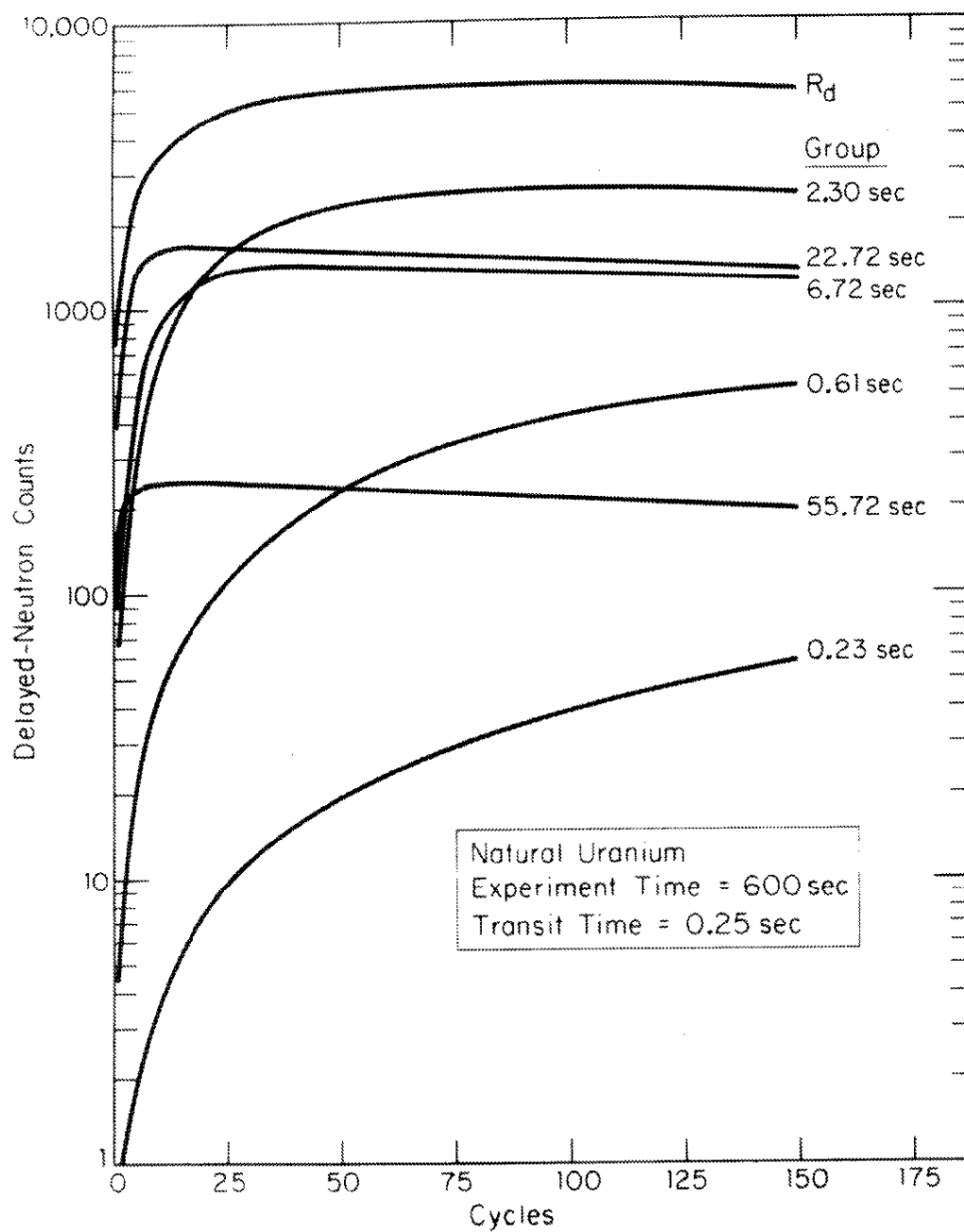


FIGURE 39. Calculated Group Response and Detector Response for Natural Uranium for Transit Time of 0.25 sec

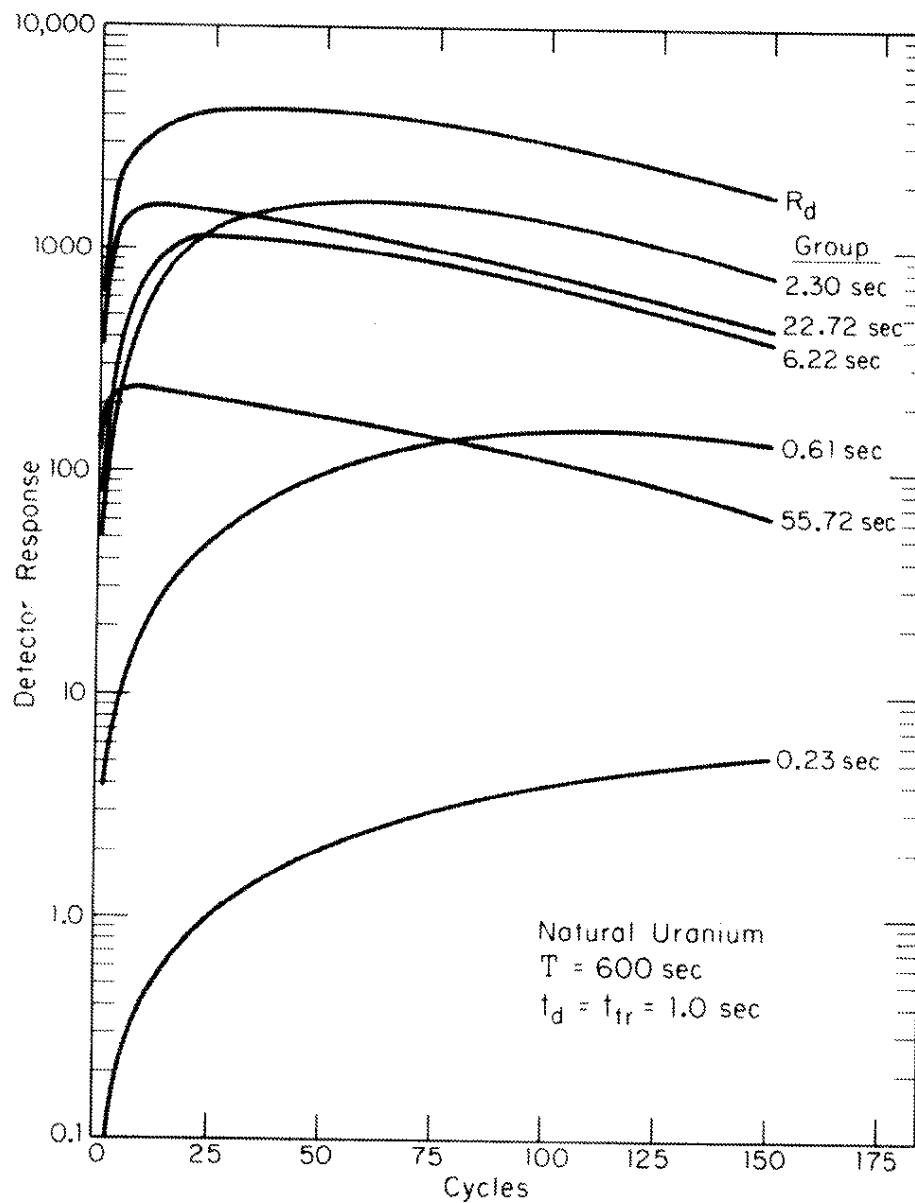


FIGURE 40. Calculated Group Response and Detector Response for Natural Uranium for Transit Time of 1.0 sec

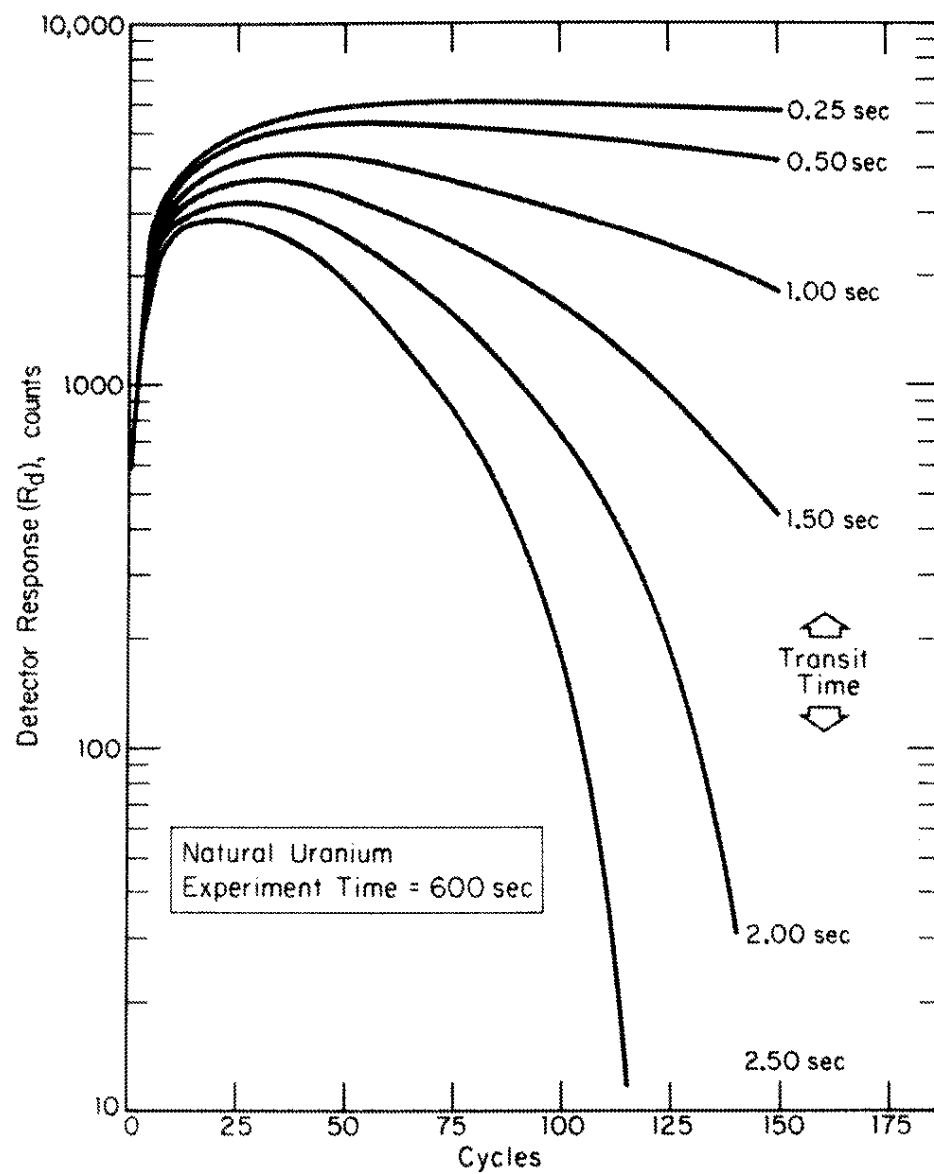


FIGURE 41. Effect of Sample Transit Time on Detector Response for Natural Uranium

TABLE 11

Changes in Calculated Detector Response with Changes in Sample Transit Time  
for the Optimum Number of Cycles for Natural Uranium<sup>a</sup>

Group	Half-Life, sec	Calculated Detector Response, % Total for Each Group										
		0.00-sec transit	0.25-sec transit	0.50-sec transit	0.75-sec transit	1.00-sec transit	1.25-sec transit	1.50-sec transit	1.75-sec transit	2.00-sec transit	2.25-sec transit	2.50-sec transit
1	55.72	3.11	3.68	4.00	4.29	4.55	4.75	5.04	5.30	5.61	5.87	6.15
2	22.72	21.39	25.33	27.42	29.33	31.08	32.40	34.28	35.98	37.94	39.60	41.47
3	6.22	19.29	22.48	25.98	25.17	26.17	26.80	27.69	28.34	28.91	29.27	29.53
4	2.30	39.36	42.00	40.72	38.67	36.44	34.52	32.05	29.73	27.08	24.91	22.64
5	0.61	12.40	0.61	5.95	3.67	2.45	1.71	1.50	0.90	0.65	0.46	0.24
6	0.23	4.43	0.52	0.20	0.08	0.04	0.03	0.01	0.00	0.00	0.00	0.00

a. Total experiment time is 600 sec.

TABLE 12

Optimum Experimental Conditions for Cyclic Analysis of Natural Uranium (1 mg)

Transit Time, sec <sup>a</sup> +	0.25	0.50	0.75	1.00	1.25	1.50	1.75	2.00	2.25	2.50
Cycles	83	57	45	38	33	30	27	24	22	20
Irradiation - count interval, sec	3.36	4.76	4.92	6.89	7.84	8.25	9.36	10.50	11.39	12.50
Neutron detector response $R_d$ , counts	6048	5262	4719	4298	3955	3667	3424	3213	3030	2868

a. Equal transit times to and from the detector are assumed.

b. Equal irradiation and counting times are assumed.

TABLE 13

Optimum Experimental Conditions for Cyclic Analysis of Common Fissile Materials

Isotope	Cycles	$t_i = t_c$ , sec <sup>a</sup>	Detector Response <sup>b</sup> $R_d$ , counts
<sup>233</sup> U	33	8.09	254,100
<sup>235</sup> U	38	6.89	553,300
<sup>239</sup> Pu	35	7.57	313,700
<sup>241</sup> Pu	41	6.32	887,800
LWR Pu	37	7.11	286,600

a. Equal irradiation and counting intervals.

b. One-milligram samples and an experiment time of 600 sec are assumed; transit time is 1.00 sec.

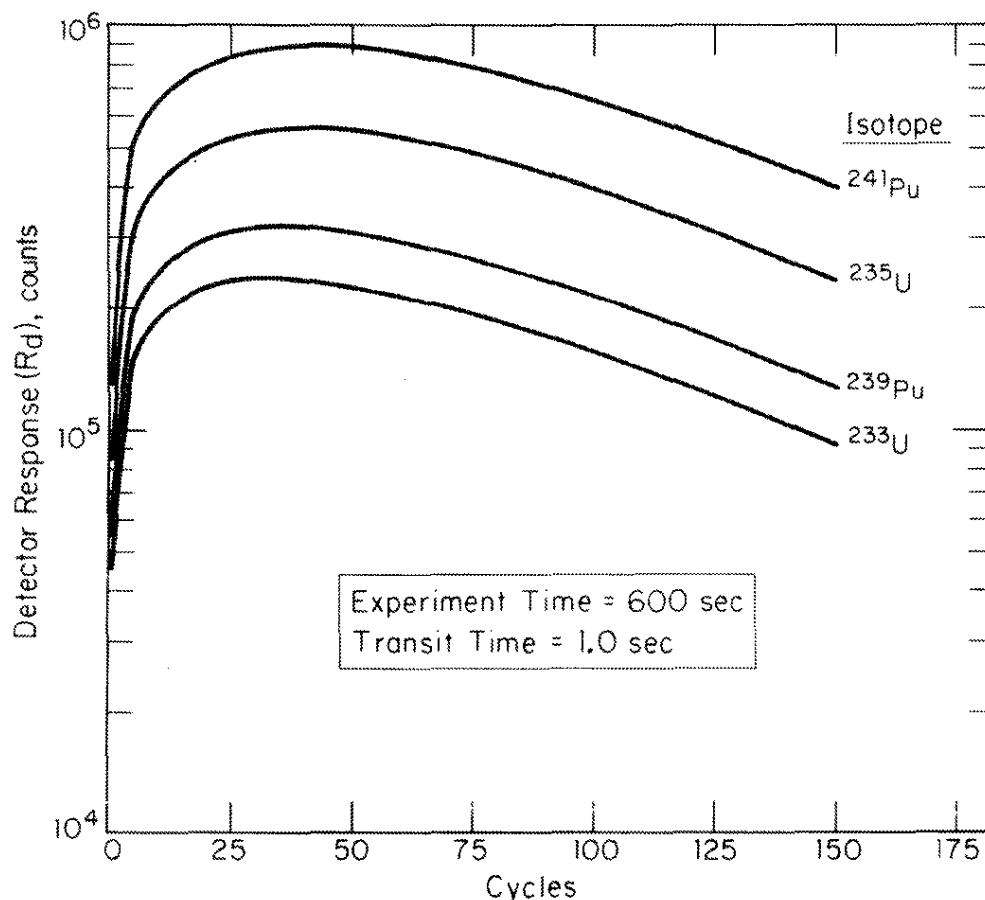


FIGURE 42. Relative Detector Response for Fissile Isotopes

#### Comparison of Calculated and Measured Detector Responses

Samples of approximately 1 mg of enriched (97.66%)  $^{235}\text{U}$  were cyclically irradiated and counted in the 17-mg  $^{252}\text{Cf}$  facility for comparison with the calculated detector response curves. The pressure of the pneumatic sample transfer system was adjusted to give transfer times of  $1.0 \pm 0.1$  sec. A total analysis time of  $600 \pm 10$  sec was maintained by adjusting irradiation and counting intervals, according to the number of cycles used. Results are shown in Figure 43. The experimental points were adjusted for sample weight and counter efficiency. Agreement is excellent except where large numbers of cycles were used. Comparison of curve shapes (Figure 41) calculated for various transit times indicates an actual experimental transit time of about 1.1 sec.

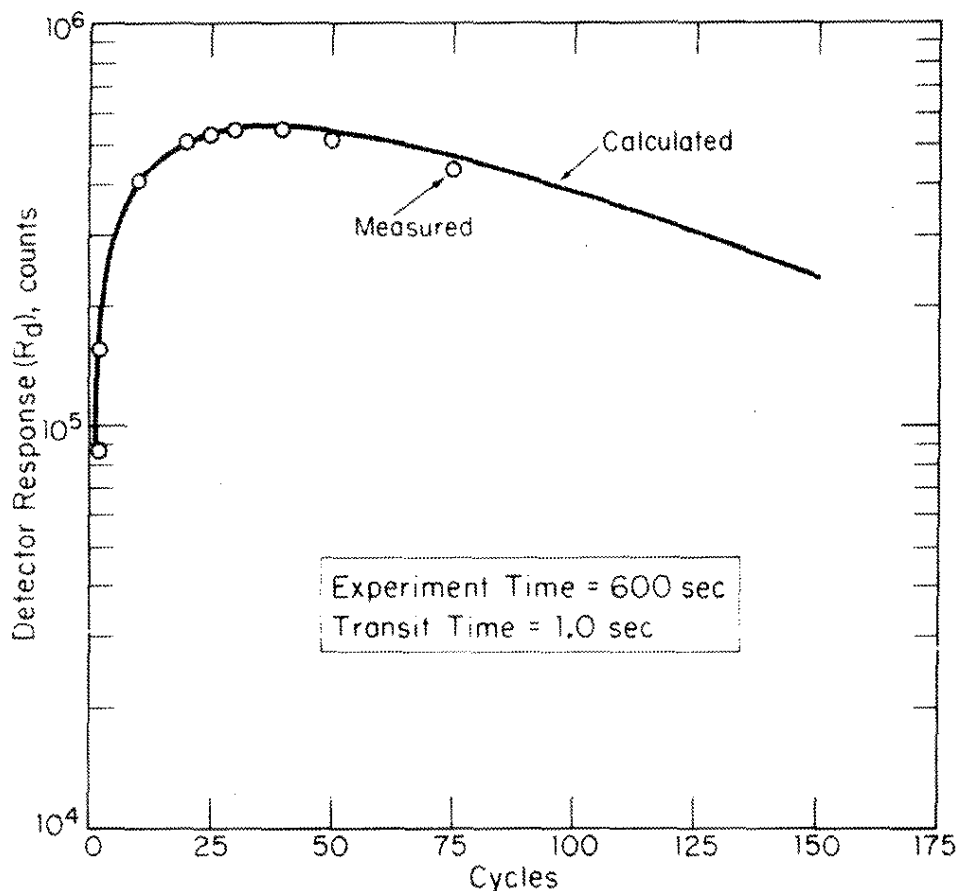
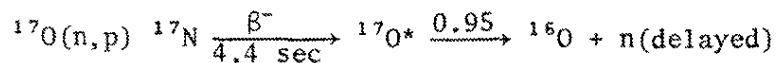


FIGURE 43. Comparison of Calculated and Measured Detector Responses for Cyclic Analysis of  $^{235}\text{U}$

#### Oxygen-17 Interference in Analysis of Low-Level Aqueous Samples

For cyclic determinations of low-level quantities of fissile materials in aqueous or oxygen-containing matrices, undesirable background from delayed neutrons produced from  $^{17}\text{O}$  by the fast-neutron reaction must be considered.



The threshold neutron energy for this reaction is 8.2 MeV. The average cross section for the fast-neutron reaction of  $^{17}\text{O}$  has been measured in the  $^{252}\text{Cf}$  facility with  $^{17}\text{O}$ -enriched (37.1%) water. If a detection efficiency for delayed neutrons produced in this reaction is assumed to be the same as for those produced in fission, and if the fast neutron flux  $\phi_F$  ( $E_n > 7.8$  MeV) is  $1.0 \times 10^6$  (as calculated by ANISN), the measured average cross section  $\sigma_{n,p}$  is 1.7 mb.

Equation 11 may be used to calculate the  $^{17}\text{O}$  interference at any irradiation location in a cyclic analysis if the fast-neutron flux is known. The saturated rate of production of delayed neutrons from the  $^{17}\text{O}$  reaction is

$$R = 0.95 \sigma_{n,p} \phi F \quad (36)$$

As an example, Figure 44 and Table 14 summarize the calculated  $^{17}\text{O}$  effect for a hypothetical 10-ml sample containing 10 ppm natural uranium analyzed in the  $^{252}\text{Cf}$  activation facility. The experimental counter background of 8 counts/min was used to calculate background counts. Equations 11 and 34 were used to calculate counts from  $^{17}\text{O}$ , and the counts from natural uranium were calculated as described previously. Transit times of 1.0 sec were assumed.

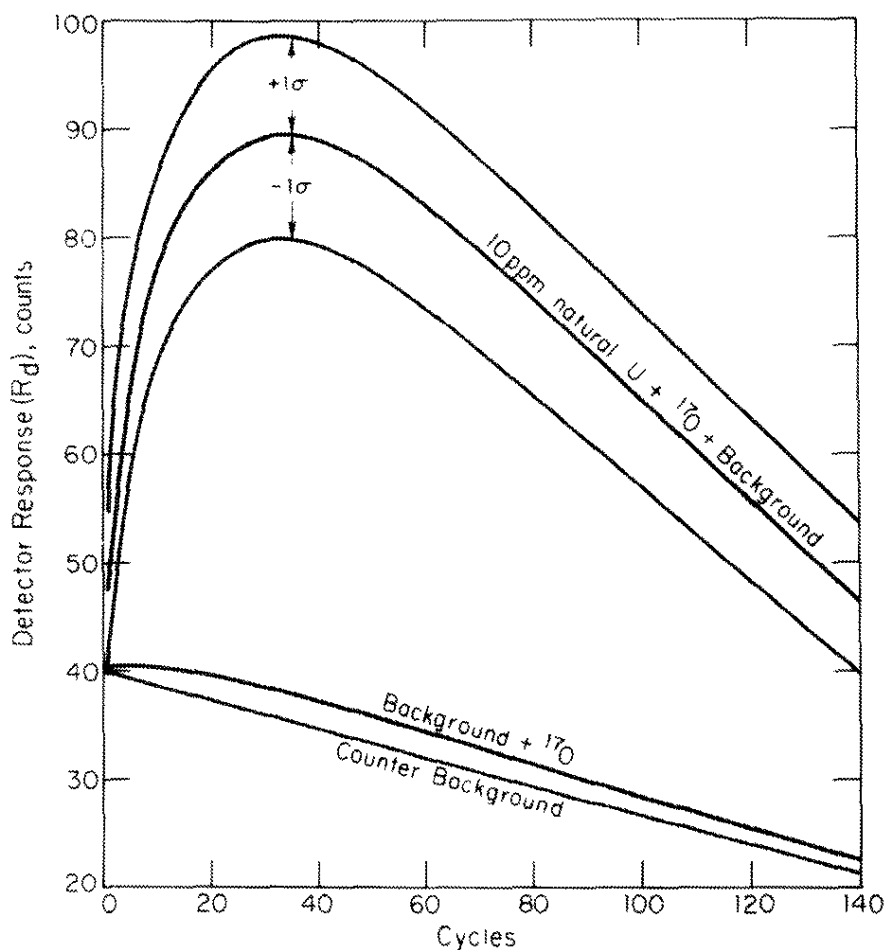


FIGURE 44. Calculated Detector Response for Aqueous Samples Containing 10 ppm Natural Uranium



TABLE 14

Delayed-Neutron Signal-to-Noise Ratios for Cyclic  
Analysis of Natural Uranium in Aqueous Solution<sup>a</sup>

<i>Cycles</i>	<i>Counts from <sup>17</sup>O</i>	<i>Background Counts</i>	<i>Counts from Uranium</i>	<i>Signal- to-Noise Ratio<sup>b</sup></i>
1	0.14	39.9	7.8	0.56
5	0.68	39.3	27.2	1.7
10	1.34	38.7	37.2	2.1
20	2.18	37.3	46.8	2.5
30	2.45	36.0	50.7	2.7
40	2.47	34.7	51.6	2.7
50	2.39	33.3	50.6	2.7
100	1.63	26.7	36.8	2.3
150	0.93	20.0	21.8	1.7

a. Equal counting and irradiation intervals;  
transit times = 1.0 sec.

b. The signal-to-noise ratio is defined as:

$$S/N = \text{counts from uranium} / 2 \sqrt{\text{sum of counts from all sources}}$$

The calculated signal-to-noise ratio (Table 14) = (ratio of calculated uranium counts)/2 (sum of neutron counts from all sources)<sup>1/2</sup>. Signal-to-noise ratios greater than one indicate that 10 ppm of natural uranium is detectable at the 2 $\sigma$  confidence level.

Identical calculations were made for the 100-mg <sup>252</sup>Cf facility to determine detection sensitivities for natural uranium (0.5 ppm). For analyses near the detection limit, the <sup>17</sup>O interference is calculated and removed from the detector response as a background contribution.

## COMPUTER DATA PROCESSING

The master equations of activation analysis has been derived previously. This equation includes cyclic considerations and is included in this section for reference; the elemental concentration in ppm is given by:

$$P = \frac{K}{EW} \cdot \frac{A \cdot 10^6}{B \cdot N_o} \cdot \frac{\lambda}{ISCDF} \cdot \frac{1}{R} \quad (37)$$

The K/EW term depends on experimental parameters:

K = photopeak area, counts

E = detector efficiency for the particular gamma ray energy

W = sample weight in grams

The  $A \cdot 10^6 / B \cdot N_o$  term depends on the target nuclei:

A = atomic weight of target

B = isotopic abundance of target

$N_o$  = avogadro's number

The  $\lambda / ISCDF$  term involves timing information and decay parameters of the product nucleus:

$\lambda$  = decay constant,  $\text{sec}^{-1}$

I = gamma ray abundance

S, C, D, F = irradiation, counting, decay, and cyclic factors previously defined.

The 1/R term depends on the cross section of the induced reaction and on the neutron flux and energy distribution at the irradiation site.

The specific rate R is the specific neutron capture reaction rate in captures/(sec-g).

Data are reduced sequentially by programs in the computer, the last of which solves this master activation analysis equation. The data reduction flow sheet is illustrated in Figure 45; boxes denote program names and all-capital names refer to tape or disc data files.

## TRANSCRIBE

The first step in the data reduction flowsheet is the accumulation of the gamma ray spectrum in the 4096-channel multichannel analyzer memory. Baseline and gain adjustments are normally set at 2.00 channels/keV. The accumulated spectrum is then transferred to the nine-track magnetic tape along with an identifier tagword. The tape containing the spectra of all samples counted during a one-day period and a header record are transferred by TRANSCRIBE to a temporary numbered storage tape. The header record contains other experimental information eventually used by program SIFTER to solve the master equation. The header information is supplied manually by the facility operator on a standard FORTRAN coding form. This operator-supplied experimental data is in a coded format listed in Table 15. The output of TRANSCRIBE is manually checked to ensure that the correct header record was attached to the spectrum. A sample TRANSCRIBE output is shown in Table A-1.

As indicated in the flowsheet, ADDER and COPY may be used to assemble a master storage tape and a duplicate tape for permanent retention of all gamma ray spectra and of header records for every sample analyzed.

## RAGS

Program RAGS<sup>16</sup> sequentially analyzes the gamma ray spectra stored on the temporary storage tape and writes the peak energies, peak areas, and the 2 $\sigma$  statistical uncertainty in the peak areas, and the header record onto disk data file RAGOUT. The hard copy output from RAGS may be examined manually before execution of SIFTER. Table A-2 is a sample RAGS output.

## SIFTER

The origin and content of each disk data file used by SIFTER, as shown in the data reduction flowsheet, are considered below. These data libraries are stored in EDIT library disk space and are called as needed by SIFTER. After RAGS has operated on the gamma ray spectrum, the RAGOUT file has all of the experimental information required for qualitative and quantitative analysis by SIFTER.

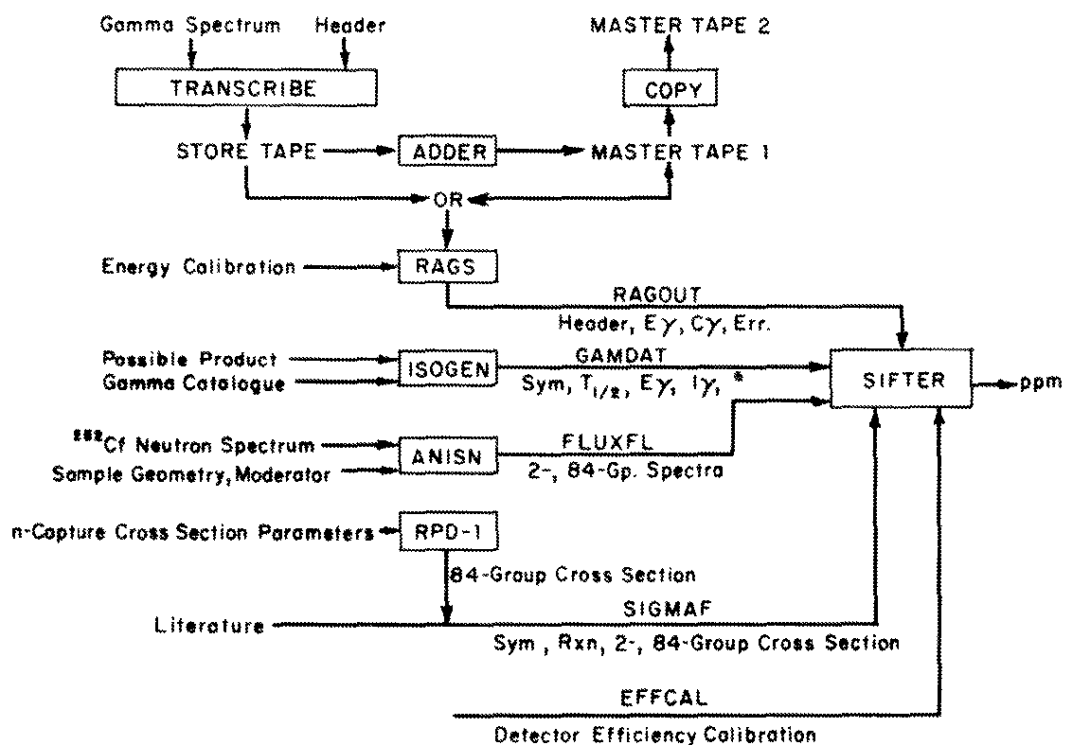


FIGURE 45. Data Reduction Flowsheet

TABLE 15

Coding Format for Header Records

Column	Information Type	Example
1,2	Year	
3,4	Month	760331144600 Count Start Occurred
5,6	Day	at 14:46:00 (2:46:00 p.m.) on
7,8	Hour	March 31, 1976
9,10	Minute	
11,12	Second	
13,14	Counting Arrangement	(01 - 05)
15-18	Counting Time	(3003 $\equiv$ $3.00 \times 10^3$ sec)
19-22	Decay Time	(1305 $\equiv$ $1.30 \times 10^5$ sec)
23-27	Sample Weight	(12343 $\equiv$ $1.234 \times 10^3$ mg)
28-31	Irradiation Time	(1003 $\equiv$ $1.00 \times 10^3$ sec)
32,33	Number of Irradiation-Counting Cycles	
34,35	Irradiation Tube	(12 $\equiv$ Ring 1, Tube 2)
36-37	Comments	
78,79	Tagword	

## EDIT Data Files

GAMDAT file (Table A-3) contains the spectroscopic decay data for all gamma rays emitted by each possible neutron activation product as well as by other commonly observed fission product nuclides. These data were obtained from Reference 6; they include product nuclide symbol, half-life, and the tabulated gamma ray energies and absolute decay abundances listed in decreasing order of abundance.

FLUX file (Table A-4) is a library of normalized 2-group and 84-group neutron fluxes for each source/moderator/sample configuration. The 2-group (thermal and epithermal) fluxes used in the 100-mg  $^{252}\text{Cf}$  facility were measured experimentally at each of the two rings of irradiation sites. The 84-group fluxes (used only in the 17-mg  $^{252}\text{Cf}$  facility) were taken from the ANISN computer code.

SIGMAF file (Table A-5) contains data specific to the particular nuclear reaction forming the product nuclide. The file includes the product nuclide symbol, the reaction symbol, the target isotopic abundance and atomic weight, and the tabulated 2200-m/sec cross section and resonance integral for the reaction. Cross sections listed in 84-group format are included when available.

EFFCAL file (Table A-6) contains the absolute detector efficiency vs. energy calibration data measured experimentally for each numbered detector-sample geometry. The reciprocal of the absolute efficiency is listed for each energy for counting arrangements used in the 100-mg  $^{252}\text{Cf}$  facility.

## SIFTER Flow Diagram

Figure 46 is a simplified flow diagram of SIFTER. After initialization, the RAGOUT data file containing header information, peak energies, areas, and uncertainties from the first spectrum are read into SIFTER. The peak energies found by RAGS are matched to a tabulated set of self-consistent and accurately measured photopeak energies of isotopes commonly produced in samples by neutron irradiation. The photopeak energies in RAGOUT are refitted by the least squares method to this consistent set. If the counting geometry contained in the header record IGEO matches that in an EFFCAL file, the photopeak areas are multiplied by the inverse of the efficiency as interpolated by a least squares energy fit from the data stored in EFFCAL. If a calibrated counting arrangement was not used, the efficiency is set to one. Next, FLUX file is searched for the appropriate flux for the irradiation position. No match means that the

absolute neutron capture rate cannot be calculated, and a dis/(min-g) value is calculated. If a tube match is found, the flux is corrected for decay of  $^{252}\text{Cf}$  from the calibration data to the date of activation. Next, the first isotope ISO listed in the GAMDAT file and its spectroscopic decay data listed in order of decreasing decay abundance are read. The photopeak energy  $\text{EN}_\gamma$  of the most-abundant gamma ray in ISO is searched against the list of RAGOUT refitted energies  $\text{E}_\gamma$ . When a match is found,  $\text{EN}_\gamma = \text{E}_\gamma \pm 0.3 \text{ MeV}$ , the S,C,D, and F terms are calculated from the listed half-life in GAMDAT, from the experimental irradiation, decay, and counting times, and from the number of irradiation cycles listed in RAGOUT. If no gamma ray match is found, the next-most-abundant gamma ray listed in ISO is searched against RAGOUT. This indexing continues through the gamma ray list of ISO. At the end of data for the ISO, the next isotope listed in GAMDAT is read, and the energy match is continued. If a gamma match has been found and the S,C,D,F terms have been calculated, the dis/(min-g) is calculated and printed out if flux data are absent. If flux parameters are available, the SIGMAF file is searched for a match between ISO and the first reaction product symbol JSO. A match signals a RATE calculation using the normalized 84-group fluxes and cross sections. If 84-group data are not available, 2-group fluxes and cross sections are used. If neither multigroup nor 2-group cross section data exist, the RATE is set to one, and a relative concentration is printed. Calculations for RATE = 1 indicate that a comparative standard must be run for that element.

At this point, all of the experimental and tabulated information required for the calculation of the concentration and the uncertainty of the neutron capture parent of ISO is available. This concentration (ppm), its uncertainty, the nuclide symbol, the reaction symbol, and the RATE calculation comment (Rate = 1, 84-group or 2-group) are printed out (Table A-7).

Often a particular nuclide can be produced by neutron reactions such as (n,p), (n, $\alpha$ ), and (n, $\gamma$ ) reactions on different parent nuclides. SIGMAF file includes all possible production mechanisms for each product JSO. To account for these reactions, the entire SIGMAF file is searched for all possible symbol matches. Very little fast neutron (n,p) or (n, $\alpha$ ) cross section data are available for inclusion in 84-group format; therefore, a RATE = 1 calculation normally signals possible interference.

The end of the SIGMAF file signals the search against RAGOUT of the next-most-abundant gamma ray in the product ISO. The process is continued until the end of the list of possible gamma rays for the product ISO is reached, and then a new ISO is searched in the same manner. This searching loop continues until the end

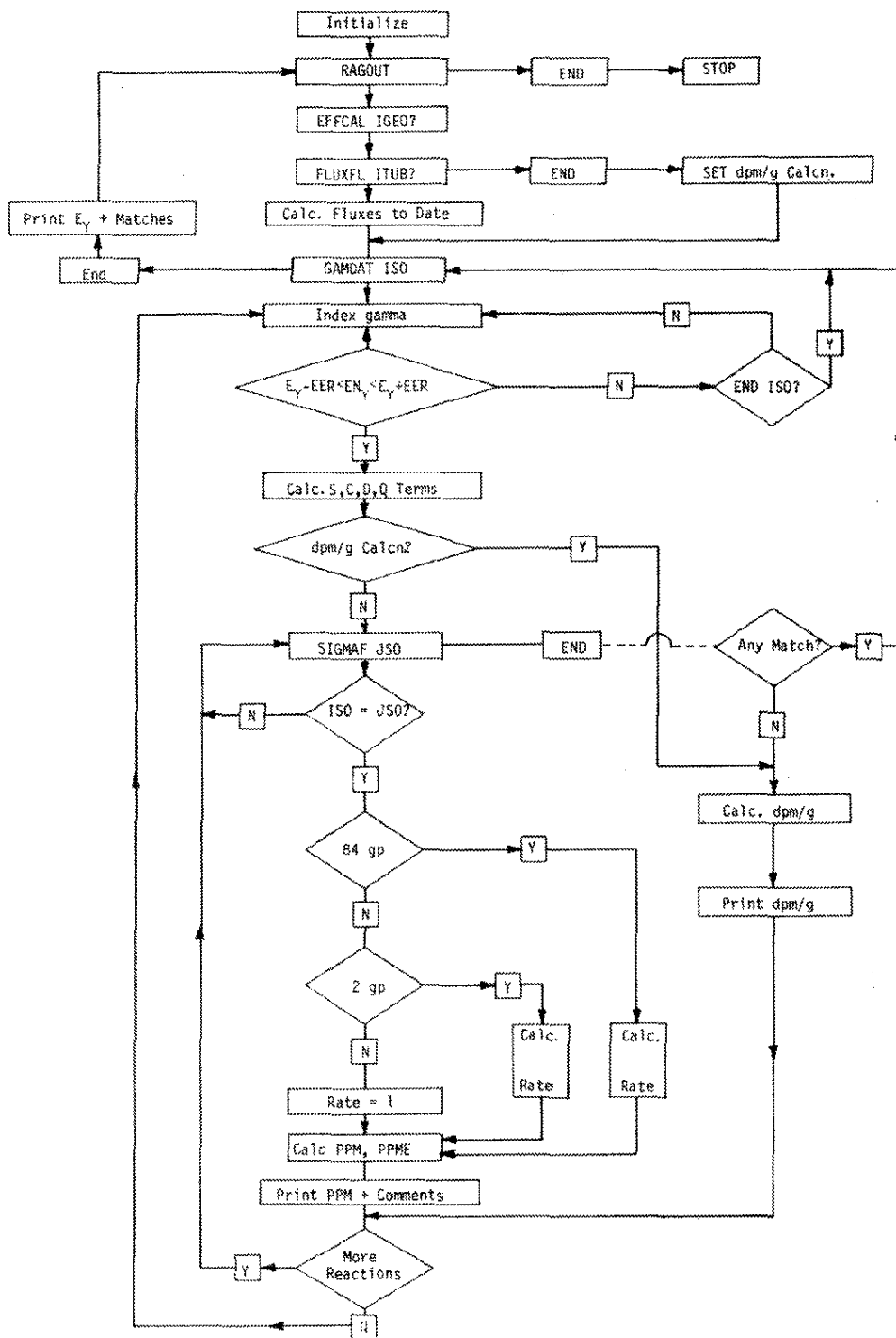


FIGURE 46. SIFTER Program Flowsheet

of the GAMDAT file is reached. Next a listing is made of each refitted RAGOUT photopeak energy  $E_\gamma$ , photopeak areas corrected for efficiency, percent uncertainty in the area, and all nuclide symbols which had a gamma ray matching that energy (Table A-7). This latter listing provides a quick check and demonstrates whether all significant gamma rays were accounted for in the search procedure and also whether legitimate interferences between isotopes have occurred which would render the calculated concentration questionable.

Following this listing, the next spectral analysis RAGOUT block is read and the entire process repeated until all spectra have been scanned.

### Interpretation of SIFTER Output

Interpreting SIFTER outputs is not always straightforward because: 1) the same product nuclide can be formed by different reaction mechanisms, e.g.,  $^{23}\text{Na}(n,\gamma)^{24}\text{Na}$  and  $^{27}\text{Al}(n,\alpha)^{24}\text{Na}$ ; 2) most nuclides have more than one intense gamma ray and multiple values for the calculated concentration. (for example,  $^{60}\text{Co}$  emits gamma rays of 1333.495 and 1172.210 MeV); 3) some judgment is required to determine whether the experimental timing conditions allow for a particular product to be present; 4) poor counting statistics may skew a peak so that the peak-centered energy calculated by RAGS does not match ( $\pm 0.3$  MeV) the gamma energy listed in GAMDAT; 5) double-escape and single-escape peaks are not recognized as such; 6) no partitioning of activity among isomers is made (for example,  $^{152}\text{Eu}$  and  $^{152\text{M}1}\text{Eu}$  both contribute to the intensity of the 121.78- and 344.31-KeV gamma ray photopeaks); 7) statistical fluctuations in the spectrum may occasionally be analyzed as a photopeak and indicates matched nuclide that may not actually be present in the sample; 8) if tabulated cross sections are not yet available for reaction, the rate is set to one and no concentration can be calculated for that element; 9) concentration values of the same element taken from multiple counts of a particular sample must be edited to arrive at a single best value.

These limitations to a straightforward interpretation currently require that SIFTER outputs be examined by trained personnel and that judgments made in the final interpretation.

Table A-7 and Table A-8 are SIFTER outputs of a freeze-dried vegetation sample. The header record information at the top of the output indicates that the spectrum tagword is 26 and that the analysis was performed at 11:17 p.m. on 3/17/76. The count time (CT) decay time DT and irradiation times TIR are indicated in seconds. The sample weight Wt, count geometry IGEO, irradiation



tube ITUB and the number of cycles ICYC are also shown. The sample description is listed next as well as the number of statistically significant photopeaks NPK. The photopeak energies (not refitted) found by RAGS are listed in the seven columns in order of increasing energy. The RAGOUT energies which matched an abbreviated list of self-consistent energies for common activation products are listed. A third-order, least squares energy refit was performed on the 18 matched photopeak energies. The columns in Figure A-7a are: product nuclide symbol, the refitted experimental gamma ray energies, the reaction symbol [for example, GO = (n, $\gamma$ ), AO = (n, $\alpha$ ), PO = (n,p), and GI = (n, $\gamma$ ) reaction leading to the first metastable state of the product isotope], the concentration (ppm) and statistical error, and a comment denoting the method of calculating the specific neutron capture rate.

Table A-10 lists each photopeak energy, peak area (corrected for efficiency), percent uncertainty in peak area, and the symbols of products having energy matches to that photopeak.

Many of the difficulties in interpreting SIFTER outputs are evident in these two tables. For example, the 312.90-keV photopeak has never proven reliable for the analysis of potassium, probably because the absolute gamma ray abundance is incorrect. The 102.70-keV photopeak attributed to  $^{81m}\text{Se}$  is actually the 103.20 keV photopeak of  $^{153}\text{Sm}$ . The five  $^{82}\text{Br}$  ppm values must be weighted to arrive at a best value; however, such multiple energy matches provide unequivocal evidence of the presence of bromine. The 487.40\* photopeak listed for tellurium is actually the 487.10-keV peak from  $^{140}\text{La}$ . (The asterisk indicates a relative gamma ray abundance and a relative ppm value.) The 121.78-keV photopeak is the result of decay of both  $^{151}\text{Eu}$  and  $^{152\text{m}}\text{Eu}$  which results in an abnormally high concentration of both. The 328.50-keV  $^{193}\text{Ir}$  peak actually is  $^{140}\text{La}$ . All other values are judged correct.

Data reduction program development in progress includes a routine to calculate "less than or equal to" values for elements not detected based on experimental parameters and on an interpolation of backgrounds between the two nearest real photopeaks. The GAMDAT library will be updated to contain a completely self-consistent set of photopeak energies which will eliminate many false energy matches. Finally, SIFTER will be replaced with RICHES,<sup>17</sup> a program designed to output a single best value for each element detected based on all counting data (multiple spectra, isotopes, and gamma rays) from each sample.

## Analysis of Test Mixture

An earlier version of SIFTER was used as the basic data reduction routine in the original 17-mg  $^{252}\text{Cf}$  facility. To verify the applicability of the absolute technique to complex mixtures, a test mixture supplied in 1973 by the USAEC as part of an evaluation of activation analysis using  $^{252}\text{Cf}$  sources was analyzed. This test mixture had been analyzed previously at Savannah River by classical comparative standard methods. The first analysis was performed before the pneumatic rabbit system was operational, and the results were based on counting of normally used longer-lives (>2 minutes) activation products. After installation of the rabbit system and development of SIFTER, the test mixture was analyzed again using automated absolute activation analysis (AAAA).

Results and comparison of the two techniques are summarized in Table 16. The precision and accuracy of AAAA is equivalent to the comparative technique. The analysis time for the absolute technique, however, is reduced because: 1) comparative standards were not prepared, irradiated, and counted; 2) the pneumatic transfer system permits analysis based on short half-life product isotopes; and 3) data reduction time using SIFTER is much less than normal reduction time for comparison to standard data.

TABLE 16

## Analysis of Test Mixture

<i>Element</i>	<i>Concentration, ppm</i>		
	<i>Comparative</i>	<i>Absolute (AAA)</i>	<i>USAEC Reported</i>
Se	-	870 $\pm$ 10	840
V	20 $\pm$ 1	17 $\pm$ 1	20
Al	420 $\pm$ 40	330 $\pm$ 20	370
Cu	130 $\pm$ 30	60 $\pm$ 30	95
Co	140 $\pm$ 8	150 $\pm$ 5	140
Mo	3200 $\pm$ 300	3300 $\pm$ 100	2910
Mn	5.8 $\pm$ 0.8	4.5 $\pm$ 0.5	5
As	81 $\pm$ 5	72 $\pm$ 2	70
Eu	0.94 $\pm$ 0.06	0.88 $\pm$ 0.06	0.9
Na	731 $\pm$ 9	630 $\pm$ 10	690
Hg	985 $\pm$ 25	900 $\pm$ 100	930
Zn	935 $\pm$ 45	680 $\pm$ 110	930
Cd	<u>2092 <math>\pm</math>44</u>	<u>2100 <math>\pm</math>80</u>	2330
Average Deviation	$\pm$ 10%	$\pm$ 11%	
Preparation, Irradiation Time	30 days	2 days	
Counting, Data Analysis	4 days	1 day	

## RESULTS AND APPLICATIONS

---

This section discusses results of the application of AAAA to many known multielement standards. Some unique applications of AAAA to Savannah River programs are presented. For comparison purposes, only those samples analyzed in the 100-mg  $^{252}\text{Cf}$  facility (since July 1975) are considered here; however, many samples were analyzed with quite similar results with the 17-mg  $^{252}\text{Cf}$  source (July 1973 - July 1975). The results shown in this section were edited from actual SIFTER outputs as described in the previous section.

### SOLID STANDARDS

#### Standard Coal (NBS Standard SRM-1632)

Two 10-ml samples of standard coal from the National Bureau of Standards (NBS) were weighed into sample irradiation containers. This material was used as received in finely ground and blended forms. Enough distilled water was added to displace all air from the containers. The first sample was irradiated (10-sec) and counted (10-sec) cyclically (40 cycles) for delayed neutrons (natural uranium analysis) and for short-lived gamma activities ( $^{46}\text{Mn}$ ,  $^{77}\text{Se}$ ,  $^{28}\text{Al}$ ,  $^{52}\text{V}$ ). The other sample was irradiated for 2 weeks, and then gamma counts were taken after decay periods of 60 seconds, 1 day, 7 days, and 14 days for medium-lived and long-lived species. Results of the absolute analysis are shown in Column 4 of Table 17. The concentration values certified by NBS are indicated as well as the values found by comparative analyses conducted by four separate laboratories using classical instrumental reactor neutron activation analysis (INAA). AAAA results are as precise and accurate as those reported by INAA using high flux [ $10^{12}$  to  $10^{13}$  neutrons/( $\text{cm}^2\text{-sec}$ )] irradiations and comparative standards.

#### Standard Fly Ash (NBS Sample SRM-1633)

Table 18 summarizes the results obtained by AAAA for the standard fly ash. As with the standard coal, agreement between INAA and AAAA values is quite good. Another very important factor involved in the absolute technique which must be considered is the effect of the matrix. Based on a comparison of 11 key elements measured by AAAA and INAA in NBS samples SRM-1632 and SRM-1633, the increase in self-absorption between the coal and fly ash is  $\leq 4\%$ . The 11 key elements are major constituents

TABLE 17

Analysis of NBS Coal Standard SRM-1632

Element <sup>a</sup>	Concentration		
	NBS	INNA <sup>a</sup>	AAAA <sup>b</sup>
← wt % →			
Al		1.85 ±0.13	1.62 ±0.13
Fe	0.87 ±0.03	0.84 ±0.04	0.89 ±0.03
K		0.28 ±0.03	0.30 ±0.02
Mg		0.20 ±0.05	0.82 ±0.20
← ppm →			
Na		414 ±20	380 ±3
Cl		890 ±125	800 ±50
Sc		3.7 ±0.3	3.98 ±0.04
Ti	800	1040 ±110	995 ±100
V	35 ±3	36 ±3	33 ±3
Cr	20.2 ±0.5	19.7 ±0.9	18.5 ±1.7
Mn	40 ±3	43 ±4	43 ±1
Co	6	5.7 ±0.4	6.0 ±0.02
Zn	37 ±4	30 ±10	52 ±4
As	5.9 ±0.6	6.5 ±1.4	4.7 ±0.5
Br		19.3 ±1.9	15 ±1
Sr		161 ±16	170 ±20
Ba		350 ±30	310 ±30
Sb		3.9 ±1.3	3.8 ±0.2
Cs		1.4 ±0.1	3.5 ±1.3
La		10.7 ±1.2	8.3 ±0.2
Ce		19.5 ±1.0	26 ±5
Sm		1.7 ±0.2	1.4 ±0.10
Yb		0.7 ±0.1	1.0 ±0.2
U		1.41 ±0.07	1.34 ±0.50
Eu		0.33 ±0.03	0.30 ±0.10
Ga			5 ±1
Dy			1.0 ±0.1
Se		3.4 ±0.2	3.1 ±0.6

a. Value reported by Instrumental Neutron Activation Analysis Round Robin, J. M. Ondov, et al., *Anal. Chem.* 47, 1102 (1975).

b. Value found by absolute activation analysis at SRL. Uncertainties based on counting statistics only.

TABLE 18

## Analysis of NBS Fly Ash Standard SRM-1633

Element	<i>Concentration</i>		
	<i>NBS</i>	<i>INAA</i>	<i>AAAA</i>
	$\longleftrightarrow$ wt % $\longleftrightarrow$		
Fe		6.2 $\pm$ 0.3	6.3 $\pm$ 0.1
Mg		1.8 $\pm$ 0.4	6.3 $\pm$ 0.3
Al		12.7 $\pm$ 0.5	10.4 $\pm$ 0.6
Si		21 $\pm$ 2	
Ca		4.7 $\pm$ 0.6	
K		1.61 $\pm$ 0.15	1.51 $\pm$ 0.05
	$\longleftrightarrow$ ppm $\longleftrightarrow$		
Na		3200 $\pm$ 400	2820 $\pm$ 50
Sc		27 $\pm$ 1	26.8 $\pm$ 0.2
Mn	493 $\pm$ 7	496 $\pm$ 19	520 $\pm$ 20
Co	38	42 $\pm$ 1	38 $\pm$ 2
As	61 $\pm$ 6	58 $\pm$ 4	54 $\pm$ 3
Sr	1380	1700 $\pm$ 300	1340 $\pm$ 100
Sb		6.9 $\pm$ 0.6	7.4 $\pm$ 0.3
Ba		2700 $\pm$ 200	3200 $\pm$ 400
La		82 $\pm$ 2	68 $\pm$ 2
Sm		12.4 $\pm$ 0.9	11 $\pm$ 1
Dy			9 $\pm$ 2
Hf		7.9 $\pm$ 0.4	7.5 $\pm$ 0.4
W		4.6 $\pm$ 1.6	6 $\pm$ 1
Cr	131 $\pm$ 2	127 $\pm$ 6	120 $\pm$ 5
Br		12 $\pm$ 4	6 $\pm$ 1
Ce		146 $\pm$ 15	176 $\pm$ 4
Yb		7 $\pm$ 3	4.7 $\pm$ 0.4
Lu		1 $\pm$ 0.1	4 $\pm$ 1
Zn	210 $\pm$ 20	216 $\pm$ 25	270 $\pm$ 30
Se	9.4 $\pm$ 0.5	10.2 $\pm$ 1.4	8.7 $\pm$ 1.8
Cs		8.6 $\pm$ 1.1	8.5 $\pm$ 0.5
Tb		1.9 $\pm$ 0.3	1.2 $\pm$ 0.2
Ta		1.8 $\pm$ 0.3	2.0 $\pm$ 0.1
Cl		42 $\pm$ 10	40 $\pm$ 8
Ti		7400 $\pm$ 300	6000 $\pm$ 400
V		235 $\pm$ 15	196 $\pm$ 10

and those elements which, by experience, have characteristically provided results which are both precise and accurate: Al, Fe, K, Na, Sc, V, Cr, Mn, Co, La, and Sm. The average difference for these elements between AAAA and INAA is 4.5% for the coal and 8.2% for the fly ash. These results and those reported below for wetted USGS rock standards provide evidence for the lack of major matrix effects.

#### Rock Standards (USGS Samples GSP-1 and BCR-1)

Tables 19 and 20 summarize results of AAAA on wetted samples of standard (powdered) rock from the U. S. Geologic Survey (USGS). Results for most elements agree with those values selected as "correct." Again, no matrix effects are evident for these solids. The serious discrepancy in the magnesium concentration by AAAA for coal, fly ash, and both rock standards is caused by  $^{27}\text{Mg}$  produced by the fast neutron interference reaction  $^{27}\text{Al}(n,p)^{27}\text{Mg}$  and by the desired thermal neutron capture of magnesium. This interference as well as other potential interferences are flagged by the SIFTER output and require validity judgment. Another interference which has been noted is the  $^{27}\text{Si}(n,p)^{28}\text{Al}$  reaction, which interferes with the analysis of aluminum in materials where the silicon/aluminum weight ratio exceeds ~100.

#### LIQUID STANDARDS

A series of dilute liquid elemental standards were analyzed by AAAA. The results and the percent deviation between the standard value and that found by AAAA are listed in Table 21. No uncertainties are listed for the standards which were prepared from commercially-available atomic absorption standards.

These results and the results of the rock, coal, and fly ash analyses indicate that AAAA can be applied to many different solid and liquid samples such as other coals, fly ash, soils, vegetation, and process samples commonly submitted for analysis.

#### ELEMENTAL DETECTION LIMITS

TFIJCL, a version of the program SIFTER which solves the master activation program in reverse was written to provide an estimate of elemental detection sensitivities for samples irradiated and counted in the 100-mg  $^{252}\text{Cf}$  facility. The detectable limit was assumed to be the 100 net counts in the photopeak of the most-abundant gamma ray derived from the neutron capture produce of each element. In the calculation, data files are the same as those in SIFTER, namely, EFFCAL, SIGMA, FILE, and

TABLE 19

## Analysis of USGS Rock Standard GSP-1

<i>Element</i>	<i>USGS Value<sup>a</sup></i>	<i>Absolute Value<sup>b,c</sup></i>
----------------	-----------------------------------	---

## a. Major constituents, wt %

Na	2.08	2.04 ±0.04
K	4.59	4.9 ±0.6
Fe	3.03	3.0 ±0.2
Al	8.07	7.64 ±0.16
F	0.32	0.32 ±0.10
Ti	0.399	0.41 ±0.03
Mg	0.58	5.0 ±0.5

## b. Minor constituents, ppm

Zn	98	150 ±30
Ce	394	440 ±100
La	191	180 ±10
Co	6.4	7.6 ±2.5
Sc	7.1	7.2 ±0.2
Sb	3.1	3.3 ±0.9
Hf	15.9	16.3 ±0.5
V	52.9	51 ±6
Eu	2.4	2.0 ±0.5
Cl	300	400 ±140
Mn	331	366 ±30
Dy	5.4	3.3 ±1.5
Sm	27.1	30 ±1
Hg	15.5	11 ±5
Au	0.0016	0.024 ±0.009
Cr	12.5	19 ±7
Tb	1.3	1.8 ±0.7
Ta	1.0	1.4 ±0.5

a. F. J. Flanagan, *Geochimica et Cosmochimica Acta* 37, 1189 (1973).

b. Value in ppm unless otherwise indicated.

c. Uncertainty based on counting statistics only.



TABLE 20

Analysis of USGS Rock Standard BCR-1

Element	USGS Value <sup>a</sup>	Absolute Value <sup>b,c</sup>
a. Major constituents, wt %		
Na	2.43	2.53 ±0.05
Mg	2.09	6.0 ±0.3
Al	7.20	6.7 ±0.2
K	1.41	1.44 ±0.5
Ti	1.28	1.29 ±0.25
Mn	0.141	0.155 ±0.001

## b. Minor constituents, ppm

Ba	675	600 ±100
V	399	405 ±10
Co	38	33 ±10
Dy	6.3	5.7 ±0.7
Sr	330	900 ±400
Sc	33	40 ±1
La	12.8	22 ±4
Sm	6.6	6 ±1
Yb	3.36	4 ±1
Lu	0.55	2.5 ±0.4
Cr	17.6	25 ±5
Ce	53.9	36 ±5
Tb	1.0	1.9 ±0.3
Hf	4.7	6 ±1
Sb	0.69	1.3 ±0.5
Nd	29	68 ±20
Ta	0.91	1.5 ±0.6

a. F. J. Flanagan, *Geochimica et Cosmochimica Acta* 37, 1189 (1973).

b. Value in ppm unless otherwise indicated.

c. Uncertainty based on counting statistics only.

TABLE 21

## Absolute Analysis of Atomic Absorption Liquid Standards

<i>Element</i>	<i>Standard Value, ppm</i>	<i>Absolute Value, ppm</i>	<i>Percent Deviation from Standard</i>
Cs	97.9	100.3 $\pm$ 2.7	+2.5
Sc	98.7	115.1 $\pm$ 1.0	+16.5
Co	98.8	109.6 $\pm$ 4.0	+10.9
Se	96.7	97.9 $\pm$ 9.8	+1.2
Cr	100.0	100 $\pm$ 5	0.0
Ta	100.5	110 $\pm$ 3	+9.5
Ge	100	95 $\pm$ 39	-5.0
Dy	9.93	10.1 $\pm$ 1.0	+1.7
Mn	99.4	94 $\pm$ 1	-5.4
Na	100.1	103 $\pm$ 4	+2.9
K	100.2	122 $\pm$ 5	+21.8
La	98.3	99 $\pm$ 3	+0.7
As	99.1	104 $\pm$ 4	+4.9
W	105.6	93 $\pm$ 2	-11.9
Sm	9.77	9.3 $\pm$ 0.3	-4.8
Ho	10.0	10.3 $\pm$ 1.0	+3.0
Yb	100.2	91 $\pm$ 19	-9.2
Hg	99.8	130 $\pm$ 30	+30.3

GAMDAT. The most-sensitive product isotope from each element was selected from one of the four irradiation, decay, and counting regimes listed in Table 22. The detection limits are interference-free, and no effect of neighboring photopeaks or Compton background under the peak of interest is considered. As such, these limits have proven to be too low. As a rule of thumb, quantitative analyses in real samples usually require about 10 times higher concentration than those listed.

## SUMMARY OF ROUTINE ANALYSES

The automated and absolute activation analysis technique has been applied successfully to many different types of samples generated in different Savannah River programs. In some programs, activation analysis has been the only source of multielement data; in others, the technique is used in conjunction with other element analysis techniques to provide more-complete elemental analysis. These other techniques include inductively coupled plasma (ICP), DC arc emission spectroscopy, X-ray fluorescence, spark source mass spectrometry, and atomic absorption spectroscopy.

TABLE 22

Interference-Free Elemental Detection Limits<sup>a</sup>  
of the 100-mg <sup>252</sup>Cf Facility

<i>Element</i>	<i>Detection Limit, ppm</i>
Eu, Dy	<0.001
Mn, In, <sup>125</sup> I, Ir, Au, Lu, Ho, Sm, Re, <sup>239</sup> Pu <sup>b</sup>	0.001 - 0.01
Na, Sc, Co, Ga, Br, Ag, Sb, I, Cs, La, Pr, Tm, Yb, Ta, W, Pt, As, Se	0.01 - 0.1
Ar, K, Cr, V, Cu, Cd, Ce, Nd, Gd, Tb, Er, Hf, Hg, Ge, Sr, Nat. U <sup>b</sup>	0.1 - 1.0
Cl, Zn, Mo, Ru, Rh, Pd, Te, Ba, Os	1.0 - 10
F, Mg, Al, Ti, Ni, Sn, Rb, Y	10 - 100
Ca, Fe, Zr	100 - 1000
Pb, O, S	>1000

a. Based on 100 counts in photopeak from 15% efficient Ge(Li) detector. 10-gram sample is assumed. The lowest detection limit for each element was selected from one of the listed regimes:

<i>Regime</i>	<i>Irradiation Time</i>	<i>Decay Time</i>	<i>Count Time</i>	<i>Cycles</i>
1	6 sec	1 sec	6 sec	50
2	1 hr	5 min	30 min	1
3	1 day	1 hr	30 min	1
4	7 days	1 hr	30 min	1

b. Based on the 25% efficiency of the delayed neutron detector.

Table 23 shows the types of samples analyzed and the range of elemental concentrations determined as a function of sample type. Many of the results were determined in the 100-mg  $^{252}\text{Cf}$  facility. The results in Table 23 were part of a study of the effects of stack releases from a coal-fired powerhouse on minor and trace element contents of neighboring soil and vegetation.

Many other routine analytical applications have been found for neutron activation analysis. Applications include:

- Chloride content of various plastic tapes and oils used at Savannah River.
- $^{129}\text{I}$  and  $^{99}\text{Tc}$  content of irradiated light water reactor fuels.
- Uranium and plutonium content of plant process streams and waste.
- Mercury content of fresh water fishes.
- Elemental composition of plant radioactive waste sludges.
- U/Al ratio measurements in reactor fuel fabrication studies.
- Analysis of trace elemental content of streams following ion-exchange pre-concentration.
- Stream pollutant source identification.
- River sediment characterization.

TABLE 23

## Elemental Concentration Ranges Measured in Typical Samples

Element	Concentration, ppm				Detection Sensitivity <sup>a</sup>
	Coals	Fly Ash	Soils	Vegetation	
Sc	3 - 5	30 - 35	1 - 5	0.3 - 0.2	0.01 - 0.1
V	15 - 30	150 - 300	10 - 30	5 - 10	0.1 - 1
Mn	30 - 300	200 - 500	100 - 500	200 - 300	0.001 - 0.01
As	5 - 60	20 - 500	0.5 - 5		0.01 - 0.1
Br	5 - 30	5 - 100	0.5 - 5	10 - 50	0.01 - 0.1
Sr	100 - 150	500 - 1000			0.1 - 1
La	5 - 10	50 - 80	10 - 50	0.5 - 5	0.01 - 0.1
Sm	1 - 3	10 - 20	1 - 5	0.1 - 0.5	0.001 - 0.01
Cr	15 - 25	100 - 250	5 - 15	1 - 15	0.1 - 1.0
Co	5 - 10	50 - 100	1 - 2	0.5 - 2	0.01 - 0.1
Ga	5 - 10	50 - 100	1 - 10		0.01 - 0.1
Sb	1 - 5	5 - 30	0.2 - 1		0.01 - 0.1
Cs	1 - 5	10 - 20	0.5 - 5	0.1 - 2	0.01 - 0.1
Ce	15 - 30	100 - 300	30 - 80	0.1 - 10	0.1 - 1
Tb	0.1 - 1	1 - 5	0.3 - 2		0.1 - 1
Yb	0.5 - 2	5 - 20	0.5 - 2		0.01 - 0.1
Lu	0.5 - 1	3 - 5	0.5 - 1.5		0.001 - 0.01
Hf	0.5 - 1	5 - 10	5 - 10		0.1 - 1
Th	1 - 5	10 - 30	5 - 20	0.05 - 0.10	0.5 - 5
U	1 - 3	5 - 15	1 - 5		0.5 - 5
Zn	40 - 50	300 - 400	10 - 50	10 - 200	1 - 10
Se	1 - 5	10 - 20	1 - 10	0.03 - 0.15	0.01 - 0.1
Nd	20 - 40	150 - 250	10 - 50		0.1 - 1
Eu	0.2 - 5	1 - 30	0.1 - 0.5		<0.001
Tm				1 - 15	0.01 - 0.1
Ta	0.2 - 0.4	1 - 2	0.5 - 1.5		0.01 - 0.1
Ba	100 - 250	300 - 2000	100 - 300	150 - 250	1 - 10
Mo	1 - 10	20 - 100			1 - 10
W		5 - 20	0.5 - 2		0.01 - 0.1
Rb	20 - 50	150 - 300	10 - 30	5 - 50	10 - 100
Dy	0.5 - 1	5 - 10	1 - 3		<0.001
Fe(%)			0.2 - 1.5		0.01 - 0.1
Na			100 - 500	10 - 100	0.01 - 0.1
Al(%)			0.5 - 2	0.007 - 0.09	0.001 - 0.01
Ti(%)			0.1 - 0.5		0.001 - 0.01
K(%)			0.05 - 0.3	0.6 - 1.1	0.001 - 0.01
Mg(%)			0.5 - 2	N.D. - 0.4	0.001 - 0.01
Cl(%)				0.14 - 0.27	0.001 - 0.01

a. The calculated detection sensitivities refer to the 100-mg Cf facility; values are interference free.



## APPENDIX A: Data Reduction Tables

Table A-1. TRANSCRIBE Output

14096	76	316	852	0	5	3.0E	02	6.0E	01	1.5E	03	1.3E	06	1	1	HORTON VEG SA 1ST CT 75-7521	1SPEC.NO=	1	
24096	76	316	852	0	5	3.0E	02	6.0E	01	1.5E	03	1.3E	06	1	1	HORTON VEG SA 1ST CT 75-7521	2SPEC.NO=	2	
34096	76	316	9	2	0	5	3.0E	02	6.0E	01	1.6E	03	1.3E	06	1	2	HORTON VEG SA 1ST CT 75-7522	3SPEC.NO=	3
44096	76	316	911	0	5	3.0E	02	6.0E	01	1.7E	03	1.3E	06	1	4	HORTON VEG SA 1ST CT 75-7523	4SPEC.NO=	4	
54096	76	316	920	0	5	3.0E	02	6.0E	01	1.7E	03	1.3E	06	1	5	HORTON VEG SA 1ST CT 75-7524	5SPEC.NO=	5	
64096	76	316	929	0	5	3.0E	02	6.0E	01	1.8E	03	1.3E	06	1	7	HORTON VEG SA 1ST CT 75-7525	6SPEC.NO=	6	
74096	76	316	942	0	5	3.0E	02	6.0E	01	1.2E	03	1.3E	06	1	8	HORTON VEG SA 1ST CT 75-7526	7SPEC.NO=	7	
84096	76	316	957	0	5	3.0E	02	6.0E	01	1.3E	03	1.3E	06	1	10	HORTON VEG SA 1ST CT 75-7527	8SPEC.NO=	8	
94096	76	316	10	5	0	5	3.0E	02	6.0E	01	1.4E	03	1.3E	06	1	11	HORTON VEG SA 1ST CT 75-7528	9SPEC.NO=	9
104096	76	316	1018	0	5	3.0E	02	6.0E	01	1.6E	03	1.3E	06	1	12	HORTON VEG SA 1ST CT 75-7529	10SPEC.NO=	10	
114096	76	316	1027	0	5	3.0E	02	6.0E	01	1.2E	03	1.3E	06	1	13	HORTON VEG SA 1ST CT 75-7530	11SPEC.NO=	11	
124096	76	316	1038	0	5	3.0E	02	6.0E	01	1.4E	03	1.3E	06	1	14	HORTON VEG SA 1ST CT 75-7531	12SPEC.NO=	12	
134096	76	316	1045	0	5	3.0E	02	6.0E	01	1.4E	03	1.3E	06	1	15	HORTON VEG SA 1ST CT 75-7532	13SPEC.NO=	13	
144096	76	316	1052	0	5	3.0E	02	6.0E	01	1.3E	03	1.3E	06	1	16	HORTON VEG SA 1ST CT 75-7533	14SPEC.NO=	14	
154096	76	316	1059	0	5	3.0E	02	6.0E	01	1.3E	03	1.3E	06	1	17	HORTON VEG SA 1ST CT 75-7534	15SPEC.NO=	15	
164096	76	317	8	6	0	5	1.0E	03	8.4E	04	1.5E	03	1.3E	06	1	1	HORTON VEG SA 2ND CT 75-7521	16SPEC.NO=	16
174096	76	317	824	0	5	1.0E	03	8.4E	04	1.6E	03	1.3E	06	1	2	HORTON VEG SA 2ND CT 75-7522	17SPEC.NO=	17	
184096	76	317	842	0	5	1.0E	03	8.5E	04	1.7E	03	1.3E	06	1	4	HORTON VEG SA 2ND CT 75-7523	18SPEC.NO=	18	
194096	76	317	9	9	0	5	1.0E	03	8.6E	04	1.7E	03	1.3E	06	1	5	HORTON VEG SA 2ND CT 75-7524	19SPEC.NO=	19
204096	76	317	928	0	5	1.0E	03	8.6E	04	1.8E	03	1.3E	06	1	7	HORTON VEG SA 2ND CT 75-7525	20SPEC.NO=	20	
214096	76	317	946	0	5	1.0E	03	8.7E	04	1.2E	03	1.3E	06	1	8	HORTON VEG SA 2ND CT 75-7526	21SPEC.NO=	21	
224096	76	317	10	4	0	5	1.0E	03	8.7E	04	1.3E	03	1.3E	06	1	10	HORTON VEG SA 2ND CT 75-7527	22SPEC.NO=	22
234096	76	317	1023	0	5	1.0E	03	8.8E	04	1.4E	03	1.3E	06	1	11	HORTON VEG SA 2ND CT 75-7528	23SPEC.NO=	23	
244096	76	317	1041	0	5	1.0E	03	8.8E	04	1.6E	03	1.3E	06	1	12	HORTON VEG SA 2ND CT 75-7529	24SPEC.NO=	24	
254096	76	317	1059	0	5	1.0E	03	8.8E	04	1.2E	03	1.3E	06	1	13	HORTON VEG SA 2ND CT 75-7530	25SPEC.NO=	25	
264096	76	317	1117	0	5	1.0E	03	8.9E	04	1.4E	03	1.3E	06	1	14	HORTON VEG SA 2ND CT 75-7531	26SPEC.NO=	26	
274096	76	317	1211	0	5	1.0E	03	9.2E	04	1.4E	03	1.3E	06	1	15	HORTON VEG SA 2ND CT 75-7532	27SPEC.NO=	27	
284096	76	317	1229	0	5	1.0E	03	9.2E	04	1.3E	03	1.3E	06	1	16	HORTON VEG SA 2ND CT 75-7533	28SPEC.NO=	28	
294096	76	317	1249	0	5	1.0E	03	9.3E	04	1.3E	03	1.3E	06	1	17	HORTON VEG SA 2ND CT 75-7534	29SPEC.NO=	29	



Table A-2. RAG Output

10 78/ 0714 13: 0: 0 1000= 1 CT= 3.000E 03 UT= 2.060E 06 WT= 3.150E 03 TIR= 1.210E 06 ICVC= 1 ITU08=15  
78-2346 KISER SA 10 NPK= 24

55.87	1.277E 05	111.731	4998.	1785.	102	118	1.541	3.296	1
122.26	6.234E 03	244.530	460.	4191.	238	253	1.967	29.650	1
140.65	1.427E 05	281.304	9301.	4418.	272	289	1.918	2.519	1
177.14	3.215E 03	354.279	169.	1314.	349	357	1.916	45.641	2
181.07	1.118E 04	362.149	571.	2299.	357	369	1.516	18.759	2
562.86	3.808E 04	1125.726	601.	890.	1116	1131	2.244	12.859	2
569.04	6.677E 04	1138.089	1041.	1868.	1131	1149	2.128	8.864	2
604.50	4.713E 05	1209.004	6908.	1168.	1197	1218	2.278	2.802	1
661.56	5.927E 04	1323.143	789.	921.	1314	1337	2.448	10.480	1
739.53	1.163E 04	1479.051	137.	709.	1464	1485	2.050	42.559	1
765.50	9.896E 03	1531.008	112.	537.	1523	1540	2.890	45.453	1
796.04	4.257E 05	1592.080	4632.	540.	1577	1599	2.470	3.105	2
802.46	6.876E 04	1604.124	527.	358.	1599	1616	2.450	11.294	2
889.77	6.459E 04	1779.541	628.	675.	1770	1793	2.562	11.491	1
934.92	7.031E 04	1869.848	651.	607.	1860	1881	2.858	10.893	1
1099.96	7.976E 04	2199.918	633.	625.	2182	2214	2.623	11.207	1
1121.33	6.748E 04	2242.664	526.	412.	2229	2252	2.772	11.649	1
1174.16	2.936E 05	2348.324	2188.	369.	2326	2359	2.731	4.622	1
1292.80	4.866E 04	2585.595	331.	216.	2556	2593	2.710	14.140	1
1333.63	2.753E 05	2687.264	1810.	88.	2652	2679	2.722	6.805	1
1366.40	1.880E 04	2733.192	121.	76.	2711	2746	2.428	23.178	1
1401.82	1.280E 04	2803.641	80.	28.	2793	2811	2.689	25.921	1
1409.67	5.691E 03	2818.143	36.	23.	2810	2829	3.223	43.128	1
1765.73	4.823E 03	3531.458	24.	12.	3521	3541	3.538	49.480	1

CODE= 1 MEMBER GAMDAT

[illegible]

Table A-3. Continued

CODE= 1 MEMBER GAMCAT										2 PAGE	
1481.90	2.57-1	1115.50	1.54-1	366.30	4.78-2	1623.50	4.83-3	1725.00	4.13-3		7.4
507.90	2.96-3	609.50	1.46-3	770.70	7.20-4	852.70	6.70-4				7.5
ZN 65	2.10816E	07	1								7.6
1115.52	5.07-1										7.7
CU 66	3.06000E	02	2								7.8
1039.00	9.00-2	833.60	2.50-3								8.1
ZN 69M	4.96800E	04	2								8.2
438.70	5.50-1	8.60	0.0 0								8.3
GA 70	1.26600E	03	4								8.4
1050.50	1.60-3	1039.40	1.60-3	175.30	1.60-3	1215.00	2.00-5				8.5
GA 72	5.07600E	04	46								8.6
834.02	9.56-1	2201.67	2.56-1	629.86	2.52-1	2507.80	1.27-1	894.22	9.95-2		8.7
2490.98	7.94-2	1050.69	6.89-2	600.85	5.45-2	1861.09	5.26-2	1596.65	4.30-2		8.8
1464.00	3.54-2	786.40	3.26-2	810.24	2.01-2	1276.75	1.56-2	1230.86	1.46-2		9.1
1260.10	1.10-2	970.54	1.09-2	2109.50	1.07-2	1680.77	9.95-3	861.11	9.18-3		9.2
1571.50	8.03-3	999.86	8.03-3	1215.16	7.84-3	2849.10	4.78-3	1710.90	4.11-3		9.3
735.90	3.73-3	381.20	2.68-3	939.35	2.58-3	2515.60	2.39-3	1878.00	2.30-3		9.4
1837.80	2.30-3	428.30	2.20-3	1567.90	2.01-3	289.30	1.72-3	2214.50	1.53-3		9.5
449.60	1.53-3	2621.00	1.43-3	1920.20	1.43-3	924.10	1.43-3	940.50	1.05-3		9.6
587.90	1.05-3	479.10	1.05-3	336.30	1.05-3	112.52	1.05-3	2030.40	9.60-4		9.7
1711.30	9.60-4										9.8
GE 75	4.96800E	03	7								10.1
264.80	1.00-1	199.20	7.80-3	418.60	2.50-3	468.70	1.80-3	65.60	8.90-4		10.2
617.80	5.00-4	353.00	1.90-4								10.3
GE 75M	4.89000E	01	5								10.4
400.70	0.0 0	304.00	0.0 0	136.00	0.0 0	121.10	0.0 0	96.70	0.0 0		10.5
SE 75	1.03680E	07	16								10.6
264.65	5.73-1	136.00	5.63-1	279.53	2.48-1	121.11	1.61-1	400.64	1.12-1		10.7
96.73	3.21-2	198.60	1.39-2	303.90	1.32-2	66.48	1.01-2	572.60	3.60-4		10.8
24.40	2.50-4	419.00	1.32-4	81.00	8.60-5	617.70	4.30-5	468.60	6.00-6		11.1
821.70	1.00-6										11.2
AS 76	9.47519E	04	47								11.3
559.47	4.10-1	657.20	5.69-2	1216.19	3.96-2	1213.25	2.22-2	554.45	1.48-2		11.4
1228.73	1.28-2	563.87	9.40-3	2097.52	6.98-3	665.62	4.02-3	2111.40	3.90-3		11.5
1788.88	3.61-3	1439.53	3.49-3	1792.75	2.46-3	654.46	2.13-3	1129.88	1.48-3		11.6
867.15	1.40-3	1454.07	1.23-3	772.17	1.19-3	740.25	1.11-3	571.90	9.80-4		11.7
1219.76	8.60-4	882.76	7.00-4	2656.72	6.20-4	1238.31	6.20-4	1054.43	6.20-4		11.8
1097.13	5.30-4	2430.25	4.90-4	1204.20	4.10-4	908.89	4.10-4	850.84	4.10-4		12.1
575.92	4.10-4	2517.83	3.70-4	1569.17	3.70-4	647.92	3.70-4	2670.46	3.30-4		12.2
1689.35	3.30-4	1542.80	3.30-4	1534.02	3.30-4	980.75	3.30-4	765.56	3.30-4		12.3
727.00	3.20-4	2443.70	2.90-4	1325.08	2.90-4	1122.00	2.90-4	811.39	2.90-4		12.4
641.37	2.80-4	1774.58	0.0 0								12.5
GE 77	4.06800E	04	50								12.6
264.40	1.00 0	211.00	5.00-1	416.30	4.90-1	215.60	4.80-1	558.50	3.40-1		12.7
367.40	3.10-1	632.40	1.90-1	714.80	1.60-1	1085.60	1.20-1	338.30	1.20-1		12.8
1368.00	5.10-2	1193.90	4.90-2	811.20	4.60-2	746.20	3.00-2	209.00	2.90-2		13.1
195.00	2.90-2	461.60	2.80-2	475.40	2.70-2	782.10	2.40-2	928.80	1.90-2		13.2
924.30	1.90-2	875.80	1.90-2	750.80	1.80-2	583.00	1.70-2	786.50	1.50-2		13.3
767.60	1.50-2	673.60	1.40-2	614.80	1.30-2	1572.80	1.20-2	1264.60	1.20-2		13.4
907.60	1.10-2	824.00	1.00-2	156.60	9.50-3	1999.60	9.10-3	2342.30	7.90-3		13.5
1309.50	7.60-3	1319.70	7.00-3	1242.70	6.90-3	1494.60	6.50-3	1313.00	6.40-3		13.6

Table A-3. Continued

CODE=	1	MEMBER	GAMCAT	3 PAGE								
914.60	6.00-3	1709.50	5.70-3	2077.90	5.60-3	2090.00	4.80-3	940.40	4.00-3	13.7		
795.60	4.00-3	1479.30	3.80-3	1215.20	3.00-3	2126.00	2.80-3	1296.20	2.80-3	13.8		
GE 77M	3.21600E	03	5							14.1		
215.50	3.91-1	159.70	2.11-1	154.80	9.00-3	419.40	1.80-3	614.30	8.20-4	14.2		
SE 77M	1.75000E	01	2							14.3		
161.60	5.00-1	11.20	0.0	0						14.4		
BR 80	1.05600E	03	8							14.5		
616.20	7.00-2	665.60	1.00-2	639.20	3.00-3	704.30	2.00-3	1256.70	7.00-4	14.6		
812.00	3.00-4	687.40	1.00-4	677.00	1.00-4					14.7		
BR 80M	1.59120E	04	11							14.8		
37.00	3.60-1	616.20	7.00-2	665.60	1.00-2	49.00	3.20-3	639.20	3.00-3	15.1		
704.30	2.00-3	1256.70	7.00-4	812.00	3.00-4	687.40	1.00-4	677.00	1.00-4	15.2		
11.90	0.0	0								15.3		
SE 81	1.11600E	03	8							15.4		
275.80	1.00-2	289.90	7.90-3	829.00	3.70-3	566.10	2.90-3	553.00	1.30-3	15.5		
539.00	6.20-4	650.40	2.60-4	180.00	9.40-5					15.6		
SE 81M	3.43800E	03	10							15.7		
102.70	1.00-1	275.80	1.00-2	289.90	7.90-3	829.00	3.70-3	1146.00	3.40-3	15.8		
566.10	2.90-3	553.00	1.30-3	539.00	6.20-4	650.40	2.60-4	180.00	9.40-5	16.1		
BR 82	1.27800E	05	33							16.2		
776.49	8.33-1	554.33	7.05-1	619.09	4.33-1	698.35	2.79-1	1043.95	2.78-1	16.3		
1317.43	2.75-1	827.81	2.43-1	1474.84	1.67-1	221.47	2.36-2	183.90	2.36-2	16.4		
1007.57	1.35-2	606.32	1.27-2	92.18	8.60-3	273.48	8.50-3	1650.27	7.60-3	16.5		
1081.35	6.40-3	952.12	3.70-3	295.00	1.50-3	73.00	1.30-3	1779.58	1.20-3	16.6		
137.40	1.20-3	1180.10	1.00-3	1072.57	9.00-4	2555.00	8.00-4	401.12	8.00-4	16.7		
100.90	7.00-4	735.62	6.00-4	1871.60	4.00-4	711.10	4.00-4	1956.50	3.00-4	16.8		
2056.00	2.00-4	1822.60	2.00-4	1770.79	2.00-4					17.1		
KR 85	3.38606E	08	1							17.2		
513.98	4.30-3									17.3		
SR 85	5.63328E	06	4							17.4		
513.98	1.00	0	880.00	1.00-4	356.00	2.00-5	733.00	0.0	0	17.5		
SR 85M	4.06200E	03	3							17.6		
231.69	8.21-1	151.28	1.15-1	238.65	2.88-3					17.7		
RB 86	1.61222E	06	1							17.8		
1076.77	8.80-2									18.1		
SR 87M	1.01160E	04	1							18.2		
388.40	8.25-1									18.3		
RB 88	1.06800E	03	43							18.4		
1836.13	2.30-1	898.01	1.16-1	2677.99	2.58-2	1382.77	7.49-3	2119.84	5.05-3	18.5		
3009.82	3.84-3	3218.75	3.57-3	2577.90	2.50-3	1779.72	2.30-3	3486.76	1.80-3	18.6		
890.68	1.61-3	2111.79	1.39-3	4743.53	1.13-3	2734.17	1.03-3	1217.67	5.50-4	18.7		
1679.90	5.00-4	1799.52	4.23-4	2388.00	2.90-4	2195.60	2.80-4	484.75	2.60-4	18.8		
1668.80	2.50-4	439.19	1.50-4	1257.20	1.40-4	625.27	1.40-4	4037.20	1.20-4	19.1		
2621.90	1.20-4	1027.30	1.20-4	916.90	1.20-4	1297.00	9.20-5	431.90	8.50-5	19.2		
4853.90	8.30-5	3966.20	6.90-5	3525.00	6.90-5	3017.60	4.60-5	1635.00	4.60-5	19.3		
1313.90	4.60-5	1239.50	4.60-5	417.00	3.90-5	3611.50	3.50-5	4633.50	2.80-5	19.4		
2199.00	2.30-5	1555.70	2.30-5	2797.40	1.60-5					19.5		
Y 90M	1.14840E	04	5							19.6		
202.40	9.70-1	479.30	9.10-1	2315.00	4.00-3	682.00	0.0	0	14.90	0.0	0	19.7
NB 94M	3.75600E	02	4									19.8
871.00	2.00-3	703.00	2.00-5	41.50	0.0	0	16.50	0.0	0			20.1

CODE# 1 MEMBER GAMDAT

[illegible]

Table A-3. Continued

CODE= 1 MEMBER GAMDAT

5 PAGE

1600.70	8.00-5	1592.70	8.00-5	1114.60	8.00-5	578.00	8.00-5	2390.80	7.00-5	26.5	
680.10	7.00-5	2317.60	6.00-5	2309.40	6.00-5	2308.70	6.00-5	2094.10	6.00-5	26.6	
1909.40	6.00-5	1789.00	6.00-5	774.60	6.00-5	2194.00	5.00-5	2193.20	5.00-5	26.7	
1108.90	5.00-5									26.8	
AG108	1.44600E	02	13							27.1	
632.98	7.76-1	433.96	2.22-1	618.86	1.16-1	1007.22	6.20-3	510.10	1.60-3	27.2	
1441.14	1.40-3	880.26	1.40-3	497.10	1.00-3	388.60	8.20-4	1106.00	7.30-4	27.3	
1540.00	4.70-4	383.20	4.00-4	931.12	2.40-4					27.4	
PD109	4.84920E	04	30							27.5	
88.04	3.80-2	44.70	7.60-4	311.40	3.40-4	647.30	2.60-4	781.40	1.20-4	27.6	
415.20	1.14-4	636.30	1.06-4	602.50	8.50-5	413.00	7.00-5	309.10	5.20-5	27.7	
701.90	3.30-5	558.10	2.60-5	736.70	1.79-5	707.00	1.69-5	778.30	1.61-5	27.8	
134.20	1.40-5	145.10	1.20-5	423.90	1.01-5	390.60	9.90-6	103.90	9.90-6	28.1	
447.60	8.80-6	551.40	6.50-6	454.30	5.80-6	822.90	2.00-6	724.40	2.00-6	28.2	
286.30	1.50-6	862.50	1.40-6	395.60	7.00-7	1010.50	2.60-7	966.30	2.60-7	28.3	
PD109M	2.81400E	02	2							28.4	
188.90	5.80-1	21.00	5.80-1							28.5	
AG110	2.47000E	01	13							28.6	
657.50	5.57-2	815.50	4.70-4	1125.80	1.90-4	818.20	1.10-4	295.30	9.50-5	28.7	
1674.30	8.90-5	1783.60	5.60-5	2004.40	4.40-5	1475.80	4.40-5	1186.30	3.30-5	28.8	
1629.90	2.80-5	1421.40	2.80-5	1074.00	1.10-5					29.1	
AG110M	2.18592E	07	50							29.2	
657.74	9.38-1	884.67	7.47-1	937.48	3.32-1	1384.22	2.63-1	763.93	2.18-1	29.3	
706.67	1.59-1	1504.91	1.40-1	677.56	1.18-1	818.02	7.10-2	686.83	6.90-2	29.4	
1475.75	4.40-2	744.25	4.10-2	446.78	3.10-2	620.24	2.50-2	1562.30	1.28-2	29.5	
667.90	7.00-3	867.00	3.80-3	1524.50	3.00-3	260.20	2.80-3	859.00	1.90-3	29.6	
626.10	1.70-3	1334.16	1.50-3	132.60	1.40-3	997.18	1.30-3	120.00	1.10-3	29.7	
1443.00	1.00-3	365.10	1.00-3	221.40	1.00-3	219.50	9.40-4	911.60	9.00-4	29.8	
846.50	9.00-4	896.00	6.00-4	1252.00	5.50-4	1085.70	5.00-4	266.40	4.70-4	30.1	
386.60	4.00-4	1117.40	3.70-4	396.70	3.40-4	1018.70	3.00-4	229.00	3.00-4	30.2	
1125.70	2.40-4	785.80	1.90-4	1903.30	1.80-4	1784.60	1.80-4	1646.00	1.80-4	30.3	
1580.10	1.60-4	67.50	9.40-5	1688.00	9.00-5	766.00	9.00-5	565.50	9.00-5	30.4	
PD111	1.32000E	03	46							30.5	
580.10	1.00	0*1458.70	8.80-1*	1388.40	8.50-1*	70.50	8.00-1*	650.60	6.80-1*	30.6	
59.90	6.30-1*	376.70	5.50-1*	547.10	4.40-1*	623.20	3.90-1*	835.80	3.40-1*	30.7	
508.90	2.80-1*	1120.20	1.80-1*	710.00	1.50-1*	298.80	9.70-2*	404.90	8.60-2*	30.8	
476.70	8.00-2*	438.70	6.30-2*	1002.20	6.00-2*	169.40	6.00-2*	775.60	4.60-2*	31.1	
685.70	4.50-2*	955.10	4.00-2*	803.90	4.00-2*	485.90	4.00-2*	391.30	4.00-2*	31.2	
1574.10	3.70-2*	808.50	3.00-2*	1542.40	2.90-2*	1644.30	2.30-2*	552.90	2.00-2*	31.3	
516.50	2.00-2*	478.50	2.00-2*	230.50	2.00-2*	316.90	1.80-2*	657.70	1.70-2*	31.4	
1067.10	1.50-2*	1059.80	1.50-2*	920.50	1.50-2*	611.40	1.50-2*	746.00	1.40-2*	31.5	
352.60	1.30-2*	1269.70	1.00-2*	1026.60	1.00-2*	950.00	1.00-2*	519.20	1.00-2*	31.6	
494.20	1.00-2*									31.7	
SN113	9.93599E	06	4							31.8	
391.40	1.00	0*	255.20	3.50-2*	648.00	1.50-3*	24.20	0.0	0	32.1	
SN113M	1.20000E	03	3							32.2	
79.30	6.00-3	25.30	0.0	0	24.20	0.0	0			32.3	
IN114	7.19000E	01	4							32.4	
1300.00	4.10-2	575.70	1.10-3	747.80	9.00-4	23.20	0.0	0		32.5	
IN114M	4.27766E	06	5							32.6	
189.90	1.77-1	558.30	4.65-2	725.20	4.55-2	1300.20	1.80-3	24.20	0.0	0	32.7

Table A-3. Continued

CODE = 1 MEMBER GAMCAT

6 PAGE

CD115	1.92168E 05	7								32.8
527.90	2.75-1	492.30	8.10-2	260.90	1.85-2	231.40	7.02-3	35.00	5.00-3	33.1
270.00	1.70-3	24.20	0.0 0							33.2
IN116	1.42000E 01	5								33.3
1270.00	1.20-2	450.00	1.20-3	950.00	1.00-3	2200.00	2.00-4	2000.00	1.00-4	33.4
IN116M1	3.24600E 03	32								33.5
1293.40	8.50-1	1097.30	5.57-1	417.02	3.24-1	2112.10	1.50-1	818.70	1.16-1	33.6
1507.80	1.02-1	138.33	3.33-2	1753.80	2.44-2	463.30	8.50-3	355.30	8.50-3	33.7
972.40	4.60-3	780.40	3.05-3	705.70	1.60-3	689.00	1.60-3	278.50	1.50-3	33.8
262.80	1.30-3	303.60	1.20-3	730.70	1.05-3	630.90	7.50-4	655.70	7.30-4	34.1
932.20	7.00-4	2225.50	4.00-4	1536.30	4.00-4	871.90	4.00-4	245.00	4.00-4	34.2
567.40	3.50-4	517.60	3.50-4	474.60	3.50-4	536.00	3.20-4	434.90	3.00-4	34.3
1072.30	2.00-4	99.70	1.50-4							34.4
CD117	1.22400E 04	49								34.5
273.31	1.99-1	1303.40	1.25-1	344.51	1.25-1	1576.90	7.60-2	434.23	7.50-2	34.6
880.75	2.90-2	89.71	2.90-2	1052.00	2.30-2	831.79	1.60-2	1723.30	1.30-2	34.7
1562.50	1.10-2	945.70	1.10-2	220.90	1.00-2	1408.70	9.00-3	1337.90	9.00-3	34.8
1142.50	9.00-3	1247.90	8.00-3	1260.00	7.20-3	1707.10	7.00-3	1116.90	7.00-3	35.1
840.22	5.80-3	463.09	5.80-3	712.60	5.70-3	71.11	5.60-3	1291.10	5.20-3	35.2
1682.40	5.00-3	1053.00	5.00-3	1272.80	4.80-3	1314.80	4.60-3	1229.20	4.10-3	35.3
1450.20	4.00-3	963.40	4.00-3	292.00	4.00-3	1475.40	3.00-3	387.93	3.00-3	35.4
1125.00	2.40-3	1652.50	2.20-3	950.10	2.10-3	1422.40	2.00-3	728.70	1.80-3	35.5
1362.20	1.60-3	1035.50	1.60-3	699.90	1.60-3	419.71	1.50-3	245.40	1.40-3	35.6
1120.30	1.20-3	787.60	1.00-3	626.70	8.00-4	1521.30	4.00-4			35.7
CD117M	9.00000E 03	20								35.8
1234.50	2.52-1	1997.40	1.28-1	1066.00	1.06-1	564.40	7.70-2	1029.00	5.30-2	36.1
1432.70	5.20-2	860.40	4.60-2	2322.90	3.60-2	747.90	3.20-2	366.94	1.80-2	36.2
931.30	1.50-2	631.70	1.50-2	762.70	9.10-3	1365.60	8.40-3	461.10	6.30-3	36.3
484.80	5.60-3	2417.00	4.90-3	2400.40	3.50-3	2096.00	3.50-3	617.30	2.40-3	36.4
SB122	2.35008E 05	9								36.5
563.90	6.60-1	564.10	6.30-1	686.00	3.40-2	692.80	3.27-2	1260.00	7.00-3	36.6
1140.00	7.00-3	1140.60	6.60-3	1256.80	6.50-3	26.40	0.0 0			36.7
SB122M	2.52000E 02	4								36.8
60.70	5.00-1	75.30	1.70-1	26.40	0.0 0	26.00	0.0 0			37.1
SN123	1.11456E 07	3								37.2
1089.00	6.00-3	1032.00	3.40-4	155.00	1.00-5					37.3
SN123M	2.40000E 03	4								37.4
160.30	10.00-1	381.30	2.70-4	542.20	1.60-4	552.00	7.00-5			37.5
TE123M	1.03421E 07	2								37.6
159.00	8.41-1	88.50	9.30-4							37.7
SB124	5.20128E 06	16								37.8
602.70	9.80-1	1691.00	4.57-1	722.80	1.06-1	645.80	7.10-2	2091.20	5.20-2	38.1
1368.30	2.45-2	713.70	2.28-2	1450.00	2.00-2	1045.10	1.84-2	968.30	1.72-2	38.2
1325.50	1.58-2	709.30	1.34-2	1298.00	1.30-2	790.80	7.00-3	1354.90	6.40-3	38.3
2280.00	6.00-3									38.4
SB124M1	9.30000E 01	3								38.5
645.00	2.00-1	603.00	2.00-1	505.00	2.00-1					38.6
SB124M2	1.21800E 03	4								38.7
645.00	2.00-1	603.00	2.00-1	505.00	2.00-1	25.00	0.0 0			38.8
SN125	8.33760E 05	47								39.1
1066.60	8.87-2	1088.90	4.29-2	822.60	3.87-2	915.50	3.76-2	2001.70	2.11-2	39.2

Table A-3. Continued

CODE= 1 MEMBER GAMCAT

7 PAGE

469.70	1.38-2	332.00	1.22-2	800.50	9.70-3	1087.40	9.30-3	1419.50	4.70-3	39.3		
1173.20	2.90-3	1017.10	2.80-3	893.70	2.50-3	1221.00	2.30-3	350.90	2.30-3	39.4		
2275.20	1.50-3	1805.70	1.50-3	934.70	1.20-3	1151.30	1.10-3	921.60	9.00-4	39.5		
1889.90	8.00-4	270.90	8.00-4	1349.40	6.00-4	2200.60	4.00-4	652.60	4.00-4	39.6		
1164.30	3.00-4	1259.00	2.00-4	434.10	2.00-4	258.30	2.00-4	1198.20	9.00-5	39.7		
282.90	9.00-5	1207.70	6.00-5	1110.70	6.00-5	684.20	6.00-5	524.30	6.00-5	39.8		
1591.20	5.00-5	1185.40	5.00-5	562.20	5.00-5	311.10	5.00-5	1982.90	4.00-5	40.1		
1557.50	4.00-5	1137.50	3.00-5	2227.00	2.00-5	398.00	5.00-6	363.00	4.00-6	40.2		
286.00	4.00-6	386.00	2.00-6							40.3		
38125	8.61504E	07	18							40.4		
427.90	3.04-1	600.60	1.81-1	635.90	1.15-1	463.40	1.07-1	176.40	7.10-2	40.5		
606.70	5.10-2	671.40	1.80-2	380.50	1.53-2	321.00	4.40-3	204.20	3.20-3	40.6		
443.30	3.10-3	117.00	2.80-3	172.50	2.50-3	208.10	2.40-3	407.90	2.00-3	40.7		
227.70	1.30-3	109.40	1.20-3	199.20	0.0	0				40.8		
TE125M	5.01120E	06	3							41.1		
35.50	7.00-2	109.30	3.00-2	27.50	0.0	0				41.2		
TE127	3.38400E	04	9							41.3		
417.90	9.70-3	360.30	1.30-3	202.90	5.70-4	215.10	3.80-4	57.63	2.90-4	41.4		
145.20	3.20-5	375.00	2.90-6	172.10	2.90-6	618.60	1.30-6			41.5		
TE127M	9.41759E	06	14							41.6		
417.90	9.70-3	57.63	5.10-3	360.30	1.32-3	88.26	1.20-3	202.90	5.70-4	41.7		
215.10	3.80-4	658.90	1.30-4	145.20	3.20-5	593.30	2.30-5	651.00	2.90-6	41.8		
375.00	2.90-6	172.10	2.90-6	618.60	1.30-6	628.60	9.00-7			42.1		
I 128	1.49820E	03	6							42.2		
442.91	2.05-1	526.62	1.97-2	969.40	4.90-3	1139.70	1.20-4	613.10	3.10-5	42.3		
1434.50	6.80-6									42.4		
TE129	4.14000E	03	33							42.5		
27.80	2.30	0*	459.60	1.00	0*	487.40	1.90-1*	278.40	8.00-2*	1084.00	7.90-2*	42.6
250.60	5.60-2*	1111.70	3.10-2*	802.20	2.73-2*	209.00	2.60-2*	281.20	2.10-2*			42.7
624.40	1.20-2*	531.80	1.20-2*	741.10	1.05-2*	833.40	5.90-3*	342.80	5.20-3*			42.8
982.40	2.30-3*	1268.00	1.60-3*	551.50	1.50-3*	1264.40	1.20-3*	1233.00	1.20-3*			43.1
768.90	1.20-3*	829.90	1.00-3*	559.70	1.00-3*	342.60	1.00-3*	270.30	6.00-4*			43.2
794.90	3.00-4*	1013.80	2.00-4*	1003.60	2.00-4*	716.80	2.00-4*	1282.10	1.00-4*			43.3
1254.20	1.00-4*	925.80	1.00-4*	1204.20	6.00-5*							43.4
TE129M	2.89613E	06	46									43.5
27.80	2.30	0*	459.60	1.00	0*	696.00	6.40-1*	487.40	1.90-1*	729.60	1.52-1*	43.6
278.40	8.00-2*	1084.00	7.90-2*	250.60	5.60-2*	1111.70	3.10-2*	105.50	3.00-2*			43.7
802.20	2.73-2*	209.00	2.60-2*	556.60	2.30-2*	281.20	2.10-2*	817.20	1.90-2*			43.8
624.40	1.20-2*	531.80	1.20-2*	741.10	1.05-2*	844.90	7.30-3*	833.40	5.90-3*			44.1
342.80	5.20-3*	672.00	5.00-3*	1022.60	4.10-3*	701.80	3.80-3*	1050.40	3.70-3*			44.2
982.40	2.30-3*	1260.80	1.60-3*	551.50	1.50-3*	1264.40	1.20-3*	1233.00	1.20-3*			44.3
768.90	1.20-3*	829.90	1.00-3*	705.60	1.00-3*	559.70	1.00-3*	342.60	1.00-3*			44.4
1401.60	9.00-4*	270.30	6.00-4*	794.90	3.00-4*	1373.80	2.00-4*	1013.80	2.00-4*			44.5
1003.60	2.00-4*	716.80	2.00-4*	1282.10	1.00-4*	1254.20	1.00-4*	925.80	1.00-4*			44.6
1204.20	6.00-5*											44.7
I 130	4.46400E	04	24									44.8
536.10	1.00	0	668.40	9.40-1	739.40	8.10-1	418.00	3.30-1	1157.30	1.10-1		45.1
586.10	1.60-2	686.00	9.30-3	1272.10	7.80-3	966.80	7.70-3	510.90	6.20-3			45.2
603.60	6.00-3	1096.40	5.00-3	1404.10	3.60-3	1122.00	2.30-3	808.50	2.10-3			45.3
1222.50	1.80-3	877.30	1.80-3	800.50	7.00-4	1607.70	4.00-4	1547.70	4.00-4			45.4
1501.10	4.00-4	1423.60	3.00-4	1202.90	2.00-4	1489.40	1.00-4					45.5



Table A-3. Continued

CODE= 1 MEMBER GAMCAT

8 PAGE

I 130M	5.52000E 02 5									45.6
538.10	1.57-1	586.10	1.40-2	1615.00	5.60-3	1122.00	2.00-3	48.20	0.0 0	45.7
TE131	1.50000E 03 42									45.8
149.80	6.77-1	452.40	1.80-1	1147.40	5.68-2	492.80	5.14-2	602.20	4.80-2	46.1
997.40	3.59-2	948.50	2.23-2	654.00	1.49-2	934.60	9.50-3	384.20	9.50-3	46.2
1008.10	8.80-3	342.90	7.40-3	1294.80	6.40-3	727.00	5.10-3	545.10	3.80-3	46.3
951.80	3.40-3	1098.70	2.10-3	841.90	1.90-3	298.30	1.80-3	696.00	1.70-3	46.4
898.60	1.50-3	1501.00	1.20-3	1278.20	1.20-3	278.30	1.20-3	1427.50	1.10-3	46.5
567.40	9.00-4	109.80	9.00-4	1351.60	6.00-4	1527.90	5.00-4	855.60	5.00-4	46.6
825.00	5.00-4	353.00	5.00-4	221.40	5.00-4	605.40	4.00-4	575.00	3.00-4	46.7
496.00	3.00-4	421.00	3.00-4	550.60	2.00-4	1652.00	7.00-5	1579.00	7.00-5	46.8
1309.00	7.00-5	402.00	7.00-5							47.1
I 131	6.94656E 05 9									47.2
364.50	8.20-1	637.00	6.80-2	284.30	5.40-2	80.20	2.60-2	723.00	1.60-2	47.3
503.00	4.00-3	325.80	2.00-3	177.20	2.00-3	29.80	0.0 0			47.4
TE132	2.80800E 05 45									47.5
667.70	9.80-1	228.20	8.80-1	772.70	7.50-1	53.00	1.70-1	954.60	1.67-1	47.6
522.60	1.56-1	630.20	1.35-1	1398.50	6.80-2	727.50	6.80-2	812.60	6.00-2	47.7
671.00	6.00-2	505.70	4.70-2	1135.20	2.92-2	810.00	2.80-2	1371.70	2.28-2	47.8
650.60	2.20-2	621.00	2.08-2	1295.00	1.84-2	1442.60	1.35-2	1142.60	1.35-2	48.1
1289.90	1.30-2	262.80	1.30-2	2001.70	1.20-2	116.50	1.20-2	1921.70	1.14-2	48.2
1172.20	1.13-2	111.90	1.10-2	877.90	1.06-2	284.70	1.02-2	546.80	1.00-2	48.3
910.90	9.40-3	984.10	6.50-3	446.10	6.40-3	864.40	5.70-3	1034.60	5.04-3	48.4
928.10	4.70-3	416.60	4.40-3	431.80	4.30-3	1757.00	3.20-3	1147.10	3.20-3	48.5
240.80	2.30-3	1271.80	1.50-3	1476.70	1.24-3	1519.90	8.40-4	28.60	0.0 0	48.6
I 132	8.20800E 03 39									48.7
667.70	9.80-1	772.70	7.50-1	954.60	1.67-1	522.60	1.56-1	630.20	1.35-1	48.8
1398.50	6.80-2	727.50	6.80-2	812.60	6.00-2	671.00	6.00-2	505.70	4.70-2	49.1
1135.20	2.92-2	810.00	2.80-2	1371.70	2.28-2	650.60	2.20-2	621.00	2.08-2	49.2
1295.00	1.84-2	1442.60	1.35-2	1142.60	1.35-2	1289.90	1.30-2	262.80	1.30-2	49.3
2001.70	1.20-2	1921.70	1.14-2	1172.20	1.13-2	877.90	1.06-2	284.70	1.02-2	49.4
546.80	1.00-2	910.90	9.40-3	984.10	6.50-3	446.10	6.40-3	864.40	5.70-3	49.5
1034.60	5.04-3	928.10	4.70-3	416.60	4.40-3	431.80	4.30-3	1757.00	3.20-3	49.6
1147.10	3.20-3	1271.80	1.50-3	1476.70	1.24-3	1519.90	8.40-4			49.7
I 133	7.55999E 04 28									49.8
529.50	8.70-1	875.30	4.50-2	1298.90	2.18-2	707.40	1.60-2	1237.50	1.57-2	50.1
510.40	1.50-2	856.10	1.20-2	680.80	7.60-3	1052.80	5.00-3	769.10	4.70-3	50.2
263.40	4.40-3	910.50	3.80-3	618.00	3.70-3	422.90	2.60-3	344.00	2.60-3	50.3
820.90	1.70-3	1351.60	1.60-3	417.20	1.40-3	266.30	1.30-3	1061.10	8.70-4	50.4
789.90	5.00-4	1590.10	4.40-4	608.00	4.00-4	1733.00	2.60-4	938.50	1.30-4	50.5
893.20	1.00-4	814.00	1.00-4	847.00	4.00-5					50.6
I 134	3.19200E 03 50									50.7
847.08	9.57-1	884.18	6.49-1	1072.88	1.49-1	595.40	1.11-1	621.80	1.07-1	50.8
1136.50	8.90-2	540.88	7.63-2	677.50	7.56-2	405.40	7.32-2	857.48	6.54-2	51.1
1806.40	5.53-2	974.80	4.80-2	135.48	4.35-2	1613.80	4.33-2	766.60	4.17-2	51.2
433.30	4.15-2	948.10	3.96-2	1741.30	2.61-2	1456.10	2.34-2	235.40	2.25-2	51.3
514.40	2.16-2	628.13	2.13-2	1040.00	2.04-2	730.70	1.77-2	488.90	1.42-2	51.4
459.03	1.36-2	565.40	9.85-3	1103.00	9.28-3	1100.00	8.70-3	188.53	8.42-3	51.5
138.90	8.18-3	1470.30	7.46-3	739.20	6.84-3	837.00	6.26-3	816.60	6.26-3	51.6
411.20	5.45-3	1542.60	4.88-3	1270.03	4.78-3	319.78	4.45-3	350.90	4.16-3	51.7
571.00	4.06-3	1644.30	3.92-3	1353.80	3.73-3	967.10	3.63-3	1159.70	3.20-3	51.8

Table A-3. Continued

CODE= 1 MEMBER GAMCAT

9 PAGE

162.58	3.15-3	217.43	2.39-3	1191.40	2.34-3	2312.60	2.10-3	1429.20	1.77-3	52.1	
CS134	6.50703E	07	9							52.2	
604.60	5.80-1	795.80	8.80-1	569.20	1.40-1	801.80	9.00-2	563.10	8.00-2	52.3	
1365.00	3.40-2	1167.70	1.90-2	475.30	1.50-2	1038.40	1.10-2			52.4	
CS134M	1.04400E	04	4							52.5	
127.10	1.40-1	137.40	0.0	0	31.00	0.0	0	10.50	0.0	0	52.6
I 135	2.41200E	04	50							52.7	
1260.50	2.91-1	1131.60	2.21-1	526.50	1.13-1	1678.30	9.90-2	1458.10	9.10-2	52.8	
1791.50	8.30-2	1038.80	7.70-2	546.50	6.30-2	836.80	5.90-2	1706.70	4.30-2	53.1	
1124.10	3.90-2	417.50	3.10-2	288.60	3.10-2	220.50	1.80-2	1101.60	1.50-2	53.2	
1566.80	1.20-2	972.70	1.20-2	2410.10	1.00-2	1503.10	1.00-2	1169.00	1.00-2	53.3	
2046.70	9.00-3	971.90	9.00-3	1240.50	8.00-3	707.60	7.00-3	2256.70	6.00-3	53.4	
1831.10	6.00-3	1368.20	6.00-3	531.00	5.00-3	434.00	5.00-3	649.50	4.00-3	53.5	
1927.80	3.00-3	1448.60	3.00-3	994.80	2.00-3	797.30	2.00-3	451.80	2.00-3	53.6	
429.90	2.00-3	414.80	2.00-3	290.40	2.00-3	264.30	2.00-3	229.80	2.00-3	53.7	
960.90	1.00-3	785.30	1.00-3	689.90	1.00-3	402.90	1.00-3	1180.40	9.00-4	53.8	
1161.20	9.00-4	362.00	9.00-4	305.60	9.00-4	808.10	6.00-4	679.30	3.00-4	54.1	
XE135	3.30120E	04	12							54.2	
249.60	9.20-1	608.60	2.60-2	408.20	3.40-3	158.50	2.60-3	358.60	2.40-3	54.3	
812.60	5.00-4	731.90	5.00-4	654.60	3.00-4	199.90	2.00-4	373.10	1.00-4	54.4	
573.30	6.00-5	1063.00	3.00-5							54.5	
CS137	9.52198E	08	3							54.6	
661.64	8.51-1	32.10	5.70-2	36.50	1.30-2					54.7	
8A131	9.89800E	05	4							54.8	
496.37	2.40-1	123.81	1.40-1	216.08	1.00-1	373.24	7.60-2			55.1	
8A137M	1.53000E	02	3							55.2	
661.64	8.51-1	32.10	5.70-2	36.50	1.30-2					55.3	
8A139	4.96260E	03	23							55.4	
165.80	7.30-1	1420.50	1.00-2	1219.10	1.50-3	1254.80	1.00-3	1310.60	5.40-4	55.5	
1090.90	3.10-4	1256.70	1.70-4	1683.40	1.20-4	1215.50	1.20-4	1370.60	1.10-4	55.6	
1536.30	1.00-4	1595.70	9.30-5	1476.60	6.10-5	1578.30	2.00-5	1053.00	1.20-5	55.7	
1765.50	1.00-5	1558.50	9.80-6	1920.60	3.00-6	1392.40	3.00-6	1381.50	3.00-6	55.8	
2060.10	2.00-6	1894.70	2.00-6	1754.50	2.00-6					56.1	
8A140	1.10506E	06	10							56.2	
537.25	3.40-1	29.97	1.90-1	162.66	8.50-2	304.85	5.90-2	423.69	4.40-2	56.3	
437.54	2.70-2	13.85	1.50-2	132.69	2.80-3	118.85	9.20-4	113.55	2.50-4	56.4	
LA140	1.44792E	05	38							56.5	
1596.40	9.60-1	487.10	4.67-1	815.70	2.28-1	328.80	2.00-1	925.20	7.10-2	56.6	
867.90	5.50-2	751.90	4.30-2	2521.80	3.40-2	432.60	2.90-2	919.70	2.70-2	56.7	
1085.30	1.10-2	2348.30	8.60-3	266.50	5.40-3	131.10	5.20-3	951.00	5.00-3	56.8	
242.00	5.00-3	2010.40	4.30-3	510.90	4.00-3	24.60	3.20-3	898.70	2.70-3	57.1	
892.00	2.30-3	109.50	2.10-3	1416.00	2.00-3	1062.00	2.00-3	798.30	2.00-3	57.2	
173.50	1.90-3	2547.80	1.00-3	1521.80	1.00-3	69.00	1.00-3	2898.90	7.00-4	57.3	
1877.30	7.00-4	653.20	4.00-4	398.00	4.00-4	64.10	4.00-4	3119.10	2.00-4	57.4	
2465.40	2.00-4	2494.00	1.20-4	3319.70	5.00-5					57.5	
CE141	2.80368E	06	2							57.6	
145.40	4.80-1	36.00	0.0	0						57.7	
PR142	6.91199E	04	1							57.8	
1575.50	3.70-2									58.1	
CE143	1.18800E	05	28							58.2	
293.26	4.13-1	57.37	1.16-1	664.55	5.20-2	721.96	5.00-2	350.58	3.30-2	58.3	

Table A-3. Continued

CODE= 1 MEMBER GAMDAT

10 PAGE

231.56	2.00-2	490.36	1.90-2	880.39	9.10-3	1102.98	3.60-3	587.28	2.40-3	58.4
433.02	1.30-3	139.67	9.70-4	1002.97	6.60-4	447.21	6.60-4	1060.52	3.40-4	58.5
497.91	3.30-4	937.81	3.10-4	389.49	2.90-4	809.93	2.50-4	806.46	2.50-4	58.6
556.86	2.50-4	371.13	2.10-4	1031.47	1.70-4	791.09	1.70-4	1324.63	1.20-4	58.7
891.10	1.20-4	1047.04	9.00-5	1339.92	3.70-5					58.8
CE144	2.45549E 07 15									59.1
133.53	1.08-1	80.12	1.54-2	656.40	1.50-2	2186.50	7.30-3	40.93	5.00-3	59.2
1489.20	2.90-3	33.57	1.50-3	53.91	9.00-4	99.95	3.80-4	1388.00	6.20-5	59.3
813.80	2.30-5	863.90	1.80-5	675.00	1.70-5	625.00	5.00-6	2655.00	4.00-7	59.4
ND147	9.48671E 05 22									59.5
91.03	1.49-1	531.40	9.00-2	319.70	1.30-2	440.30	8.30-3	275.70	5.70-3	59.6
686.70	5.60-3	398.60	5.50-3	120.60	2.80-3	78.00	2.00-3	595.70	1.80-3	59.7
197.00	1.30-3	489.60	9.00-4	410.80	9.00-4	299.70	5.00-4	154.00	5.00-4	59.8
589.80	3.00-4	680.20	2.00-4	312.60	2.00-4	260.00	2.00-4	232.00	2.00-4	60.1
170.00	2.00-4	182.00	1.00-4							60.2
ND149	6.48000E 03 40									60.3
211.30	2.30-1	114.30	1.60-1	270.10	9.20-2	654.40	8.40-2	423.50	8.10-2	60.4
540.60	6.60-2	267.60	5.20-2	155.90	5.20-2	326.40	4.00-2	240.20	3.40-2	60.5
208.10	2.50-2	74.30	2.20-2	188.60	1.70-2	443.50	1.30-2	349.30	1.30-2	60.6
97.30	1.30-2	58.90	1.30-2	198.90	1.20-2	556.40	1.00-2	245.80	8.90-3	60.7
288.10	5.90-3	366.60	5.70-3	282.40	5.20-3	275.20	5.10-3	192.00	5.10-3	60.8
294.80	5.00-3	311.10	4.40-3	230.30	4.30-3	213.80	3.50-3	301.40	3.30-3	61.1
258.10	3.30-3	384.70	2.90-3	273.10	2.00-3	122.30	2.00-3	630.20	1.90-3	61.2
177.80	1.40-3	126.60	1.00-3	117.10	1.00-3	38.70	0.0 0	30.00	0.0 0	61.3
ND151	7.44000E 02 38									61.4
116.80	2.22-1	1180.90	1.00-1	255.70	7.60-2	138.90	4.30-2	175.10	4.20-2	61.5
736.20	4.00-2	423.60	3.60-2	797.50	3.20-2	1122.60	3.00-2	170.70	2.30-2	61.6
724.20	1.90-2	678.00	1.50-2	85.10	1.40-2	739.20	1.20-2	300.60	1.10-2	61.7
90.00	1.10-2	402.30	9.60-3	69.00	8.70-3	914.20	8.20-3	755.60	7.40-3	61.8
585.20	7.40-3	841.10	6.50-3	658.60	4.50-3	324.60	3.30-3	102.90	3.30-3	62.1
81.80	3.30-3	239.50	3.00-3	238.70	3.00-3	183.10	2.50-3	58.30	2.40-3	62.2
149.50	2.20-3	208.10	2.10-3	589.60	2.00-3	199.70	2.00-3	197.20	1.80-3	62.3
829.10	1.50-3	1297.80	1.30-3	38.70	0.0 0					62.4
EU152	4.16551E 08 48									62.5
121.78	2.54-1	344.31	2.45-1	1408.02	1.98-1	964.01	1.32-1	1112.04	1.24-1	62.6
778.87	1.20-1	1085.83	9.70-2	244.66	6.80-2	867.33	3.80-2	443.98	2.90-2	62.7
411.13	2.00-2	1089.73	1.70-2	1299.20	1.60-2	1212.94	1.30-2	688.68	8.00-3	62.8
367.80	8.00-3	1005.15	6.00-3	1457.64	5.00-3	564.08	5.00-3	919.31	4.00-3	63.1
678.61	4.00-3	586.34	4.00-3	488.72	4.00-3	295.97	4.00-3	810.42	3.00-3	63.2
719.34	3.00-3	1528.12	2.00-3	1249.91	2.00-3	1108.90	2.00-3	926.23	2.00-3	63.3
764.86	2.00-3	963.36	1.00-3	841.53	1.00-3	674.68	1.00-3	656.52	1.00-3	63.4
566.64	1.00-3	503.50	1.00-3	416.06	1.00-3	329.41	1.00-3	1292.75	9.00-4	63.5
712.81	9.00-4	768.90	8.00-4	901.20	7.00-4	324.87	7.00-4	271.05	7.00-4	63.6
251.62	7.00-4	930.58	6.00-4	520.30	5.00-4					63.7
EU152M1	3.34800E 04 48									63.8
121.78	2.20-1	344.31	2.10-1	1408.02	1.70-1	1112.04	1.10-1	964.01	1.10-1	64.1
778.87	1.00-1	1085.83	8.00-2	244.66	6.00-2	867.33	3.00-2	443.98	2.00-2	64.2
411.13	2.00-2	1299.20	1.00-2	1212.94	1.00-2	1089.73	1.00-2	367.80	7.00-3	64.3
688.68	6.00-3	1005.15	5.00-3	1457.64	4.00-3	678.61	4.00-3	586.34	4.00-3	64.4
564.08	4.00-3	520.30	4.00-3	919.31	3.00-3	719.34	3.00-3	488.72	3.00-3	64.5
295.97	3.00-3	1528.12	2.00-3	926.23	2.00-3	810.42	2.00-3	1249.91	1.00-3	64.6

Table A-3. Continued

CODE= 1 MEMBER GAMDAT

11 PAGE

1108.90	1.00-3	963.36	1.00-3	841.53	1.00-3	764.86	1.00-3	674.68	1.00-3	64.7
656.52	1.00-3	503.50	1.00-3	329.41	1.00-3	566.64	9.00-4	1292.75	8.00-4	64.8
712.81	8.00-4	416.06	8.00-4	901.20	6.00-4	768.90	6.00-4	324.87	6.00-4	65.1
271.05	6.00-4	251.62	6.00-4	930.58	5.00-4					65.2
EU152M2	5.76000E 03	3								65.3
90.00	7.40-1	39.70	0.0 0	18.30	0.0 0					65.4
SM153	1.67184E 05	28								65.5
103.20	2.80-1	69.60	4.76-2	97.40	7.29-3	83.40	2.10-3	75.40	1.71-3	65.6
89.50	1.62-3	531.40	6.45-4	172.90	5.88-4	533.20	3.36-4	539.10	1.68-4	65.7
463.60	1.40-4	609.10	1.18-4	151.60	9.00-5	521.30	7.00-5	636.00	5.04-5	65.8
555.20	5.00-5	603.10	3.90-5	411.50	3.90-5	424.30	3.60-5	450.00	3.10-5	66.1
578.60	2.80-5	438.00	2.80-5	54.10	1.68-5	68.20	1.20-5	598.20	0.0 0	66.2
596.90	0.0 0	41.50	0.0 0	19.80	0.0 0					66.3
EU154	2.68234E 08	50								66.4
123.07	3.90-1	1274.49	3.36-1	723.26	2.02-1	1004.75	1.70-1	873.16	1.17-1	66.5
996.29	9.90-2	247.90	6.80-2	591.79	5.00-2	756.81	4.30-2	1596.70	1.70-2	66.6
692.43	1.70-2	1246.20	8.00-3	904.10	8.00-3	582.03	8.00-3	1494.20	6.00-3	66.7
444.50	6.00-3	845.40	5.00-3	815.50	5.00-3	892.80	4.00-3	1128.50	3.00-3	66.8
625.20	3.00-3	1140.70	2.00-3	850.70	2.00-3	557.60	2.00-3	478.30	2.00-3	67.1
401.20	2.00-3	188.20	2.00-3	1241.40	1.00-3	1118.20	1.00-3	715.70	1.00-3	67.2
676.50	1.00-3	649.80	9.00-4	1188.30	8.00-4	880.60	7.00-4	613.30	7.00-4	67.3
467.90	7.00-4	924.70	6.00-4	511.20	6.00-4	1538.00	5.00-4	518.20	5.00-4	67.4
321.80	5.00-4	397.20	4.00-4	1160.30	3.00-4	232.10	3.00-4	146.30	3.00-4	67.5
1316.40	2.00-4	1290.40	2.00-4	404.20	2.00-4	329.90	1.00-4	1418.20	9.00-5	67.6
SM155	1.38000E 03	27								67.7
104.32	7.25-1	41.50	1.71-1	245.73	3.90-2	141.41	2.30-2	141.40	2.30-2	67.8
78.50	1.20-2	26.60	6.30-3	61.80	4.00-3	460.80	6.90-4	1301.20	6.70-4	68.1
228.70	6.60-4	664.00	6.10-4	138.60	6.00-4	169.10	5.00-4	167.50	4.80-4	68.2
203.10	4.50-4	1223.00	1.90-4	571.80	1.80-4	522.50	1.50-4	631.20	1.40-4	68.3
1002.70	1.20-4	462.20	1.20-4	307.30	1.20-4	510.20	1.10-4	957.90	1.00-4	68.4
90.10	1.00-4	41.50	0.0 0							68.5
EU155	1.56522E 08	6								68.6
86.54	3.20-1	105.30	2.00-1	60.01	1.28-2	26.50	1.28-2	45.30	7.40-3	68.7
18.90	3.20-4									68.8
EU156	1.31069E 06	50								69.1
811.60	9.00-2	1230.40	8.70-2	88.90	8.00-2	2205.00	7.00-2	646.20	7.00-2	69.2
1242.10	6.60-2	1064.90	6.10-2	723.30	6.00-2	1153.30	5.90-2	1153.90	5.60-2	69.3
1965.40	3.80-2	2186.30	3.10-2	2026.10	3.10-2	2097.20	3.00-2	960.30	2.80-2	69.4
944.10	2.48-2	2180.50	1.90-2	1937.20	1.90-2	599.50	1.70-2	1366.10	1.60-2	69.5
867.00	1.50-2	1876.50	1.30-2	2270.00	8.00-3	105.10	6.80-3	1248.30	5.42-3	69.6
915.60	4.54-3	1183.60	3.70-3	969.70	3.50-3	841.20	2.46-3	434.30	2.40-3	69.7
1681.90	2.25-3	490.00	2.03-3	1258.40	9.80-4	199.20	7.20-4	1277.20	0.0 0	69.8
1168.00	0.0 0	1079.00	0.0 0	1049.30	0.0 0	1040.30	0.0 0	1018.30	0.0 0	70.1
1011.60	0.0 0	985.80	0.0 0	865.90	0.0 0	860.00	0.0 0	858.30	0.0 0	70.2
757.40	0.0 0	709.90	0.0 0	585.80	0.0 0	293.70	0.0 0	43.00	0.0 0	70.3
GD159	6.48000E 04	18								70.4
363.60	1.00-1	58.00	1.80-2	348.20	2.00-3	226.00	1.80-3	581.10	5.50-4	70.5
305.60	5.40-4	79.40	3.80-4	290.20	2.40-4	559.90	1.70-4	617.70	1.30-4	70.6
210.80	9.00-5	274.20	6.50-5	236.90	5.50-5	137.70	4.20-5	536.70	1.80-5	70.7
854.50	1.40-5	616.30	9.00-6	44.50	0.0 0					70.8
TB160	6.22944E 06	34								71.1

Table A-3. Continued

CODE= 1 MEMBER GAMDAT

12 PAGE

879.36	3.00-1	298.58	2.71-1	966.15	2.47-1	1177.94	1.48-1	86.79	1.37-1	71.2
962.30	1.02-1	1271.85	7.40-2	197.04	5.22-2	215.65	3.93-2	1311.95	2.79-2	71.3
1200.00	2.24-2	765.19	2.03-2	1115.20	1.50-2	392.51	1.36-2	1003.26	9.80-3	71.4
309.56	9.00-3	682.35	5.45-3	1102.90	5.00-3	337.32	3.30-3	871.95	1.74-3	71.5
1251.40	5.40-4	486.08	8.00-4	1069.10	7.60-4	230.63	7.10-4	93.92	6.70-4	71.6
246.49	1.80-4	379.45	1.40-4	349.94	1.40-4	432.72	1.30-4	1285.90	1.10-4	71.7
237.64	7.00-5	1300.00	5.00-5	176.49	4.70-5	242.50	4.00-5			71.8
GD161	2.22000E	02 15								72.1
361.00	6.60-1	315.30	2.50-1	102.40	1.10-1	283.80	8.00-2	165.30	4.63-2	72.2
180.60	2.26-2	482.00	2.07-2	258.80	1.94-2	531.00	1.68-2	273.00	1.29-2	72.3
56.60	8.50-3	105.50	6.47-3	77.60	4.70-4	133.70	0.0 0	44.50	0.0 0	72.4
DY165	8.35199E	03 18								72.5
94.70	4.00-2	361.50	1.10-2	716.00	7.00-3	633.00	7.00-3	279.60	6.00-3	72.6
545.00	1.70-3	566.00	1.40-3	1080.00	1.00-3	621.00	1.00-3	575.00	8.00-4	72.7
995.00	6.00-4	1056.00	3.00-4	514.00	3.00-4	479.00	3.00-4	695.00	2.00-4	72.8
588.00	8.00-5	501.00	6.00-5	47.60	0.0 0					73.1
DY165M	7.55999E	01 7								73.2
108.20	3.00-2	515.50	1.80-2	361.70	6.00-3	153.70	3.00-3	650.00	3.00-4	73.3
750.00	1.00-4	46.00	0.0 0							73.4
H0166	9.61199E	04 10								73.5
80.60	6.20-2	1380.00	9.30-3	1582.40	1.90-3	1663.00	1.20-3	1750.00	3.10-4	73.6
675.10	3.00-4	706.00	1.90-4	786.10	1.50-4	1830.30	9.30-5	49.10	0.0 0	73.7
H0166M	3.78683E	10 32								73.8
184.50	1.00 0	810.80	7.60-1	711.80	7.20-1	280.20	3.90-1	752.50	1.60-1	74.1
411.00	1.60-1	80.60	1.40-1	830.80	1.20-1	530.10	1.00-1	670.40	7.00-2	74.2
570.50	6.80-2	300.60	4.80-2	779.40	3.80-2	215.20	3.80-2	951.60	3.60-2	74.3
451.60	3.50-2	365.90	2.90-2	465.00	2.00-2	691.00	1.90-2	260.10	1.80-2	74.4
1241.80	1.20-2	594.80	1.20-2	875.90	1.10-2	1401.40	8.00-3	1427.50	7.00-3	74.5
996.80	7.00-3	896.60	7.00-3	121.60	7.00-3	111.80	7.00-3	1283.30	4.00-3	74.6
1275.00	4.00-3	1147.60	4.00-3							74.7
Y8169	2.76480E	06 16								74.8
63.12	4.42-1	197.97	3.61-1	177.24	2.18-1	109.78	1.81-1	130.53	1.17-1	75.1
307.70	1.01-1	93.60	2.60-2	118.20	1.91-2	261.00	1.71-2	20.75	2.40-3	75.2
240.40	1.21-3	117.25	3.40-4	394.00	1.30-4	156.66	8.10-5	625.00	3.60-5	75.3
515.00	2.90-5									75.4
TM170	1.12320E	07 2								75.5
84.30	3.30-2	52.40	0.0 0							75.6
ER171	2.70720E	04 50								75.7
308.20	6.44-1	295.90	2.89-1	111.60	2.05-1	124.00	9.10-2	116.60	2.30-2	75.8
210.50	6.42-3	796.20	6.40-3	907.80	6.35-3	277.40	5.80-3	237.10	3.02-3	76.1
675.70	2.85-3	372.00	2.57-3	670.70	2.52-3	783.80	2.40-3	732.20	9.76-4	76.2
620.60	8.90-4	175.80	8.90-4	419.80	8.30-4	912.80	7.70-4	85.60	6.00-4	76.3
869.70	5.50-4	559.10	4.66-4	882.00	3.85-4	608.60	3.05-4	197.70	2.70-4	76.4
966.40	2.64-4	506.60	2.27-4	424.80	2.24-4	671.70	2.20-4	363.00	1.97-4	76.5
518.80	1.77-4	547.60	1.67-4	609.00	1.65-4	693.20	1.50-4	705.80	1.20-4	76.6
573.50	9.80-5	286.50	8.00-5	1109.00	6.79-5	744.90	6.60-5	455.60	6.00-5	76.7
630.70	5.00-5	487.90	5.00-5	767.80	4.50-5	586.00	4.00-5	1395.50	2.80-5	76.8
1220.50	2.80-5	1400.50	2.50-5	1279.90	2.50-5	1284.40	2.40-5	495.40	2.00-5	77.1
Y8175	3.63600E	05 6								77.2
396.32	6.98-2	282.52	3.25-2	113.80	2.02-2	144.86	3.60-3	137.66	1.10-3	77.3
251.47	9.60-4									77.4

Table A-3. Continued

CODE= 1		MEMBER GAMDAT		13 PAGE							
HF175	6.04800E 06	8									77.5
343.40	8.50-1	89.40	3.40-2	433.00	1.40-2	229.60	6.00-3	113.80	3.00-3		77.6
161.30	3.00-4	318.90	0.0 0	54.10	0.0 0						77.7
LUI76M	1.33200E 04	10									77.8
88.35	8.45-2	1159.30	7.00-6	1061.61	3.80-6	1138.26	1.10-6	936.42	9.00-7		78.1
201.84	8.00-7	1226.85	6.00-7	1204.85	4.00-7	1247.68	1.00-7	957.40	1.00-7		78.2
YB177	6.84000E 03	22									78.3
150.39	1.72-1	1080.10	4.72-2	1241.40	2.90-2	121.62	2.90-2	138.61	1.10-2		78.4
941.70	9.00-3	1199.70	6.00-3	899.20	6.00-3	1119.60	5.00-3	1028.00	5.00-3		78.5
1230.70	3.00-3	1109.00	2.00-3	147.17	2.00-3	779.30	1.00-3	268.80	1.00-3		78.6
760.40	5.00-4	162.49	5.00-4	967.40	3.00-4	458.10	3.00-4	1214.80	2.00-4		78.7
961.50	2.00-4	1336.40	1.00-4								78.8
YB177M	6.50000E 00	3									79.1
104.00	6.50-1	228.00	1.30-1	52.40	0.0 0						79.2
LUI77	5.79744E 05	7									79.3
208.40	6.10-2	113.00	2.80-2	321.40	1.00-3	249.70	9.00-4	71.60	7.00-4		79.4
136.70	2.00-4	55.80	0.0 0								79.5
HF178M1	4.30000E 00	5									79.6
426.37	9.71-1	325.56	9.26-1	213.44	7.96-1	88.88	6.20-1	93.18	1.67-1		79.7
HF179M	1.86000E 01	3									79.8
214.30	9.40-1	160.60	3.00-2	375.00	5.00-3						80.1
HF180M	1.98000E 04	6									80.2
332.31	9.30-1	443.18	8.40-1	215.25	8.00-1	57.55	4.80-1	93.33	1.70-1		80.3
500.71	1.30-1										80.4
HF181	3.67200E 06	8									80.5
482.00	8.60-1	133.02	4.30-1	345.85	1.40-1	136.25	6.10-2	136.68	1.80-2		80.6
476.00	4.30-3	615.50	2.50-3	619.00	3.00-4						80.7
W 181	1.05002E 07	3									80.8
6.21	9.80-3	152.50	9.80-4	136.25	4.10-4						81.1
TA182	9.93599E 06	33									81.2
67.80	4.10-1	1121.30	3.58-1	1221.40	2.77-1	1189.05	1.66-1	100.10	1.44-1		81.3
1231.01	1.17-1	222.11	7.60-2	152.44	7.30-2	229.32	3.70-2	264.07	3.60-2		81.4
179.39	3.10-2	156.39	2.70-2	84.70	2.70-2	65.70	2.70-2	1001.70	2.10-2		81.5
113.70	1.80-2	1257.30	1.60-2	1289.10	1.50-2	198.40	1.50-2	1157.40	1.00-2		81.6
927.70	7.00-3	1273.70	6.90-3	31.70	4.60-3	1113.20	4.10-3	959.10	4.00-3		81.7
116.40	4.00-3	1342.60	2.80-3	1373.80	2.40-3	42.70	2.40-3	1387.20	9.00-4		81.8
1410.00	5.00-4	1453.00	4.00-4	125.40	2.00-4						82.1
TA182M	9.90000E 02	5									82.2
171.59	4.00-1	146.79	3.00-1	184.95	2.00-1	318.40	2.00-2	356.47	2.40-3		82.3
W 183M	5.30000E 00	8									82.4
107.90	1.90-1	52.60	1.10-1	99.10	9.00-2	46.50	8.00-2	160.50	6.00-2		82.5
102.50	4.00-2	210.30	1.00-2	59.30	0.0 0						82.6
W 185	6.48864E 06	1									82.7
125.40	1.70-4										82.8
RE186	3.20040E 05	7									83.1
137.15	9.18-2	767.51	2.86-4	630.34	2.54-4	333.40	6.00-7	296.90	5.00-7		83.2
773.28	2.00-7	476.42	0.0 0								83.3
W 187	8.60399E 04	45									83.4
685.70	3.20-1	479.50	2.60-1	72.00	1.10-1	134.20	1.00-1	618.20	7.40-2		83.5
551.50	6.00-2	772.80	4.80-2	601.20	1.60-2	625.40	1.30-2	478.20	1.00-2		83.6
511.70	7.70-3	466.90	6.00-3	864.60	4.00-3	745.20	3.40-3	473.80	3.00-3		83.7

Table A-3. Continued

CODE= 1 MEMBER GAMCAT

14 PAGE

437.50	3.00-3	879.50	2.80-3	529.60	2.00-3	302.20	2.00-3	252.20	2.00-3	83.8
197.30	2.00-3	206.40	1.50-3	246.30	1.40-3	200.50	1.00-3	239.10	9.00-4	84.1
211.60	7.00-4	735.60	6.00-4	223.10	6.00-4	760.00	3.00-4	220.70	3.00-4	84.2
225.60	1.00-4	180.20	0.0 0	145.10	0.0 0	136.30	0.0 0	132.20	0.0 0	84.3
128.00	0.0 0	122.50	0.0 0	113.70	0.0 0	106.50	0.0 0	98.20	0.0 0	84.4
62.10	0.0 0	61.10	0.0 0	57.20	0.0 0	49.20	0.0 0	36.20	0.0 0	84.5
RE188	6.01200E 04 35									84.6
155.00	1.00-1	633.00	9.00-3	478.00	6.00-3	932.00	4.00-3	829.00	3.00-3	84.7
1610.00	7.00-4	1132.80	6.00-4	672.00	6.00-4	485.00	5.00-4	1307.90	4.00-4	84.8
452.00	4.00-4	1803.00	3.00-4	1732.00	2.00-4	1150.00	2.00-4	824.00	2.00-4	85.1
1957.00	1.00-4	1786.00	1.00-4	1457.00	1.00-4	1176.00	1.00-4	1019.00	1.00-4	85.2
967.00	1.00-4	881.00	1.00-4	321.00	1.00-4	297.00	1.00-4	1322.00	8.00-5	85.3
1191.00	8.00-5	963.00	8.00-5	641.00	8.00-5	1368.00	7.00-5	1171.00	7.00-5	85.4
1866.00	4.00-5	1230.00	4.00-5	977.00	4.00-5	846.00	4.00-5	63.00	0.0 0	85.5
RE188M	1.12200E 03 6									85.6
63.60	3.00-1	106.00	2.10-1	92.40	1.00-1	156.00	1.20-2	169.50	2.00-3	85.7
61.10	0.0 0									85.8
OS191	1.33056E 06 4									86.1
129.40	1.00 0*	47.05	1.50-3*	82.43	1.00-3*	41.85	0.0 0			86.2
OS191M	4.69080E 04 1									86.3
74.38	0.0 0									86.4
IR192	6.39533E 06 22									86.5
316.50	8.31-1	468.06	4.76-1	308.45	2.98-1	295.95	2.91-1	604.40	8.07-2	86.6
612.45	5.18-2	588.57	4.44-2	205.79	3.36-2	484.57	3.17-2	374.48	7.39-3	86.7
416.46	6.60-3	201.31	4.96-3	489.04	3.96-3	884.52	2.74-3	283.26	2.29-3	86.8
136.35	1.33-3	1061.60	4.80-4	176.98	1.00-4	110.09	6.60-5	280.03	3.30-5	87.1
1090.40	1.30-5	1378.50	1.00-5							87.2
IR192M1	8.51999E 01 4									87.3
58.00	3.92-4	316.50	1.01-4	295.95	2.15-5	612.45	3.50-6			87.4
OS193	1.13400E 05 50									87.5
64.90	6.32-2	138.89	4.27-2	460.49	3.95-2	63.28	3.87-2	73.01	3.24-2	87.6
557.36	1.30-2	73.58	1.30-2	321.56	1.28-2	387.46	1.26-2	280.43	1.24-2	87.7
106.99	6.40-3	75.63	5.14-3	559.26	4.86-3	361.81	2.96-3	219.13	2.77-3	87.8
251.62	2.17-3	181.81	1.94-3	298.83	1.86-3	180.03	1.82-3	484.25	1.70-3	88.1
288.79	1.42-3	96.82	9.90-4	532.02	8.30-4	142.13	7.50-4	377.31	7.10-4	88.2
234.58	5.10-4	154.74	3.00-4	874.36	1.90-4	573.33	1.90-4	98.70	1.70-4	88.3
420.30	1.66-4	524.98	1.60-4	712.10	1.54-4	379.04	1.38-4	514.95	1.10-4	88.4
486.11	1.10-4	357.70	9.90-5	440.95	9.20-5	639.09	7.50-5	350.20	7.10-5	88.5
418.35	5.50-5	413.80	4.70-5	197.40	4.70-5	848.85	4.30-5	891.26	2.80-5	88.6
695.12	2.80-5	333.30	2.80-5	201.50	2.80-5	516.30	2.40-5	337.70	1.20-5	88.7
IR194	6.98399E 04 43									88.8
328.50	1.30-1	293.55	2.80-2	645.32	1.13-2	1150.86	6.00-3	530.10	6.00-3	89.1
938.87	5.70-3	300.71	3.50-3	622.05	3.10-3	1183.63	2.90-3	1469.22	1.80-3	89.2
589.39	1.50-3	1622.40	6.90-4	593.72	6.80-4	509.70	6.50-4	890.30	6.40-4	89.3
482.83	5.90-4	1218.90	5.80-4	1175.42	5.70-4	364.97	5.00-4	1293.90	4.60-4	89.4
1000.17	4.40-4	497.00	4.00-4	1342.41	3.70-4	699.00	3.60-4	1512.40	3.40-4	89.5
1048.65	3.10-4	925.28	2.90-4	528.95	2.90-4	1807.50	2.70-4	1104.08	2.70-4	89.6
1797.40	2.00-4	532.00	2.00-4	1562.81	1.80-4	1488.00	1.80-4	1803.00	1.70-4	89.7
1785.60	1.00-4	1670.70	8.70-5	2043.67	6.50-5	492.00	6.00-5	1432.20	4.00-5	89.8
2114.20	3.00-5	1924.33	2.90-5	1832.00	2.60-5					90.1
PT195M	3.47328E 05 10									90.2

Table A-3. Continued

CODE= 1 MEMBER GAMDAT

15 PAGE

98.86	1.14-1	129.74	2.83-2	30.88	1.95-2	239.21	5.60-4	211.28	3.80-4	90.3
140.50	2.90-4	130.05	0.0 0	79.94	0.0 0	28.40	0.0 0	19.80	0.0 0	90.4
PT197	6.48000E 04	3								90.5
77.35	8.00-1	191.50	2.43-1	269.20	1.70-2					90.6
HG197	2.34000E 05	3								90.7
77.35	2.41-1	191.50	8.90-3	268.00	6.00-4					90.8
AU198	2.32934E 05	3								91.1
411.80	9.47-1	675.88	1.05-2	1087.69	2.27-3					91.2
PT199	1.86000E 03	31								91.3
542.70	1.00 0*	493.50	3.80-1*	317.00	3.40-1*	185.80	2.30-1*	246.50	1.60-1*	91.4
191.70	1.60-1*	714.10	1.20-1*	474.50	7.80-2*	967.70	7.30-2*	791.20	7.30-2*	91.5
468.00	6.80-2*	465.70	6.20-2*	323.60	2.60-2*	219.40	2.60-2*	417.50	2.50-2*	91.6
240.00	1.20-2*	225.90	1.10-2*	425.10	9.40-3*	644.30	5.20-3*	505.30	5.10-3*	91.7
298.10	4.50-3*	664.60	3.10-3*	752.60	2.80-3*	1103.20	1.90-3*	890.60	1.70-3*	91.8
1072.00	1.60-3*	746.00	1.40-3*	835.30	1.30-3*	779.40	1.30-3*	786.20	1.20-3*	92.1
609.80	1.00-3*									92.2
HG203	4.04006E 06	1								92.3
279.21	8.15-1									92.4
TL206	2.52000E 02	1								92.5
803.30	5.50-5									92.6
BI210M	8.20480E 13	6								92.7
265.70	1.00 0*	304.80	5.40-1*	649.80	5.60-2*	344.00	1.40-2*	369.60	1.30-2*	92.8
329.10	1.10-2*									93.1
TH233	1.33200E 03	44								93.2
86.60	2.70-2	29.20	2.10-2	459.20	1.00-2	169.00	7.00-3	195.00	3.00-3	93.3
670.00	2.50-3	890.00	1.40-3	935.00	0.0 0	875.00	0.0 0	816.00	0.0 0	93.4
805.00	0.0 0	764.00	0.0 0	758.00	0.0 0	740.00	0.0 0	725.00	0.0 0	93.5
717.00	0.0 0	678.00	0.0 0	643.00	0.0 0	610.00	0.0 0	600.00	0.0 0	93.6
596.00	0.0 0	574.00	0.0 0	563.00	0.0 0	553.00	0.0 0	527.00	0.0 0	93.7
514.00	0.0 0	499.00	0.0 0	491.00	0.0 0	448.00	0.0 0	441.00	0.0 0	93.8
433.00	0.0 0	377.00	0.0 0	360.00	0.0 0	257.00	0.0 0	210.00	0.0 0	94.1
202.00	0.0 0	190.00	0.0 0	179.00	0.0 0	162.00	0.0 0	153.00	0.0 0	94.2
143.00	0.0 0	131.00	0.0 0	95.90	0.0 0	56.70	0.0 0			94.3
PA233	2.33300E 06	6								94.4
311.89	3.40-1	98.4	1.35-1	300.12	5.80-2	340.47	3.90-2	415.78	1.60-2	94.5
398.47	1.30-2									94.6
NP239	2.03000E+05	5								94.7
106.11	2.34-1	277.56	1.45-1	228.14	1.10-1	209.73	3.30-2	334.27	2.10-2	94.8
STOP										95.1



Table A-4. Flux File

CODE= 1 MEMBER FLUXFL

1 PAGE

00 3.480E-03 6.120E-03 84 RING 1 100MG 252CF SOURCE	1.1
3.696E-05 9.837E-05 1.937E-04 2.956E-04 3.925E-04 4.762E-04 4.475E-04	1.2
4.448E-04 4.120E-04 3.737E-04 3.823E-04 3.101E-04 2.329E-04 2.781E-04	1.3
2.301E-04 1.990E-04 1.777E-04 1.605E-04 1.459E-04 1.323E-04 2.477E-04	1.4
2.190E-04 1.966E-04 1.873E-04 1.847E-04 1.821E-04 1.787E-04 1.741E-04	1.5
1.700E-04 1.670E-04 1.638E-04 1.605E-04 7.753E-05 7.700E-05 7.619E-05	1.6
7.537E-05 7.455E-05 7.373E-05 7.291E-05 7.209E-05 7.127E-05 7.046E-05	1.7
6.966E-05 6.886E-05 6.806E-05 6.727E-05 6.649E-05 6.571E-05 6.495E-05	1.8
6.405E-05 6.398E-05 6.110E-05 7.325E-05 1.420E-05 5.689E-05 5.721E-05	2.1
5.646E-05 5.530E-05 5.640E-05 6.464E-05 7.930E-05 1.231E-04 1.861E-04	2.2
2.660E-04 3.521E-04 4.761E-04 5.852E-04 6.734E-04 7.282E-04 7.434E-04	2.3
8.027E-04 8.371E-04 8.413E-04 8.121E-04 7.500E-04 6.592E-04 5.474E-04	2.4
4.251E-04 3.043E-04 1.963E-04 1.099E-04 4.968E-05 1.548E-05 2.000E-06	2.5
10 1.370E-03 1.990E-03 84 RING 2 100MG 252CF SOURCE	2.6
3.696E-05 9.837E-05 1.937E-04 2.956E-04 3.925E-04 4.762E-04 4.475E-04	2.7
4.448E-04 4.120E-04 3.737E-04 3.823E-04 3.101E-04 2.329E-04 2.781E-04	2.8
2.301E-04 1.990E-04 1.777E-04 1.605E-04 1.459E-04 1.323E-04 2.477E-04	3.1
2.190E-04 1.966E-04 1.873E-04 1.847E-04 1.821E-04 1.787E-04 1.741E-04	3.2
1.700E-04 1.670E-04 1.638E-04 1.605E-04 7.753E-05 7.700E-05 7.619E-05	3.3
7.537E-05 7.455E-05 7.373E-05 7.291E-05 7.209E-05 7.127E-05 7.046E-05	3.4
6.966E-05 6.886E-05 6.806E-05 6.727E-05 6.649E-05 6.571E-05 6.495E-05	3.5
6.405E-05 6.398E-05 6.110E-05 7.325E-05 1.420E-05 5.689E-05 5.721E-05	3.6
5.646E-05 5.530E-05 5.640E-05 6.464E-05 7.930E-05 1.231E-04 1.861E-04	3.7
2.660E-04 3.521E-04 4.761E-04 5.852E-04 6.734E-04 7.282E-04 7.434E-04	3.8
8.027E-04 8.371E-04 8.413E-04 8.121E-04 7.500E-04 6.592E-04 5.474E-04	4.1
4.251E-04 3.043E-04 1.963E-04 1.099E-04 4.968E-05 1.548E-05 2.000E-06	4.2
999	4.3

Table A-5. Cross Section File

CODE= 1 MEMBER SIGMAF

1 PAGE

N 16	O16	PO	0	9.976E-01	1.600E	01	0.0	0.0	1.1
F 20	F19	GO	0	1.000E 00	1.900E	01	9.600E-27	1.700E-26	1.2
NA 24	NA23	GO	0	1.000E 00	2.299E	01	5.300E-25	3.100E-25	1.3
NA 24	AL27	AO	0	1.000E 00	2.698E	01	0.0	0.0	1.4
MG 27	MG26	GO	0	1.101E-01	2.598E	01	3.800E-26	2.500E-26	1.5
MG 27	AL27	PO	0	1.000E 00	2.698E	01	0.0	0.0	1.6
AL 28	AL27	GO	0	1.000E 00	2.698E	01	2.310E-25	1.100E-25	1.7
AL 28	SI28	PO	0	9.220E-01	2.798E	01	0.0	0.0	1.8
AL 28	P31	AO	0	1.000E 00	3.097E	01	0.0	0.0	2.1
S 37	S36	GO	0	1.500E-04	3.597E	01	1.500E-25	0.0	2.2
CL 38	CL37	GO	0	2.423E-01	3.697E	01	4.330E-25	4.000E-25	2.3
AR 41	AR40	GO	0	9.959E-01	3.996E	01	6.400E-25	4.100E-25	2.4
K 42	K41	GO	0	6.700E-02	4.096E	01	1.460E-24	1.400E-24	2.5
CA 49	CA48	GO	0	1.900E-03	4.795E	01	1.100E-24	5.000E-25	2.6
SC 46	SC45	GO	0	1.000E 00	4.496E	01	2.600E-23	8.600E-24	2.7
SC 46M	SC45	G1	0	1.000E 00	4.496E	01	1.700E-23	0.0	2.8
TI 51	TI50	GO	0	5.300E-02	4.994E	01	1.790E-25	1.200E-25	3.1
V 52	V51	GO	0	9.975E-01	5.094E	01	4.880E-24	2.700E-24	3.2
CR 51	CR50	GO	0	4.350E-02	4.995E	01	1.590E-23	7.600E-24	3.3
CR 55	CR54	GO	0	2.360E-02	5.394E	01	3.800E-25	2.500E-25	3.4
MN 56	MN55	GO	0	1.000E 00	5.493E	01	1.330E-23	1.420E-23	3.5
MN 56	FE56	PO	0	9.170E-01	5.593E	01	0.0	0.0	3.6
FE 59	FE58	GO	0	3.100E-03	5.793E	01	1.140E-24	1.100E-24	3.7
CD 60	CO59	GO	0	1.000E 00	5.893E	01	3.700E-23	7.500E-23	3.8
CD 60M	CO59	G1	0	1.000E 00	5.893E	01	1.900E-23	7.500E-23	4.1
NI 65	NI64	GO	0	9.000E-03	6.393E	01	1.490E-24	1.000E-24	4.2
CU 64	CU63	GO	0	6.910E-01	6.293E	01	4.400E-24	5.000E-24	4.3
CU 66	CU65	GO	0	3.090E-01	6.493E	01	2.170E-24	2.200E-24	4.4
ZN 65	ZN64	GO	0	4.890E-01	6.393E	01	7.800E-25	1.400E-24	4.5
ZN 69M	ZN68	G1	0	1.860E-01	6.792E	01	7.200E-26	2.000E-25	4.6
GA 70	GA69	GO	0	6.000E-01	6.893E	01	1.700E-24	1.600E-23	4.7
GA 72	GA71	GO	0	4.000E-01	7.192E	01	4.700E-24	3.100E-23	4.8
GE 75	GE74	GO	0	3.640E-01	7.392E	01	5.200E-25	1.100E-24	5.1
GE 77	GE76	GO	0	7.700E-02	7.592E	01	1.600E-25	2.000E-24	5.2
GE 75M	GE74	G1	0	3.640E-01	7.392E	01	1.600E-25	0.0	5.3
GE 77M	GE76	G1	0	7.700E-02	7.592E	01	1.000E-25	0.0	5.4
AS 76	AS75	GO	0	1.000E 00	7.492E	01	4.400E-24	6.100E-23	5.5
SE 75	SE74	GO	0	9.000E-03	7.392E	01	5.800E-23	6.000E-22	5.6
SE 77M	SE76	G1	0	9.000E-02	7.592E	01	2.100E-23	0.0	5.7
SE 79M	SE78	G1	0	2.350E-01	7.792E	01	3.000E-25	3.700E-24	5.8
SE 81	SE80	GO	0	5.000E-01	7.992E	01	7.000E-25	3.000E-25	6.1
SE 81M	SE80	G1	0	5.000E-01	7.992E	01	1.300E-24	2.000E-24	6.2
BR 80	BR79	GO	0	5.069E-01	7.892E	01	1.080E-23	0.0	6.3
BR 80M	BR79	G1	0	5.069E-01	7.892E	01	2.400E-24	3.600E-23	6.4
BR 82	BR81	GO	0	4.931E-01	8.092E	01	2.700E-24	5.300E-23	6.5
RB 86	RB85	GO	0	7.217E-01	8.492E	01	4.470E-25	7.000E-24	6.6
RB 88	RB87	GO	0	2.783E-01	8.692E	01	1.200E-25	3.000E-24	6.7
SR 85	SR84	GO	0	5.600E-03	8.391E	01	8.900E-25	1.200E-23	6.8
SR 85M	SR84	G1	0	5.600E-03	8.391E	01	5.900E-25	0.0	7.1
SR 87M	SR86	G1	0	9.900E-02	8.591E	01	8.400E-25	0.0	7.2
Y 90M	Y89	G1	0	1.000E 00	8.891E	01	1.000E-27	0.0	7.3

Table A-5. Continued

CODE# 1 MEMBER SIGMAF

2 PAGE

ZR 95	ZR94	GO	0	1.750E-01	9.391E	01	5.500E-26	3.000E-25	7.4
ZR 97	ZR96	GO	0	2.800E-02	9.591E	01	2.000E-26	5.000E-25	7.5
NB 94M	NB93	G1	0	1.000E 00	9.290E	01	0.0	0.0	7.6
MD 99	MD98	GO	0	2.440E-01	9.791E	01	1.300E-25	6.600E-24	7.7
MD101	MD100	GO	0	9.600E-02	9.991E	01	2.000E-25	3.800E-24	7.8
RU 97	RU96	GO	0	5.500E-02	9.591E	01	2.500E-25	6.000E-24	8.1
RU103	RU102	GO	0	3.160E-01	1.019E	02	1.300E-24	4.200E-24	8.2
RU105	RU104	GO	0	1.860E-01	1.039E	02	4.700E-25	4.600E-24	8.3
RH104	RH103	GO	0	1.000E 00	1.029E	02	1.340E-22	1.100E-21	8.4
RH104M	RH103	G1	0	1.000E 00	1.029E	02	1.100E-23	8.000E-23	8.5
PD103	PD102	GO	0	1.000E-02	1.019E	02	5.000E-24	0.0	8.6
PD109	PD108	GO	0	2.670E-01	1.079E	02	1.119E-23	2.030E-22	8.7
PD109M	PD108	G1	0	2.670E-01	1.079E	02	1.900E-25	3.000E-24	8.8
PD111	PD110	GO	0	1.180E-01	1.099E	02	1.100E-23	2.000E-22	9.1
AG108	AG107	GO	0	5.183E-01	1.069E	02	3.700E-23	9.400E-23	9.2
AG110	AG109	GO	0	4.817E-01	1.089E	02	8.800E-23	1.400E-21	9.3
AG110M	AG109	G1	0	4.817E-01	1.089E	02	4.000E-24	7.000E-23	9.4
CD111M	CD110	G1	0	1.240E-01	1.099E	02	1.000E-25	1.000E-24	9.5
CD115	CD114	GO	0	2.880E-01	1.139E	02	3.000E-25	2.300E-23	9.6
CD115M	CD114	G1	0	2.880E-01	1.139E	02	2.500E-26	0.0	9.7
CD117	CD116	GO	0	7.600E-02	1.159E	02	5.000E-26	2.000E-25	9.8
CD117M	CD116	G1	0	7.600E-02	1.159E	02	2.500E-26	0.0	10.1
IN114	CD113	GO	0	4.300E-02	1.129E	02	3.000E-24	2.500E-22	10.2
IN114M	CD113	G1	0	4.300E-02	1.129E	02	7.800E-24	0.0	10.3
IN116	CD115	GO	0	9.570E-01	1.149E	02	2.020E-22	3.300E-21	10.4
IN116M1	CD115	G1	0	9.570E-01	1.149E	02	1.610E-22	2.700E-21	10.5
SN113	SN112	GO	0	1.000E-02	1.119E	02	7.000E-25	3.000E-23	10.6
SN113M	SN112	G1	0	1.000E-02	1.119E	02	3.000E-25	0.0	10.7
SN120	SN122	GO	0	4.700E-02	1.219E	02	1.510E-25	1.000E-24	10.8
SN123M	SN122	G1	0	4.700E-02	1.219E	02	1.000E-27	0.0	11.1
SN125M	SN124	G1	0	5.800E-02	1.239E	02	1.300E-25	7.000E-24	11.2
SB122	SB121	GO	0	5.730E-01	1.209E	02	6.160E-24	2.050E-22	11.3
SB122M	SB121	G1	0	5.730E-01	1.209E	02	6.000E-26	0.0	11.4
SB124	SB123	GO	0	4.270E-01	1.229E	02	4.040E-24	1.200E-22	11.5
SB124M1	SB123	G1	0	4.270E-01	1.229E	02	4.000E-26	0.0	11.6
SB124M2	SB123	G2	0	4.270E-01	1.229E	02	2.000E-26	0.0	11.7
TE123M	TE122	G1	0	2.400E-02	1.219E	02	0.0	0.0	11.8
TE125M	TE124	G1	0	4.600E-02	1.239E	02	5.000E-26	0.0	12.1
TE127	TE126	GO	0	1.870E-01	1.259E	02	9.000E-25	1.000E-23	12.2
TE127M	TE126	G1	0	1.870E-01	1.259E	02	1.300E-25	0.0	12.3
TE129	TE128	GO	0	3.180E-01	1.279E	02	2.000E-25	1.500E-24	12.4
TE129M	TE128	G1	0	3.180E-01	1.279E	02	1.600E-26	8.000E-26	12.5
TE131	TE130	GO	0	3.450E-01	1.299E	02	2.000E-25	5.000E-25	12.6
I 128	I127	GO	0	1.000E 00	1.269E	02	6.100E-24	1.500E-24	12.7
I 130	I129	GO	0	1.000E 00	1.289E	02	2.700E-23	3.600E-23	12.8
I 130M	I129	G1	0	1.000E 00	1.289E	02	1.800E-23	0.0	13.1
CS134	CS133	GO	0	1.000E 00	1.329E	02	2.950E-23	4.300E-22	13.2
CS134M	CS133	G1	0	1.000E 00	1.329E	02	2.500E-24	3.000E-23	13.3
BA131	BA130	GO	0	1.000E-03	1.309E	02	1.050E-23	3.000E-22	13.4
BA137M	BA136	G1	0	7.800E-02	1.359E	02	1.100E-26	1.000E-25	13.5
BA139	BA138	GO	0	7.190E-01	1.379E	02	4.000E-25	3.000E-25	13.6

Table A-5. Continued

CODE=	1	MEMBER	SIGMAF				3	PAGE
LA140	LA139	GO	0 9.991E-01	1.389E	02	9.200E-24	1.140E-23	13.7
CE141	CE140	GO	0 8.850E-01	1.399E	02	5.600E-25	4.800E-25	13.8
CE143	CE142	GO	0 1.110E-01	1.419E	02	9.500E-25	1.400E-24	14.1
PR142	PR141	GO	0 1.000E 00	1.409E	02	1.150E-23	0.0	14.2
ND147	ND146	GO	0 1.720E-01	1.459E	02	1.300E-24	3.000E-24	14.3
ND149	ND148	GO	0 5.700E-02	1.479E	02	2.500E-24	1.600E-23	14.4
ND151	ND150	GO	0 5.600E-02	1.499E	02	1.200E-24	1.700E-23	14.5
SM153	SM152	GO	0 2.670E-01	1.519E	02	2.040E-22	3.000E-21	14.6
SM155	SM154	GO	0 2.280E-01	1.539E	02	6.000E-24	3.000E-23	14.7
EU152	EU151	GO	0 4.780E-01	1.509E	02	9.000E-21	3.300E-21	14.8
EU152M1	EU151	G1	0 4.780E-01	1.509E	02	3.200E-21	0.0	15.1
EU152M2	EU151	G2	0 4.780E-01	1.509E	02	4.000E-24	0.0	15.2
EU154	EU153	GO	0 5.220E-01	1.529E	02	3.800E-22	1.700E-21	15.3
GD159	GD158	GO	0 2.470E-01	1.579E	02	2.400E-24	6.000E-23	15.4
GD161	GD160	GO	0 2.170E-01	1.599E	02	7.700E-25	1.000E-23	15.5
TB160	TB159	GO	0 1.000E 00	1.589E	02	2.500E-23	4.500E-22	15.6
DY165	DY164	GO	0 2.820E-01	1.639E	02	2.700E-21	4.000E-22	15.7
DY165M	DY164	G1	0 2.820E-01	1.639E	02	1.800E-21	0.0	15.8
HQ166	HQ165	GO	0 1.000E 00	1.649E	02	6.500E-23	7.000E-22	16.1
HQ166M	HQ165	G1	0 1.000E 00	1.649E	02	3.000E-24	0.0	16.2
ER171	ER170	GO	0 1.500E-01	1.699E	02	5.700E-24	4.000E-23	16.3
TM170	TM169	GO	0 1.000E 00	1.689E	02	1.060E-22	1.700E-21	16.4
YB169	YB168	GO	0 1.400E-03	1.679E	02	3.500E-21	3.000E-20	16.5
YB175	YB174	GO	0 3.180E-01	1.739E	02	6.500E-23	3.000E-23	16.6
YB177	YB176	GO	0 1.270E-01	1.759E	02	2.400E-24	8.000E-24	16.7
YB177M	YB176	G1	0 1.270E-01	1.759E	02	0.0	0.0	16.8
LU176M	LU175	G1	0 9.740E-01	1.749E	02	1.600E-23	0.0	17.1
LU177	LU176	GO	0 2.600E-02	1.759E	02	2.100E-21	1.000E-21	17.2
HF178M1	HF177	G1	0 1.850E-01	1.769E	02	1.000E-24	0.0	17.3
HF179M1	HF178	G1	0 2.720E-01	1.779E	02	5.000E-23	4.000E-22	17.4
HF180M	HF179	G1	0 1.380E-01	1.789E	02	3.400E-25	0.0	17.5
HF175	HF174	GO	0 1.700E-03	1.739E	02	4.000E-22	5.000E-22	17.6
HF181	HF180	GO	0 3.510E-01	1.799E	02	1.400E-23	4.000E-23	17.7
TA182	TA181	GO	0 9.999E-01	1.809E	02	2.100E-23	7.000E-22	17.8
TA182M	TA181	G1	0 9.999E-01	1.809E	02	1.000E-26	0.0	18.1
W 181	W180	GO	0 1.300E-03	1.799E	02	1.000E-23	0.0	18.2
W 183M	W182	G1	0 2.630E-01	1.819E	02	2.100E-23	5.900E-22	18.3
W 185	W184	GO	0 1.430E-01	1.840E	02	1.800E-24	1.500E-23	18.4
W 187	W186	GO	0 3.070E-01	1.860E	02	3.800E-23	5.000E-22	18.5
RE186	RE185	GO	0 3.750E-01	1.850E	02	1.100E-22	1.800E-21	18.6
RE188	RE187	GO	0 6.250E-01	1.870E	02	7.500E-23	3.000E-22	18.7
RE188M	RE187	G1	0 6.250E-01	1.870E	02	1.000E-24	0.0	18.8
OS191	OS190	GO	0 2.640E-01	1.900E	02	1.300E-23	2.000E-23	19.1
OS191M	OS190	G1	0 2.640E-01	1.900E	02	9.000E-24	0.0	19.2
OS193	OS192	GO	0 4.100E-01	1.920E	02	2.010E-24	5.000E-24	19.3
IR192	IR191	GO	0 3.740E-01	1.910E	02	9.400E-22	4.000E-21	19.4
IR192M1	IR191	G1	0 3.740E-01	1.910E	02	4.000E-22	1.000E-21	19.5
IR194	IR193	GO	0 6.260E-01	1.930E	02	1.100E-22	1.400E-21	19.6
PT195M	PT194	G1	0 3.290E-01	1.940E	02	9.000E-26	0.0	19.7
PT197	PT196	GO	0 2.350E-01	1.960E	02	7.500E-24	8.000E-24	19.8
PT199	PT198	GO	0 7.200E-02	1.980E	02	3.727E-24	5.000E-23	20.1
PT199M	PT198	G1	0 7.200E-02	1.980E	02	2.700E-26	0.0	20.2
AU198	AU197	GO	0 1.000E 00	1.970E	02	9.880E-23	1.560E-21	20.3
HG197	HG196	GO	0 1.500E-03	1.960E	02	1.200E-22	6.000E-22	20.4
HG197M	HG196	G1	0 1.500E-03	1.960E	02	3.000E-21	4.000E-22	20.5
HG203	HG202	GO	0 2.970E-01	2.020E	02	5.000E-24	5.000E-24	20.6
TL206	TL205	GO	0 7.050E-01	2.050E	02	1.000E-25	1.000E-24	20.7
BI210M	BI209	G1	0 1.000E 00	2.090E	02	1.900E-26	1.900E-25	20.8
PA233	TH232	GO	0 1.0000-00	2.320E	02	7.400E-24	8.500E-23	21.1
NP239	U238	GO	0 9.928E-01	2.380E	02	2.700E-24	2.800E-22	21.2
STOP								21.3

Table A-6. EFFCAL Data File

CODE= 1 MEMBER EFFCAL

1 PAGE

00	EFFCAL ENERGIES							1.1
	20.00	25.00	30.00	35.00	40.00	45.00	50.00	001 1.2
	55.00	60.00	65.00	70.00	75.00	80.00	85.00	002 1.3
	90.00	95.00	100.00	110.00	120.00	130.00	140.00	003 1.4
	150.00	165.00	180.00	200.00	225.00	250.00	300.00	004 1.5
	350.00	400.00	500.00	600.00	700.00	800.00	1000.00	005 1.6
	1200.00	1400.00	1600.00	2000.00	2500.00	3000.00	3500.00	006 1.7
01	FLUSH DROP TUBE EFFICIENCY							1.8
	377.4	208.3	128.2	86.55	60.24	44.44	33.90	031 2.1
	26.32	21.98	18.52	16.67	15.38	14.39	13.51	032 2.2
	13.07	12.83	12.66	12.82	13.33	14.29	15.27	033 2.3
	16.26	17.70	19.42	21.74	24.39	27.25	32.89	034 2.4
	38.46	44.44	56.18	67.57	80.00	92.59	114.94	035 2.5
	137.00	158.70	181.80	224.70	277.00	327.90	381.700	036 2.6
03	1-INCH RABBIT EFFICIENCY							2.7
	1000.	540.5	333.3	222.2	153.80	111.1	85.5	031 2.8
	65.79	54.35	46.51	42.19	40.49	40.00	40.00	032 3.1
	40.49	40.98	41.49	42.92	44.84	46.51	48.78	033 3.2
	51.55	55.60	59.50	65.80	74.10	82.00	98.00	034 3.3
	116.30	132.80	166.10	198.00	230.40	263.20	327.90	035 3.4
	392.20	454.50	520.80	653.60	840.30	994.20	1139.00	036 3.5
04	EFFICIENCIES FOR FAR POSITION							3.6
	6250.00	3077.00	1754.00	1064.00	714.30	487.80	350.90	041 3.7
	263.20	204.10	166.70	135.10	125.00	119.00	116.50	3.8
	116.30	116.30	119.00	125.00	135.10	140.80	151.50	4.1
	161.30	175.40	188.70	208.30	232.60	256.40	303.00	4.2
	344.80	392.20	476.20	571.40	645.20	740.70	888.90	4.3
	1041.70	1204.80	1351.00	1667.00	2041.00	2381.00	2740.00	4.4
05	BM3 POLY SPACER DISTANCE							4.5
	540.50	307.70	181.80	125.00	88.89	64.52	50.00	4.6
	38.46	31.25	25.64	22.22	20.41	19.42	18.87	052 4.7
	18.52	18.69	18.94	20.00	21.51	22.73	24.10	4.8
	25.64	27.78	30.30	33.90	38.46	42.55	51.28	5.1
	59.70	68.96	85.11	102.00	119.00	135.10	170.90	5.2
	206.20	240.90	274.00	341.90	425.50	512.80	606.10	056 5.3
06	CLOSE RABBIT PGT DETECTOR							5.4
	606.	370.	250.	175.00	130.00	100.00	80.00	5.5
	64.10	52.60	44.40	38.50	34.50	31.70	29.60	052 5.6
	27.70	26.50	25.80	25.20	25.80	26.70	27.80	5.7
	29.00	31.10	33.60	36.80	40.80	45.20	54.10	5.8
	59.50	72.50	91.70	112.00	134.00	152.00	187.00	6.1
	222.00	258.00	294.00	361.00	444.00	562.00	610.00	056 6.2
99	DEFAULT EFFS							6.3
	1.00	1.00	1.00	1.00	1.00	1.00	1.00	991 6.4
	1.00	1.00	1.00	1.00	1.00	1.00	1.00	992 6.5
	1.00	1.00	1.00	1.00	1.00	1.00	1.00	993 6.6
	1.00	1.00	1.00	1.00	1.00	1.00	1.00	994 6.7
	1.00	1.00	1.00	1.00	1.00	1.00	1.00	995 6.8
	1.00	1.00	1.00	1.00	1.00	1.00	1.00	996 7.1

Table A-7. SIFTER Output

TAG- 20 3/17/76 11:17:00 CI- 1.000E 01 OT- 8.830E 04 TIR- 1.280E 06 WT- 1.376E 03 ISFO- 5 ITUR-14 ICYC- 1  
 HORTIN VEG SA 2ND CT 75-7531 20 NPK- 22  
 51.890 70.870 104.750 133.500 123.360 313.230 329.660  
 487.440 554.860 619.690 698.960 777.110 815.280 828.510  
 847.350 869.360 1044.830 1318.690 1365.770 1476.660 1526.210  
 1597.740  
 MATCH 1369.770 1368.596  
 MATCH 1526.210 1524.665  
 MATCH 847.350 846.751  
 MATCH 554.860 554.334  
 MATCH 619.690 619.088  
 MATCH 698.960 698.359  
 MATCH 777.110 776.502  
 MATCH 828.510 827.809  
 MATCH 1044.830 1043.973  
 MATCH 1318.690 1317.440  
 MATCH 1476.660 1474.853  
 MATCH 329.660 328.760  
 MATCH 487.440 487.039  
 MATCH 815.280 815.775  
 MATCH 1597.740 1596.110  
 MATCH 70.870 69.668  
 MATCH 104.750 103.180  
 MATCH 123.360 121.783  
 ORDER= 3 QJMB= 19  
 KING 2 100MG 252CF SOURCE  
 NA 24 1368.53 NA23 G0 3.788E 01+/- 5.307E 00 PPM 2 GP  
 NA 24 1359.53 AL27 G0 6.490E-15+/- 9.093E-16 RATE =1.0  
 K 42 1524.70 K41 G0 4.112E 03+/- 4.250E 02 PPM 2 GP  
 K 42 312.90 K41 G0 2.528E 04+/- 7.203E 03 PPM 2 GP  
 MY 56 846.50 MY55 G0 3.417E 02+/- 6.073E 01 PPM 2 GP  
 MY 56 846.60 EF56 P0 1.414E-12+/- 2.515E-13 RATE =1.0  
 SE 31M 102.70 SE80 G1 8.651E 09+/- 6.033E 08 PPM 2 GP  
 BR 82 776.49 BR81 G0 1.374E 11+/- 1.770E 00 PPM 2 GP  
 BR 82 554.33 BR81 G0 1.594E 01+/- 1.589E 00 PPM 2 GP  
 BR 82 519.39 BR81 G0 1.384E 01+/- 2.373E 00 PPM 2 GP  
 BR 82 698.35 BR81 G0 1.361E 01+/- 3.213E 00 PPM 2 GP  
 BR 82 1043.95 BR81 G0 1.232E 01+/- 4.253E 00 PPM 2 GP  
 TEL29 437.40\* TEL29 G1 3.459E 09+/- 4.341E 03 PPM 2 GP  
 I 134 847.08 7.408E 10 +/- 1.313E 10 OPM/GM AT TO  
 LA140 1596.40 LA139 G0 7.312E 00+/- 9.557E-01 PPM 2 GP  
 LA140 437.10 LA139 G1 6.361E 00+/- 7.983E-01 PPM 2 GP  
 LA140 815.70 LA139 G0 8.887E 00+/- 2.162E 00 PPM 2 GP  
 LA140 328.30 LA139 G0 7.113E 00+/- 1.136E 00 PPM 2 GP  
 EJ152 121.73 EJ151 G0 5.437E-01+/- 2.881E-01 PPM 2 GP  
 EJ152\*1 121.73 EJ151 G1 2.862E-02+/- 1.202E-02 PPM 2 GP  
 S4153 175.20 S4152 G1 1.067E 00+/- 7.433E-02 PPM 2 GP  
 S4153 69.60 S4152 G1 1.002E 00+/- 3.885E-01 PPM 2 GP  
 IR194 328.50 IR193 G0 2.292E 00+/- 3.660E-01 PPM 2 GP  
 PA233 311.44 TH232 G1 6.500E 00+/- 1.880E 00 PPM 2 GP

Table A-7. Continued

50.278	1.589E 05	3.34	0			
69.232	4.029E 03	38.76	1	SM153		
103.336	2.523E 04	6.97	3	SF 81M	SM153	Y8177M
107.099	1.552E 03	42.21	1	W 183M		
122.010	2.246E 03	44.79	2	EU152	EU152M1	
312.379	6.981E 03	28.48	2	K 42	PA233	
328.840	1.431E 04	15.97	2	LA140	IR194	
486.827	2.988E 04	12.55	2	TE129	LA140	
554.291	4.353E 04	10.60	1	BR 82		
619.140	2.321E 04	17.13	2	BR 82	AG108	
698.407	1.471E 04	23.61	1	BR 82		
775.526	4.433E 04	12.93	1	BR 82		
815.672	2.038E 04	24.33	2	AG110	LA140	
827.894	1.180E 04	32.14	0			
846.719	2.471E 04	17.79	2	MN 56	I 134	
868.411	9.258E 03	36.06	0			
1043.586	1.327E 04	34.52	1	BR 82		
1317.434	1.255E 04	39.33	0			
1368.432	6.351E 04	14.01	1	NA 24		
1475.155	8.369E 03	48.41	0			
1524.628	1.022E 05	10.35	1	K 42		
1596.055	7.061E 04	13.07	1	LA140		





## APPENDIX B: Calculation of Flux Depression Factors

---

The gold wires used in the flux mapping experiments in the 17-mg  $^{252}\text{Cf}$  activation facility were 20 mil in diameter and 1/2 inch length; each weighed about 50 mg. Both bare wires (surrounded completely by  $\text{H}_2\text{O}$  and polyethylene) and wires within cylindrical cadmium pillboxes (30-mil-thick) were activated at seven different distances from the  $^{252}\text{Cf}$  source. Because of the thickness of the wires, a correction factor for both thermal and epithermal (resonance) flux depression was required.

The flux depression factor is defined here as the measured specific activity of the wire relative to the specific activity of a wire of infinitely small diameter. In calculating this factor, the wire of radius  $R$  was assumed to be activated in the same manner as a foil of thickness  $R$ . Thermal flux depression factors for these experiments were calculated for a thick  $1/v$  detector in a Maxwellian spectrum. Resonance flux depression factors were calculated for both cadmium-covered  $1/v$  detector foil and for a thick detector foil with Doppler-broadened resonance in an isotropic  $1/E$  flux.

### THERMAL FLUX DEPRESSION

The thermal flux depression factor was calculated according to the method of Baumann.<sup>18</sup> For a slab  $1/v$  detector such as gold in an isotropic Maxwellian flux, the thermal flux depression factor,  $F$ , is given by

$$F = \frac{1 - 2E_3(KY_0)}{2KY_0}$$

$Y_0$  is the product of the atom density of the foil per unit area and the microscopic absorption cross section per atom.  $Y_0$  thus expresses the foil thickness in units of absorption mean free paths evaluated at the most-probable velocity of the incident flux. The effective foil thickness<sup>19</sup> is  $KY_0$  and allows the Maxwellian average flux depression value to be expressed in terms of equivalent monoenergetic cross sections which would give identical flux depression values. The  $En(x)$  mathematical functions are defined in Reference 20. For the particular conditions in this experiment,

$$Y_o = (0.0254 \text{ cm}) (19.32 \text{ g/cm}^3) \frac{6.022 \times 10^{23}}{196.97 \text{ g}} (98.8 \text{ cm}^2) = 0.148$$

and, from Reference 19

$$K = 1.045 \text{ so that } E = 0.379 \text{ at } (KY_o) = 0.155$$

Solving for the thermal flux depression factor,

$$F = \frac{1-2 (0.379)}{2 (0.155)} = 0.781$$

## RESONANCE FLUX DEPRESSION

The cadmium cutoff energy,  $E_c$ , an activated gold cadmium 30-mil-thick wier inside a cylindrical pillbox is calculated from Reference 20 for 2/3 beam and 1/3 isotropic flux to be

$$E_c = \frac{2}{3} E_c(\text{beam}) + 1/3 E_c(150) =$$

$$2/3 (0.475) + 1/2 (0.625) = 0.52 \text{ eV}$$

The gold absorption cross section in the resonance region may be considered to be  $1/v$  upon which large resonances are superimposed. Therefore,  $RI_{\text{total}} = RI_{1/v} + RI_{\text{res}}$ .

This cutoff is actually not sharp, and the cadmium itself shields some of the epithermal resonances of the gold cross section. A correction factor given by Martin<sup>20</sup> for this effect is about 1%.

Calculation of the resonance flux depression factor  $F$  includes depression factors for the  $1/v$  portion  $F_{1/v}$  of the epithermal cross section and for 48 separate resonances,  $F_{\text{res}}$ . The epithermal activation of gold is dominated by the large resonance at 4.90 eV. The method of Baumann<sup>19</sup> was used in these calculations. For the case of thick resonance detector foils in an  $1/E$  isotopic flux, the effect of Doppler broadening is included by the parameter

$$\theta = \frac{4 E_m E_o}{A \Gamma^2}$$

where

$E_m$  = the temperature of the absorber (in electron volts),

$E_o$  = the resonance energy,

$\Gamma$  = the total resonance width, and

A = the ratio of the mass of the absorber atom to that of the neutron.

The changes in resonance flux depression factors F with foil thickness  $Y_0$  in absorption mean free paths at the peak of the resonance have been reported for different values of  $\theta$ . The total resonance integral is the sum of  $1/v$  portion,  $RI_{1/v}$  plus the contributions of each individual resonance  $\Sigma RI_{res}$ . The resonance integral for each resonance is found from the peak absorption cross section  $\sigma_{max}$  and from reported resonance parameters.<sup>21</sup>

$$RI_{res} = \frac{\pi \sigma_{max} \Gamma_Y}{2E_0}$$

where

$$\sigma_{max} = \frac{2.6036 \times 10^6}{E_0} \frac{\Gamma_Y \Gamma_Y}{\Gamma^2} g$$

The average epithermal flux depression factor  $\bar{F}$  for the gold wire was found to be 0.1446 from

$$\bar{F} = \frac{(RI)_i F_{i_{res}} + RI_{1/v} F_{1/v}}{(\text{all resonances}) (RI_{total})}$$

Individual resonance integral and flux depression contributions to the total resonance integral and to the average flux depression factors are summarized in Table 2.

The  $1/v$  flux depression factor was calculated for a  $1/v$  detector in an isotropic  $1/E$  flux from

$$F_{1/v} = \frac{1 - 2 E_3 (KY_0/2)}{KY_0} = 0.95$$

Because,  $Y_0 = 0.0325$ ,

then  $K = 0.956$  (2/3 beam + 1/3 isotropic)

and  $KY_0 = 0.0311$

Interpolating from Table 1<sup>21</sup> gives  $E_3 = 0.4852$

The  $1/v$  portion of the resonance integral is given by

$$RI_{1/v} = \int_{0.525 \text{ ev}}^{10 \text{ Mev}} \sigma_{2200} \sqrt{\frac{E_{2200}}{E}} \frac{dE}{E} = 43 \text{ barns}$$



## REFERENCES

---

1. R. Hofstadter. "Alkali Halide Scintillation Counters." *Phys. Rev.* 74, 100 (1948).
2. D. V. Freck and J. Wakefield. "Gamma-Ray Spectrum Obtained with a Lithium-Drifted Junction in Germanium." *Nature* 193, 669 (1962).
3. W. L. Lyon. *Anal. Chem.* 45, 386A (1973).
4. W. W. Ergle. *A One-Dimensional Discrete Ordinates Transport Code with Anisotropic Scattering*. USAEC Report K-1693, Union Carbide Nuclear Division, Oak Ridge, TN (1967).
5. M. K. Drake. *Data Formats and Procedures for the ENDF Neutron Cross Section Library*, ENDF-102, Vol. 1, USAEC Report BNL-50274, Brookhaven National Laboratory, Upton, NY (1970).
6. W. W. Bowman and K. W. MacMurdo. "Radioactive Decay Gamma Ordered by Energy and Nuclide." *Atomic and Nuclear Data Tables* 13 (No. 2-3) (1974).
7. *Chart of the Nuclides*, General Electric Co., Schenectady, NY (1972).
8. G. Rudstam and F. Lund. "Delayed Neutron Activities Produced in Fission: Mass Range 79-98." *Phys. Rev. C* 13, 321 (1976).
9. G. Ruacham, S. Shalev, and O. Johnson. "Delayed Neutron Emission from Separated Fission Products." *Nucl. Instrum. Methods* 120, 33 (1974).
10. M. Asghar, J. Crancon, J. Gautheron, and C. Ristori. "Delayed Neutron Emission Probabilities of  $^{92,93}\text{Kr}$ ,  $^{92,93}\text{Rb}$ ,  $^{141,142}\text{Xe}$ , and  $^{141,142}\text{Cs}$  Precursors." *J. Inorg. Nucl. Chem.* 37, 1563 (1975).
11. G. Rudstam and S. Shalev. "Energy Spectra of Delayed Neutrons from Separated Fission Products." *Nucl. Phys. A* 235, 397 (1974).
12. G. R. Keepin. *Physics of Nuclear Kinetics*, p. 82, 86, 90, 146, Addison-Wesley, Reading MA (1965).

13. E. J. Onega, P. W. Forbes, A. K. Furr, and A. Robeson. "The Measurement of Short-Lived Delayed Photoneutrons from Fission-Fragment Gamma Rays." *Trans. Am. Nucl. Soc.* 12, 289 (1969); see also *Nucl. Sci. Eng.* 32, 49 (1968).
14. W. W. Graham, III, D. S. Harmer, and C. E. Cohern. "Accurate Delayed-Neutron Parameter Measurements in a Heavy-Water Reactor." *Nucl. Sci. Eng.* 38, 33 (1969).
15. J. P. Church. "Evaluation of Published Delayed-Neutron Parameters for Uranium-235 and Uranium-235 Heavy Water Systems." *Nucl. Sci. Eng.* 43, 229 (1971).
16. W. W. Bowman. "Rapid Analysis of Germanium Spectra." *Nucl. Instrum. Methods* 96, 135 (1971).
17. *Savannah River Laboratory Quarterly Report. Hydrogeochemical and Stream Sediment Reconnaissance — Eastern United States National Uranium Resource Evaluation Program. Report DPST-76-138-3, Savannah River Laboratory, E. I. du Pont de Nemours & Co., Aiken, SC (1976).*
18. N. P. Baumann. *Resonance Integrals and Self Shielding Factors for Detector Foils.* USAEC Report DP-817, Savannah River Laboratory, E. I. du Pont de Nemours & Co., Aiken, SC (1963).
19. N. P. Baumann and M. B. Stroud. "Self Shielding of Detector Foils in Reactor Fluxes." *Nucl. Sci. Eng.* 23 (8), 98 (1965).
20. D. H. Martin. "Correction Factors for Cd-Covered-Foil Measurements." *Nucl. Sci. Eng.* 13 (3), 52 (1955).
21. *Neutron Cross Sections, Vol. I, Resonance Parameters.* USAEC Report BNL-325, Third Edition, Brookhaven National Laboratory, Upton, NY (1973).